Memoranda on Full-Scale Upholstered Furniture Testing, 2016

Andrew Lock, Ph.D.
U.S. Consumer Product Safety Commission
Directorate for Laboratory Sciences
Division of Engineering
5 Research Place
Rockville, MD 20850
November 2017

This analysis was prepared by the CPSC staff and it has not been reviewed or approved by, and may not necessarily reflect the views of, the Commission.

The U.S. Consumer Product Safety Commission (CPSC) has a long-standing interest in fire safety, particularly as it relates to upholstered furniture. Upholstered furniture is estimated to be the first item ignited in an average of 4,500 residential fires causing 440 fire deaths annually.[1] The majority of fires or deaths are reported to be caused by smoldering ignitions. However, furniture designed to have improved resistance to small open flames has the potential to address fire scenarios involving upholstered furniture ignited by other sources, such as arcing, embers, hot surfaces, or when the upholstered furniture item is not the first item ignited, but is the item contributing the most to flame spread. In 2014, CPSC staff conducted a study that assessed chair designs built with textile components having enhanced flammability performance or "barriers." The chairs with barrier components were assessed in full-scale tests. The data suggested that fire barriers used in upholstered chair designs may be a way to improve the chair's flammability performance, when subjected to an open-flame ignition source, by reducing fire growth and energy output.

Following the 2014 study, CPSC staff developed a limited test program to evaluate the effects of different chair construction and other materials on flammability performance. In previous studies, including the 2014 study and studies before then, chairs with a foam seat and foam back were tested for flammability performance. However, chairs constructed with a foam seat and foam back are not representative of modern construction in which chairs are often built with a loose fill, usually polyester batting, in the back cushion of the chair. This program was developed to evaluate the flammability behavior of chairs constructed with a loose fill back cushion.

In this study, 30 chairs were constructed using a convenience sampling, i.e. a non-probability sample which does not necessarily represent the market, of a few components with the loose fill construction. Chairs were built with combinations of two cover fabrics using traditional construction, as well as two barriers, and two modified loose fills. These chairs were ignited using a small open-flame ignition source, the same as used in previous tests.

The attached memoranda detail the findings of the test study, as well as a NIST analysis of previous test work. This package includes three reports, A through C, which are listed in the Table of Contents below.

Table of Contents

[1] David Miller, Directorate for Epidemiology, U. S. Consumer Product Safety Commission, 2017, "2012-2014 Residential Fire Loss Estimates"

UNITED STATES
CONSUMER PRODUCT SAFETY COMMISSION
BETHESDA, MD 20814

Memorandum

Date: July 28, 2017

TO	:	Andrew Lock, Ph.D., Fire Protection Engineer, Laboratory Sciences, Upholstered Furniture Project Manager
THROUGH	:	Andrew G. Stadnik, P.E., Associate Executive Director, Directorate for Laboratory Sciences Allyson Tenney, Division Director, Division of Engineering
FROM	:	Linda Fansler, Division of Engineering Andrew Lock, PhD, Division of Engineering
SUBJECT	:	Summary Report of Open Flame Tests on Upholstered Chairs

Introduction

As part of the Upholstered Furniture Project, U.S. Consumer Product Safety Commission (CPSC) staff has conducted bench-scale and full-scale furniture testing, reviewed fire data, and assessed strategic approaches to manage risk from fires involving upholstered furniture. In 2012, CPSC staff conducted a full-scale upholstered chair test program, which included using a fire barrier in some chairs.[1] The analysis of the data from this study indicated that fire barrier use may be a way to improve flammability performance.

In 2014, CPSC staff continued research on fire barrier performance. [2] The 2014 test program included a series of full-scale smoldering and open-flame tests to evaluate the potential effectiveness of a limited number of fire barrier products in reducing the severity of upholstered furniture fires. The results of the 2014 test program indicated that, in general, for the open-flame tests, the use of barriers reduced the severity of the fires and delayed the most intense burning to different degrees. Two fire barriers were able to prevent fire from occurring some of the time.

In 2016, CPSC conducted additional barrier testing using the same chair design, cover fabrics, and barriers in the seat cushion. However, the back cushions in the 2016 tests were filled with loose, fibrous versions of fire barriers. Currently, constructed furniture usually includes loose filling material in the back cushion rather than polyurethane foam, which was generally phased out due to a shortage in 2005. Typically, back cushions are filled with polyester fibers, which is a characteristic of modern construction. This memorandum provides the details of the limited test program using modified (other than traditional polyester fiber) loose fills in chair back cushion constructions.

Test Program

The test program was designed to evaluate modified fill materials to assess their potential effectiveness in improving the flammability performance of upholstered furniture constructed with loose fill cushions. The test program did not specify a performance threshold, but rather, the test was intended to obtain additional information on the general performance of these modified fills when included in a specific chair construction. CPSC staff had 30 full-scale upholstered chairs, built using specific materials and construction to evaluate effectiveness (of the modified fills with barriers over foam seats) at reducing the potential hazard from fires involving upholstered furniture as compared to other upholstered furniture. The chairs were constructed in 10 combinations of two different upholstery fabrics, two different fire barriers, two different modified fills, and one conventional (polyester fibers) construction, and one type of foam. There were three replicates of each combination. Every combination was evaluated experimentally using an open flame; the specific combinations used are outlined in the following sections of this report. The test order of the chairs followed a randomization scheme provided by the CPSC's Directorate for Epidemiology.[3] However, the convienience sample was not conducive to a straightforward statistical analysis and not all of the combinations were included in the statistical analysis provided by Epidemology. The complete test protocol is provided in Appendix A.

The chairs used in this evaluation were made-to-order, based on CPSC staff's specifications for fabrics, fire barriers, modified fills, and a non-fire-retardant polyurethane foam (PU), which were installed on a basic wooden frame that was identical to previous tests.[4] Figure 1 illustrates the dimensional construction of the chairs.

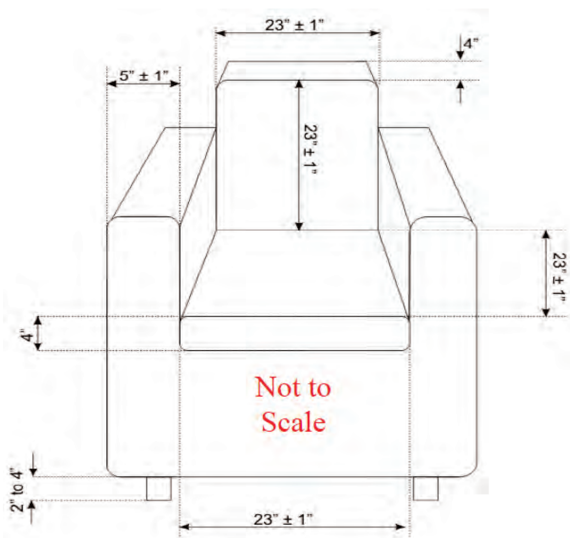

Figure 1. Schematic representation of the dimensions of the test chairs used in this series.

Chair Construction Materials

The materials, including materials with improved flammability performance, specifically fire barriers and modified loose fill fibers, were all purchased by the furniture manufacturer from vendors identified by CPSC staff. The justification for material selection is discussed later in this report. The chairs evaluated with the open-flame igntion source used 10 combinations of materials (1 foam, 2 fire barriers, 2 modified fills, and 2 cover fabrics; chairs with traditional construction without fire barriers or modified fills, were also included with 2 cover fabrics). The materials used are discussed below.

Upholstery Fabrics

Two upholstery fabrics were included in this study. They are described in Table 1. Both fabrics were used in prior testing by CPSC staff.[2,4]

Table 1. Upholstery Fabrics for Full-Scale Tests

Fabric Code	Fiber Content	Weight (oz/yd^2)	Fabric Construction
F2	100% cotton	13	Twill (denim)
F3	56% rayon/34% polyester/10% cotton	10	Jacquard

Foam

The chairs' construction was specified with the same commercially available foam in the seats, used in previous tests.

Non-Flame Retardant Polyurethane Foam:

- Density: 1.8 $\pm$ 0.1 lb/ft^3;
- Indentation Load Deflection (ILD): 25% to 30%;
- Air Permeability: Greater than 4.0 ft^3/min; and
- No flame retardant (FR) chemical treatment

Fire Barrier

Staff was interested in evaluating the flammability performance of upholstered chairs constructed with barriers and modified fill in this limited study. Two fire barriers (FB) were evaluated in this study. They are described in Table 2. These commercially available fire barriers were originally developed for use in mattress designs that meet the performance requirements specified in 16 C.F.R. part 1633--The Standard for the Flammability (Open Flame) of Mattress Sets. Because a performance threshold has not been established for upholstered chairs, the barriers were selected based on conversations with fire barrier manufacturers regarding each barrier's potential performance and the results of the previous study.[2] The manufacturers identified products they thought would likely have enhanced flammability performance in upholstered chair constructions. A subset was selected based on previous experience. The fiber content and construction specifications for each of the fire barriers were provided by each manufacturer. The barriers used here are a subset of those used in a previous study.[2]

Table 2. Fire Barriers for Full-Scale Tests

Fire Barrier Code*	Fiber Content	Construction	Chemical Analysis	Comments
FB2	Fibrous glass/modacrylic/polyester	Needle punched	2.6% Antimony	Indicates possible FR chemical additive
FB4	Rayon/polyester	High loft	1.0% Phosphorous 0.3% Chlorine	Indicates possible FR chemical additive

* Fire Barrier (FB)

The fire barriers were placed in the following locations on the chair:

- Six-sided wrap on seat cushion;
- Inside arms facing seating area;
- Across the top of the arms, down the outside of the chair; and
- Inside the back (behind back cushion) from below the crevice up to the top of the chair frame.

Polyester Batting
The 100 percent polyester batting was nominally 8 oz./yd.^{2}, 0.75-inch thick, nonwoven. The polyester batting was included in the seat and back cushion constructions in one of the following configurations:

- Used by itself on top of the foam, as in test combinations 1 and 2, or;
- Placed on top of the foam and under the fire barrier in all other test combinations.

Loose Fills
Two different modified loose fills were used in the backs of the chairs, in addition to standard loose polyester fill. Polyester fill is typically blown into a pillow or cushion by a machine. The other loose fills were filled into the cushions by hand, because the modified fills behave differently than polyester fill and the CPSC's relatively small custom order did not warrant automation. The loose fills are denoted as Fiber Fill (FF).

Table 3. Modified loose fills in back of chair for Full-Scale Tests

Fire Barrier Code*	**Fiber Content**	**Construction**
FF3	100% FR Polyester	Loose Fill
FF4	FR Rayon and modacrylic	Loose Fill

* Fiber Fill (FF)

Chair Construction Combinations
Combination "Combo" numbers were used internally to distinguish between the different chair constructions. Not all of the initially planned combinations were used, but the original numbering was maintained to ensure traceability within our records. The list of chair combinations can be found in Table 4. There were 10 combinations in total.

Table 4. Chair Material Combinations for Full-Scale, Open-Flame Testing

Combo	**Foam**	**Poly Bat**	**Poly Fill**	**FB********	**FB_Back*********	**Fabric**********
1	PU*	Yes	Yes	No	No	F2
2	PU	Yes	Yes	No	No	F3
7	PU	*No*	*No*	*FB2*	*FF3*	*F2*
8	PU	*No*	*No*	*FB2*	*FF3*	*F3*
9	PU	*No*	*No*	*FB2*	*FF4*	*F2*
10	PU	No	No	FB2	FF4	F3
15	PU	*No*	*No*	*FB4*	*FF3*	*F2*
16	PU	*No*	*No*	*FB4*	*FF3*	*F3*
17	PU	*No*	*No*	*FB4*	*FF4*	*F2*
18	PU	No	No	FB4	FF4	F3

* Polyurethane (PU), ** Fire Barrier (FB), *** Fiber Fill (FF), **** Fabric (F)

The furniture manufacturer labeled each chair to identify the fire barrier used in the construction of the chair. The chairs were tested following a randomized test scheme.[3] CPSC staff verified the components used in the test chairs before testing.

Testing Order
The combinations were tested in a predetermined randomized order developed by our epidemiology group. The chairs were labeled as OF# for open-flame testing (where # is the number in the test series). The testing order is listed in Table 5. Each combination was repeated three times.

Table 5. Open-Flame test order.

Testing Order	Combo	Foam	Poly Bat	Poly Fill	FB	FB_Back	Fabric
OF1	17	PU	No	No	FB4	FF4	F2
OF2	15	PU	No	No	FB4	FF3	F2
OF3	8	PU	No	No	FB2	FF3	F3
OF4	15	PU	No	No	FB4	FF3	F2
OF5	16	PU	No	No	FB4	FF3	F3
OF6	9	PU	No	No	FB2	FF4	F2
OF7	7	PU	No	No	FB2	FF3	F2
OF8	15	PU	No	No	FB4	FF3	F2
OF9	8	PU	No	No	FB2	FF3	F3
OF10	9	PU	No	No	FB2	FF4	F2
OF11	18	PU	No	No	FB4	FF4	F3
OF12	2	PU	Yes	Yes	No	No	F3
OF13	16	PU	No	No	FB4	FF3	F3
OF14	7	PU	No	No	FB2	FF3	F2
OF15	16	PU	No	No	FB4	FF3	F3
OF16	1	PU	Yes	Yes	No	No	F2
OF17	1	PU	Yes	Yes	No	No	F2
OF18	1	PU	Yes	Yes	No	No	F2
OF19	17	PU	No	No	FB4	FF4	F2
OF20	2	PU	Yes	Yes	No	No	F3
OF21	17	PU	No	No	FB4	FF4	F2
OF22	8	PU	No	No	FB2	FF3	F3
OF23	9	PU	No	No	FB2	FF4	F2
OF24	10	PU	No	No	FB2	FF4	F3
OF25	2	PU	Yes	Yes	No	No	F3
OF26	18	PU	No	No	FB4	FF4	F3
OF27	10	PU	No	No	FB2	FF4	F3
OF28	18	PU	No	No	FB4	FF4	F3
OF29	7	PU	No	No	FB2	FF3	F2
OF30	10	PU	No	No	FB2	FF4	F3

Test Method
The upholstered chairs were evaluated following the protocol outlined in Test Protocol – Full-Scale Chair Evaluations (Appendix A). Each chair was conditioned for a minimum of 48 hours at a temperature of 20 ± 3^oC (70 ± 5^oF) and a relative humidity of $50 \pm 5\%$ before testing.[*] Tests were conducted in the open calorimetry laboratory at the CPSC National Product Testing and Evaluation Center. One chair was tested at a time to capture the heat release rate (HRR) measurement of each tested chair. In addition to the physical measurement data, each test was video recorded and photographs were taken before and after the test.

The open-flame source was chosen to be consistent with previous test work and was intended to simulate a small, open-flame source.[†] A 240 mm butane flame was applied to the center of the crevice of the seat and back cushions of the tested chair for 70 ± 1 seconds.[5] During the test, the HRR data were monitored; the test was allowed to continue until the peak heat release rate (PHRR) was observed. Visual observations, such as progression of the flame spread, time to flame out and time to flaming through the back of the chair, were also annotated while tests were being conducted.

Data and Observations

During the tests, staff observed and recorded relevant events in each test. Heat flux was measured in three places around the chair. CO, CO_2 and O_2 levels were recorded from the effluent gases in the exhaust hood. Flame spread across the cushions, melt dripping, and full involvement of the chair were also observed. The HRR was also measured via oxygen consumption calorimetry in the hood.

Heat Release Rate Data
The Heat Release Rate (HRR) is a measure of the rate at which energy is released by the fire. The HRR can be determined as a function of the gas flow rate, O_2, CO, and CO_2 quantities in the effluent coming off of a burning hydrocarbon fuel source, in this case, upholstered furniture. This quantitative measure provides an understanding of how severe the fire is, how the fire is likely to be affecting tenability in the environment, and the likelihood of the fire spreading to nearby items.

The Peak Heat Release Rate (PHRR) is the maximum instantaneous HRR measured during a test. The PHRR is important because it provides a measure of the potential maximum severity of a fire. The time to PHRR (*TTPHRR*) is also recorded because of implications for escape and response time. The shorter the time before the PHRR, the less time occupants and emergency responders have to react to the fire.

Plots of all the HRR data from all 30 chairs are detailed in Appendix B for open-flame tests. A summary of each test is provided in Table 6. The table includes information on the test number, the combination number, fabric ID, and barrier ID. The data columns relate to the HRR measurements taken during each test. The *Peak at 15 min* indicates the highest HRR observed within the first 15 minutes of the test from when the ignition burner was removed from the specimen. The *Peak HRR* indicates the maximum HRR observed throughout the entire test. The *TTPeak HRR* refers to the amount of time from when the ignition burner was removed until the maximum overall HRR peak (previous column) was observed. The *TT 200 kW* refers the amount of time after the ignition burner was removed until the fire reached 200 kW. The

---

[*] These conditioning requirements were chosen to be consistent with other large-scale flammability test methods, *e.g*., 16 C.F.R. part 1633, "Standard for the Flammability (Open Flame) of Mattress Sets"
[†] This ignition source is specified in the British Standard, BS 5852, as Source 3. The flame size and duration are needed to evaluate the interior fire barrier's ability to prevent the spread of fire to underlying materials. Because interior fire barriers would be located between flammable cover fabrics and filling materials, it is critical that interior fire barriers be capable of withstanding the heat exposure presented by an ignited cover fabric.

figure 200 kW was chosen as a benchmark for the tests because of its use in the mattress open-flame regulation at 16 C.F.R. part1633. The *THR @ 10 min*, measured in Joules, indicates the total amount of heat produced in the first 10 minutes of the fire. Again, this is a benchmark related to the total heat release requirement in 16 C.F.R. part 1633. In each of the data columns, a value of zero indicates that a value below the measurement threshold was observed.

The highest PHRR observed in this testing was 1907 kW from a non-barrier chair. The lowest recorded PHRR was 374 kW. In general, the barriers reduced the intensity of the fire, but none of the barrier/fill combinations in this study successfully prevented a chair from burning.

Figure 2 through Figure 9 present comparisons of heat release rate curves for the various combinations of cover fabric, barrier, and back fill. In every case, the chair with no barrier and the traditional poly fill produced the highest PHRR and had the fastest fire growth. In nearly every case, the combinations of fire barrier and modified back fill resulted in a decrease of more than 50 percent in the PHRR and at least double the TTPHRR.

In these tests, the type of fill in the back of the chair seemed to have a greater effect on the performance of the chair than the fire barrier did. For example, Figure 4 and Figure 6 represent the F3, FF3 combination and F2, FF4 combinations, respectively; and in these cases, the HRR curves for FB4 and FB2 are nearly indistinguishable. In Figure 5 and Figure 7, representing F3, FF4 and F2, FF3, respectively, are likewise quite similar, showing more of a difference in the TTPHRR than other parameters.

Figure 2, Figure 3, Figure 8, and Figure 9 show the influence of the back fill as well; in every case, the chairs with FF3 in the back reach their TTPHRR faster than the FF4 chairs. Likewise, most of the FF3 chairs have a higher PHRR than the FF4 chairs.

Figure 10 through Figure 13 present comparisons of the PHRR for the various combinations of cover fabric, barrier, and back fill. Because the higher PHRR is loosely correlated with the lower TTPHRR, Figure 10 and Figure 11 show the inverse trends of Figure 12 and Figure 13. Once again, all of the barrier and fill combinations result in decreased PHRR and increased TTPHRR. A different, yet similar, observation about the loose fill in the chair backs can be made. For both F2 and F3, the chairs with FF4 had both the lowest PHRR and largest TTPHRR. In every case, the three replicates of the chairs with different barriers, but the same loose fill overlap for both TTPHRR and PHRR. This indicates that the loose fill has a larger influence than the sheet barrier on the burning behavior of these chairs. However, the different cover fabrics still play a large role in the performance of the chair. Comparing the same barrier/fill combinations between the cover fabrics for PHRR in Figure 10 and Figure 11, the peaks observed from cover fabric F3 were slightly higher. Making the same comparison for TTPHRR in Figure 12 and Figure 13, the fires on chairs with cover fabric F3 burned faster.

Table 6. Summary of Open-Flame test data.

Test Name	Fabric	FB*	FB_Back**	Peak HRR (kW)	TTPHRR	Peak HF (kW/m^2)	TT 200 kW	THR @ 10 min	Peak at 15 min
OF1	*F2*	*FB4*	*FF4*	563.02	31.48	10.75	26.05	2.08	31.98
OF2	*F2*	*FB4*	*FF3*	512.89	19.50	10.75	15.38	32.45	169.15
OF3	*F3*	*FB2*	*FF3*	653.52	16.88	14.15	4.45	38.97	380.70
OF4	*F2*	*FB4*	*FF3*	738.97	17.62	10.81	8.13	41.53	342.31
OF5	*F3*	*FB4*	*FF3*	656.14	11.00	11.70	4.12	105.96	656.14
OF6	*F2*	*FB2*	*FF4*	373.74	33.88	7.67	29.22	3.09	13.75
OF7	*F2*	*FB2*	*FF3*	485.70	19.60	10.06	16.77	31.36	190.85
OF8	*F2*	*FB4*	*FF3*	918.49	19.15	13.00	8.25	32.37	218.78
OF9	*F3*	*FB2*	*FF3*	663.94	10.77	16.75	3.92	89.30	663.94
OF10	F2	FB2	FF4	464.10	37.28	9.80	26.07	3.30	14.32
OF11	F3	FB4	FF4	619.71	13.35	11.70	9.10	30.29	619.71
OF12	F3	No	No	1568.73	4.47	24.02	2.27	222.62	1568.73
OF13	F3	FB4	FF3	686.26	18.25	12.14	3.85	45.51	305.19
Of14	F2	FB2	FF3	630.94	19.52	13.64	9.48	32.66	250.58
OF15	F3	FB4	FF3	599.04	12.98	12.49	4.07	105.64	599.04
OF16	F2	No	No	1339.99	13.13	18.96	9.12	29.20	1339.99
OF17	F2	No	No	1332.18	11.33	17.34	7.17	63.92	1332.18
OF18	F2	No	No	941.86	10.67	13.94	7.15	73.38	941.86
OF19	F2	FB4	FF4	598.91	29.33	9.02	24.42	4.79	34.93
OF20	F3	No	No	1906.72	4.67	25.22	2.57	233.25	1906.72
OF21	F2	FB4	FF4	441.71	26.37	9.02	23.97	5.13	29.06
OF22	F3	FB2	FF3	741.81	14.08	15.79	4.37	50.47	741.81
OF23	F2	FB2	FF4	477.27	29.37	11.29	26.72	4.75	31.47
OF24	F3	FB2	FF4	615.31	18.67	10.08	16.75	8.58	133.32
OF25	F3	No	No	1879.33	4.78	28.19	2.45	220.54	1879.33
OF26	F3	FB4	FF4	631.50	15.98	8.41	12.22	21.67	284.71
OF27	F3	FB2	FF4	496.54	16.10	13.38	13.98	11.36	430.21
OF28	F3	FB4	FF4	572.18	16.00	10.28	9.63	26.49	398.34
OF29	F2	FB2	FF3	576.02	21.50	13.67	8.35	30.95	207.30
OF30	F3	FB2	FF4	493.93	17.23	9.39	12.52	11.38	382.90

* Fire Barriers (FB), ** Fiber Fill (FF)

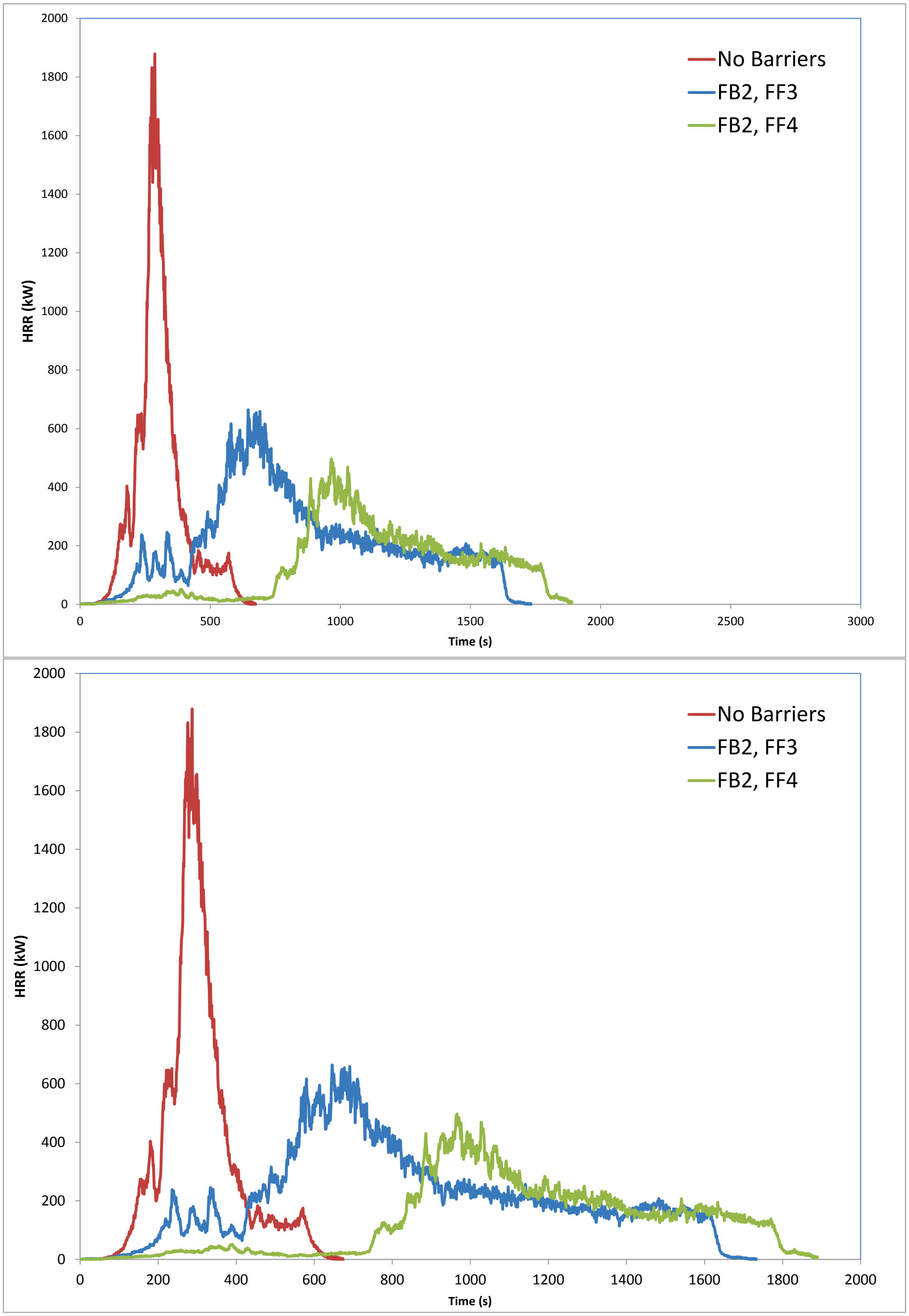

Figure 2. Example comparison of different back fills with fire barrier FB2 and cover fabric F3.

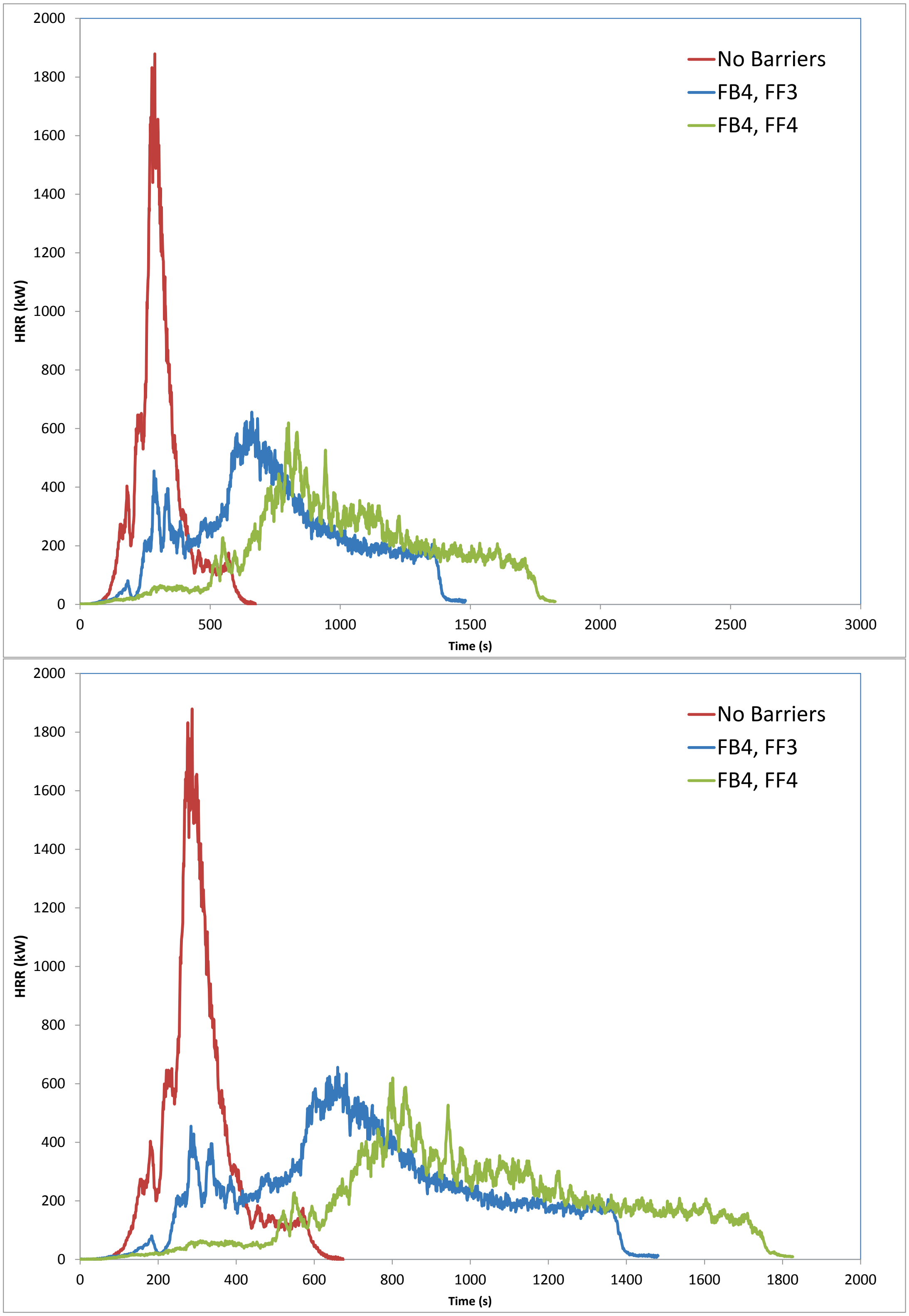

Figure 3. Example comparison of different back fills with fire barrier FB4 and cover fabric F3.

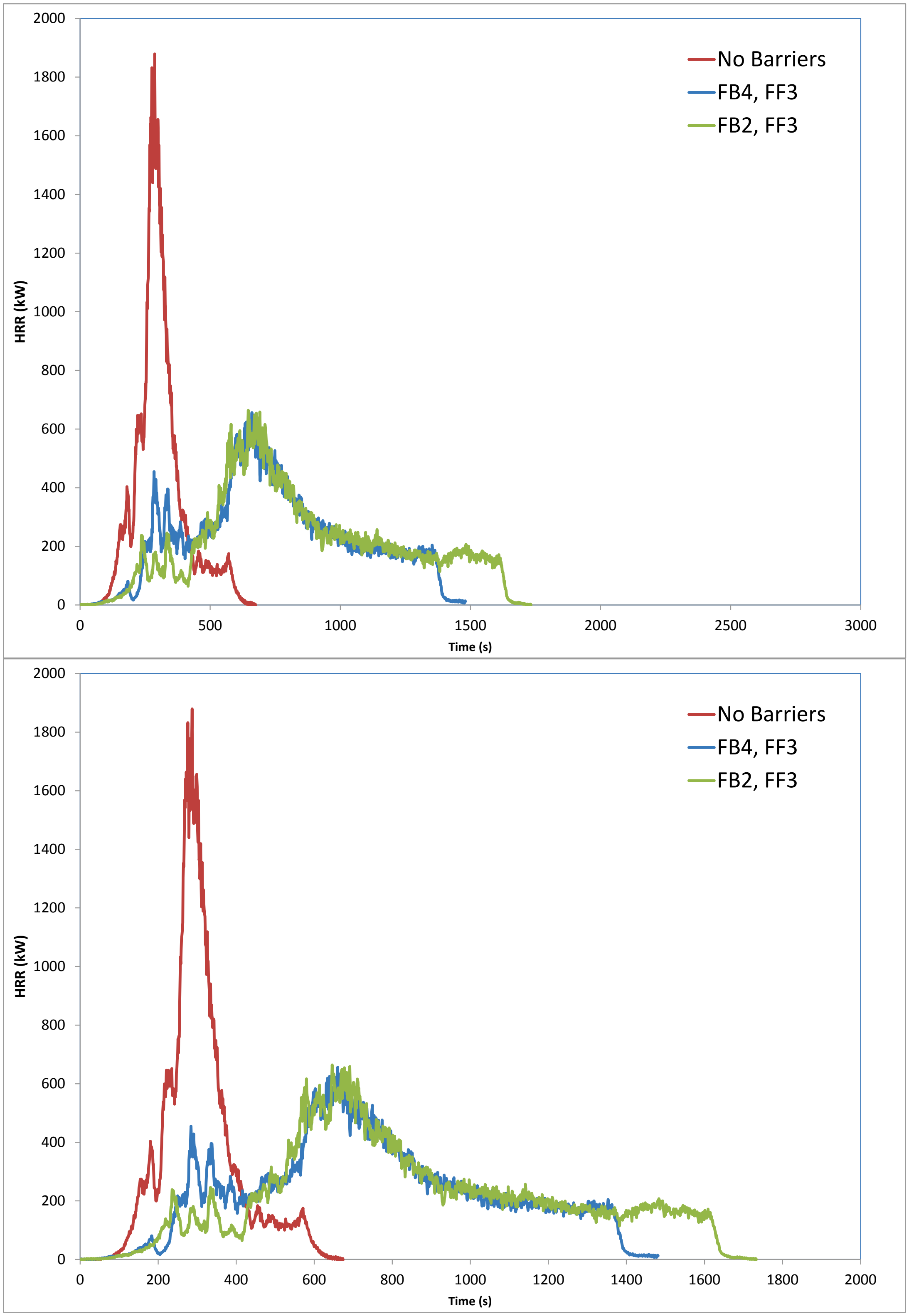

Figure 4. Example comparison of different fire barriers with back fill FF3 and cover fabric F3.

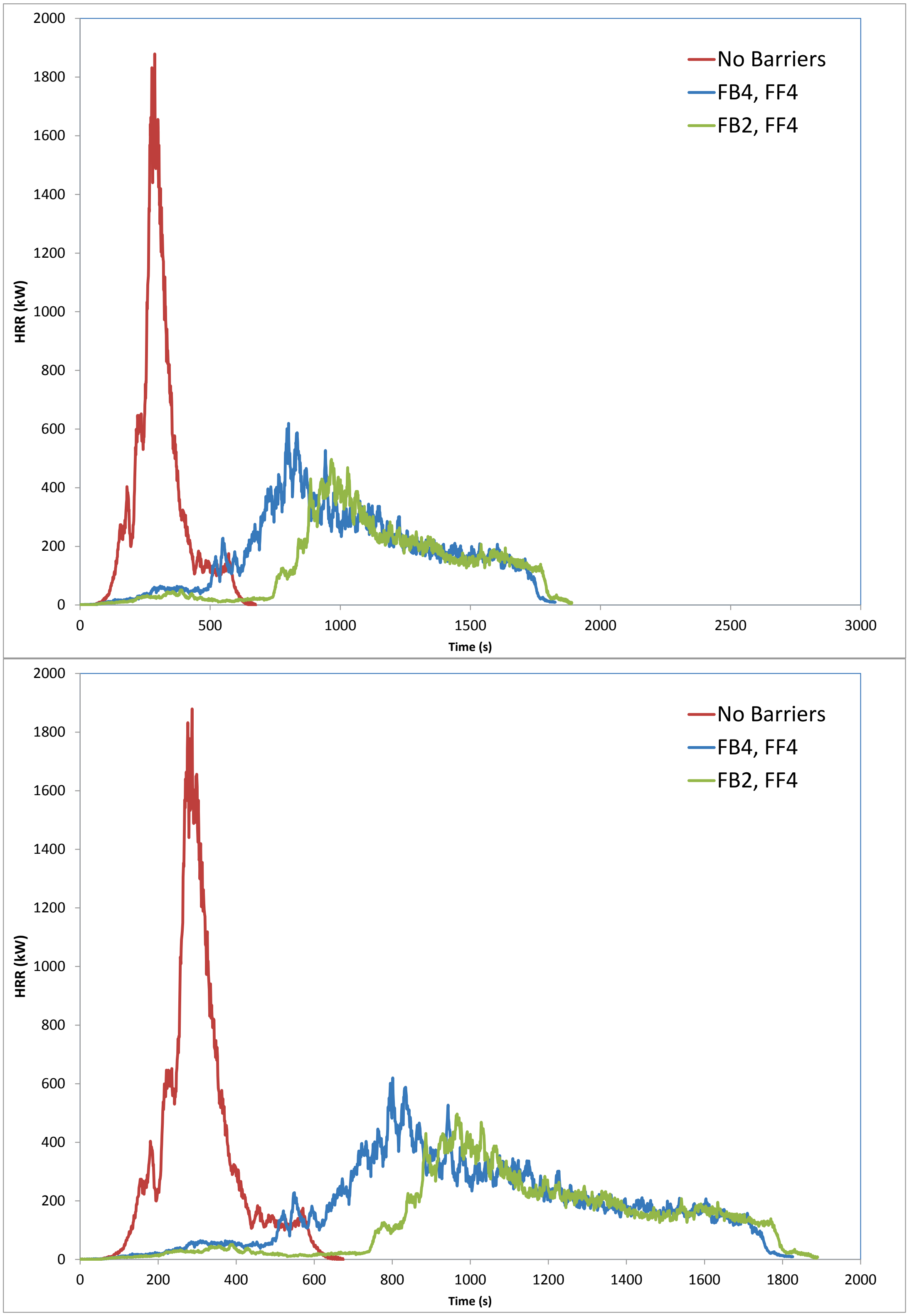

Figure 5. Example comparison of different fire barriers with back fill FF4 and cover fabric F3.

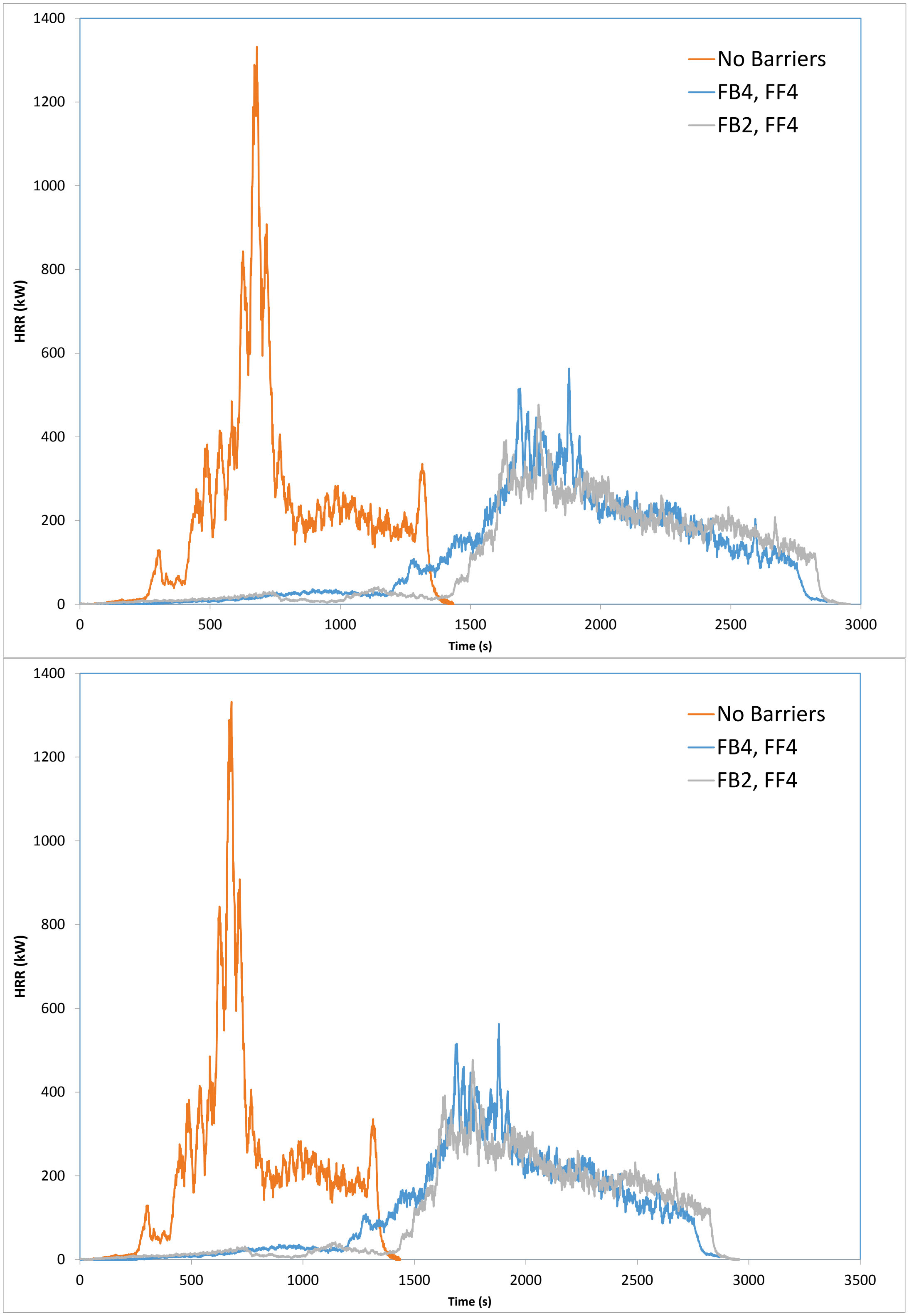

Figure 6. Example comparison of different fire barriers with back fill FF4 and cover fabric F2

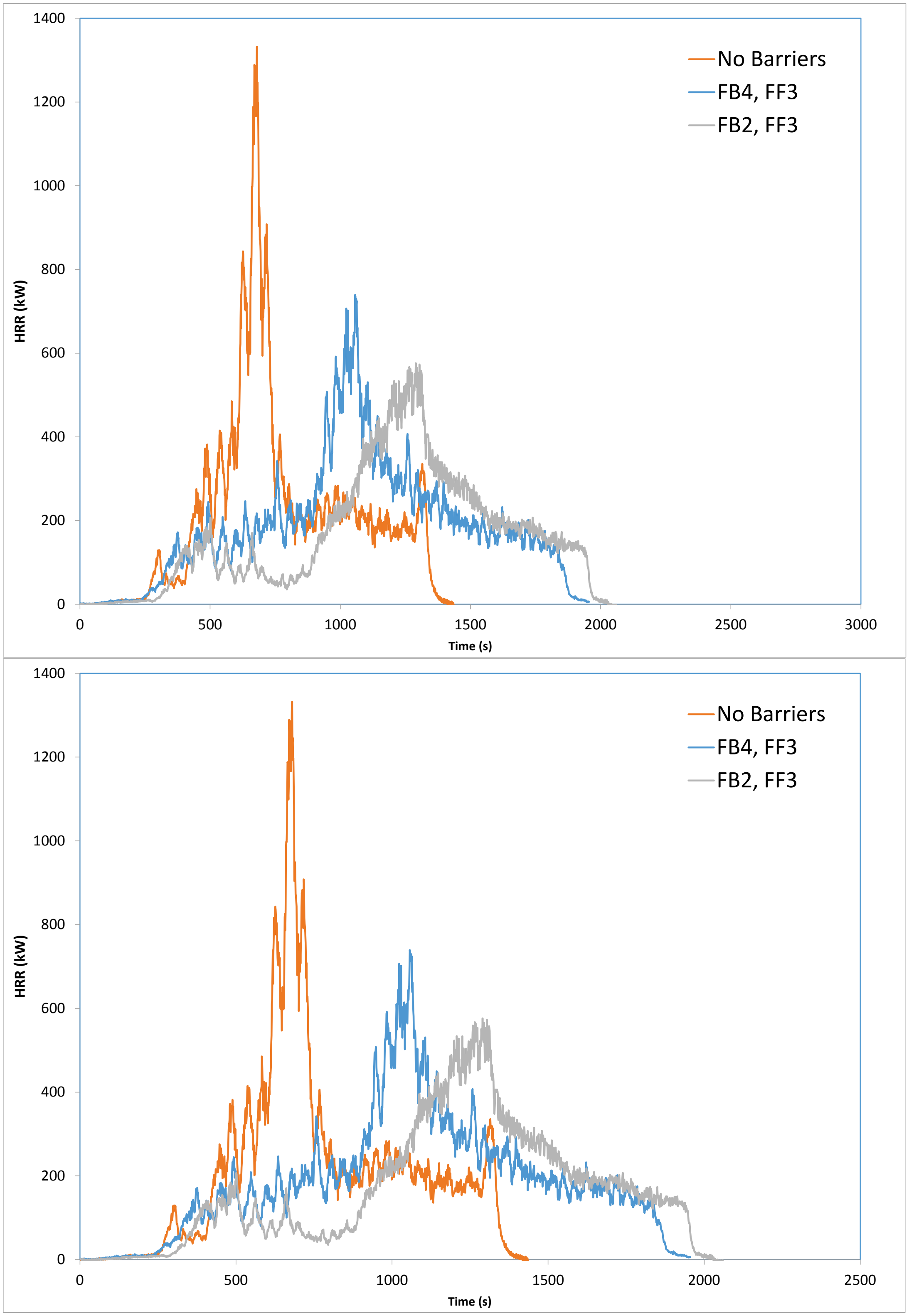

Figure 7. Example comparison of different fire barriers with back fill FF3 and cover fabric F2.

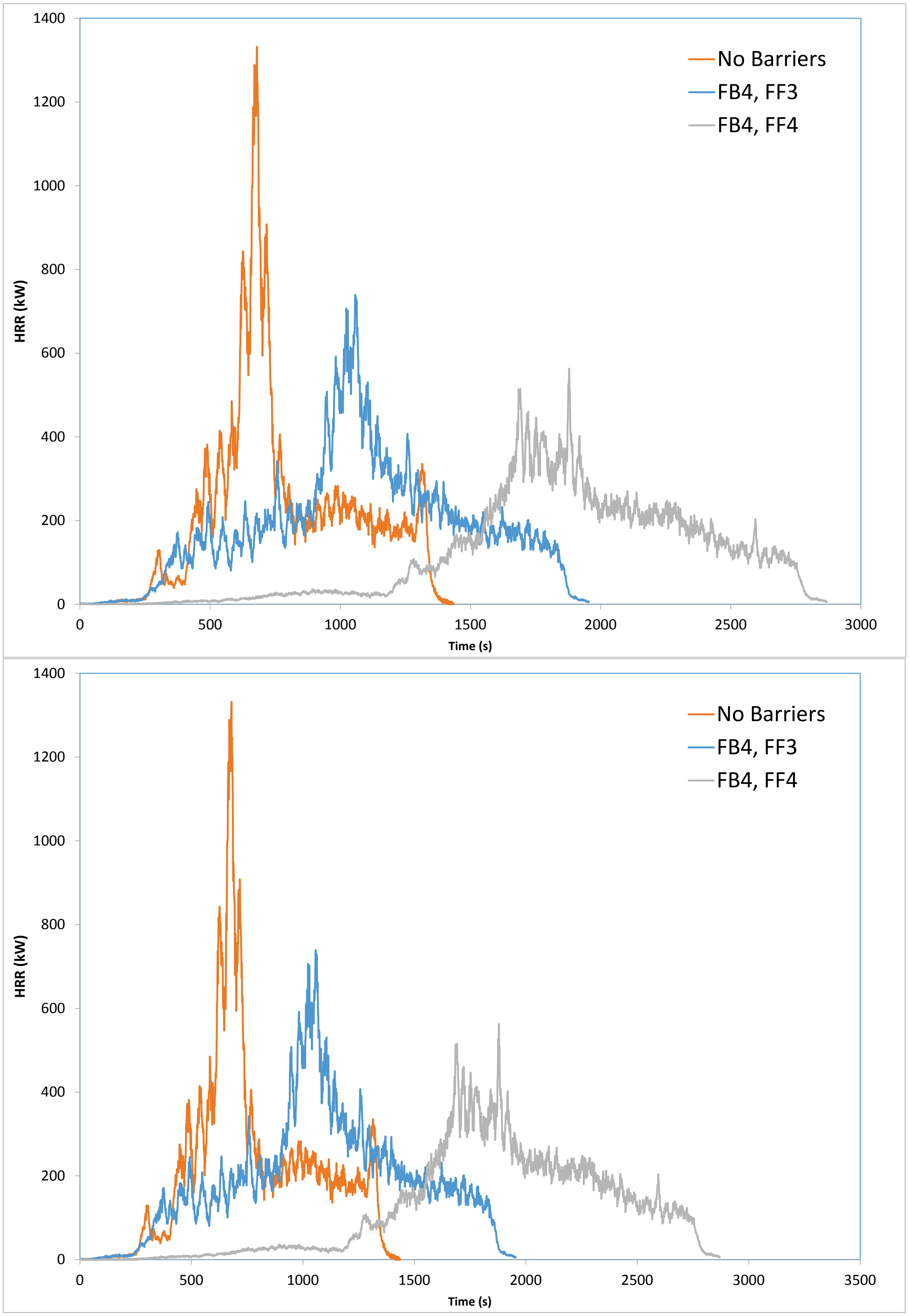

Figure 8. Example comparison of different back fills with fire barrier FB4 and cover fabric F2.

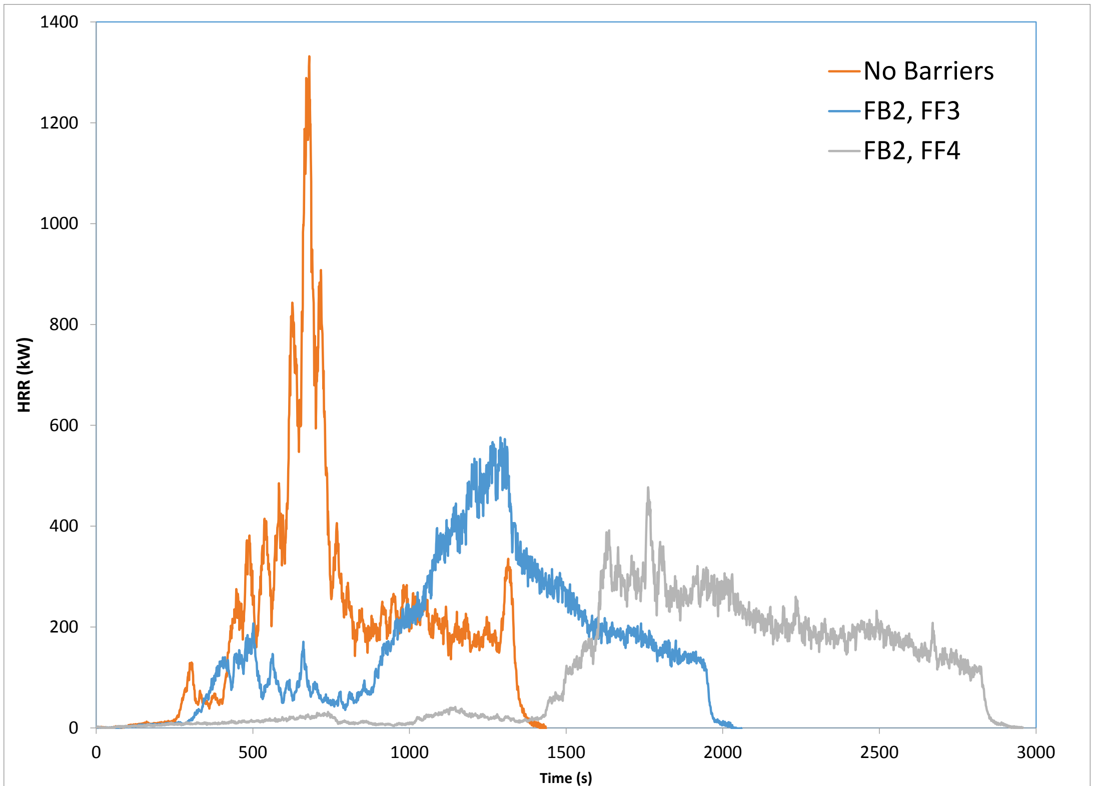

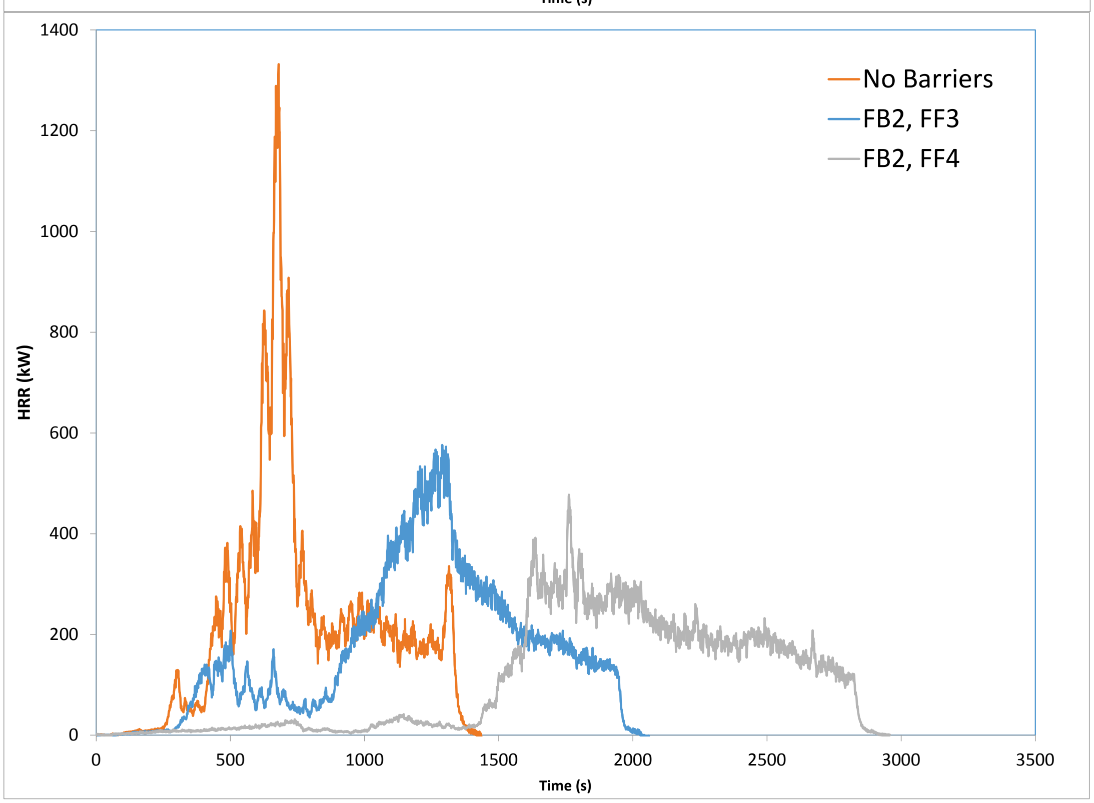

Figure 9. Example comparison of different back fills with fire barrier FB2 and cover fabric F2.

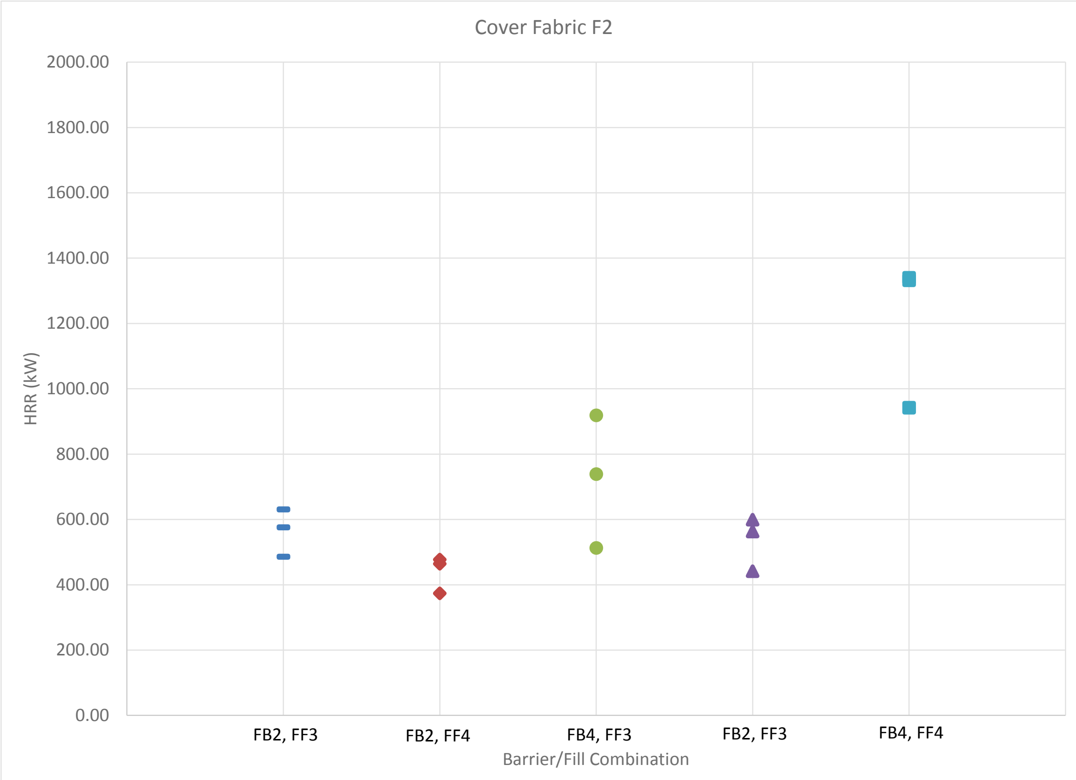

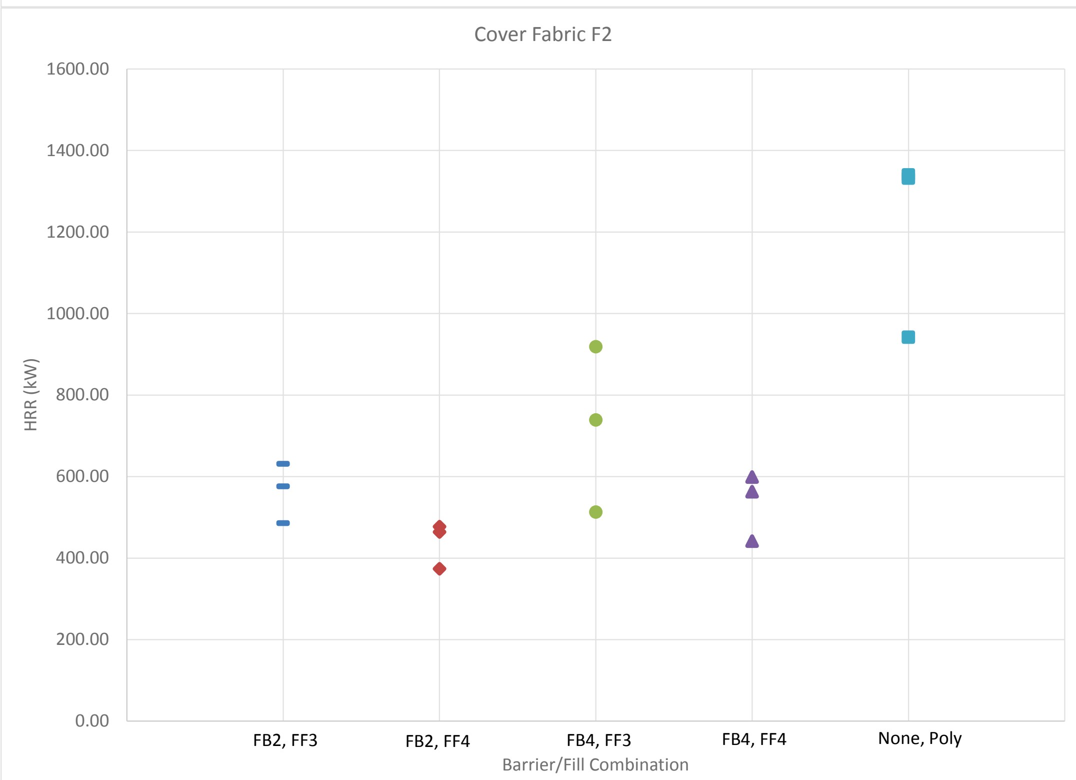

Figure 10. Peak HRR (PHRR) for all of the chairs using cover fabric F2.

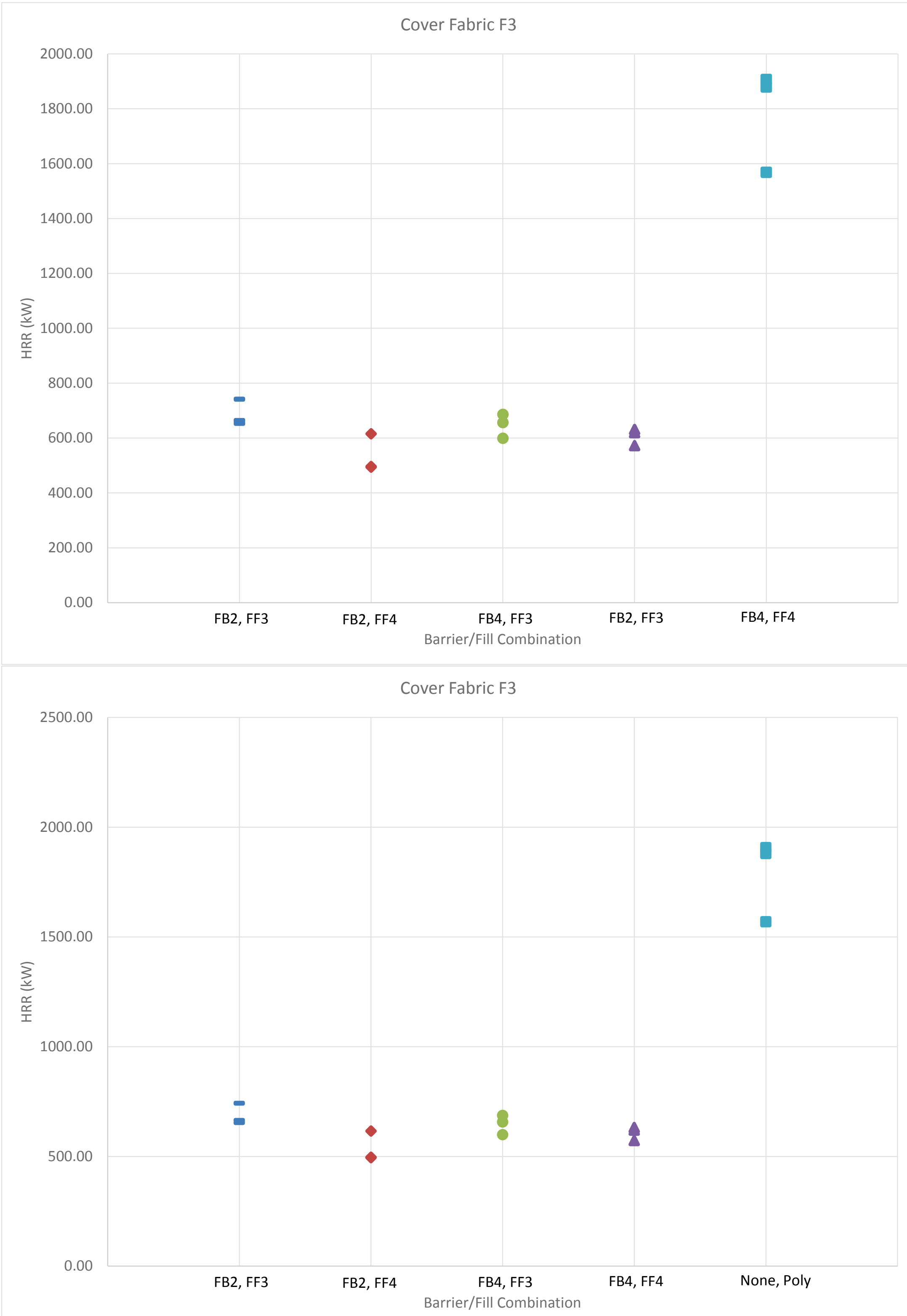

Figure 11. Peak HRR (PHRR) for all of the chairs using cover fabric F3.

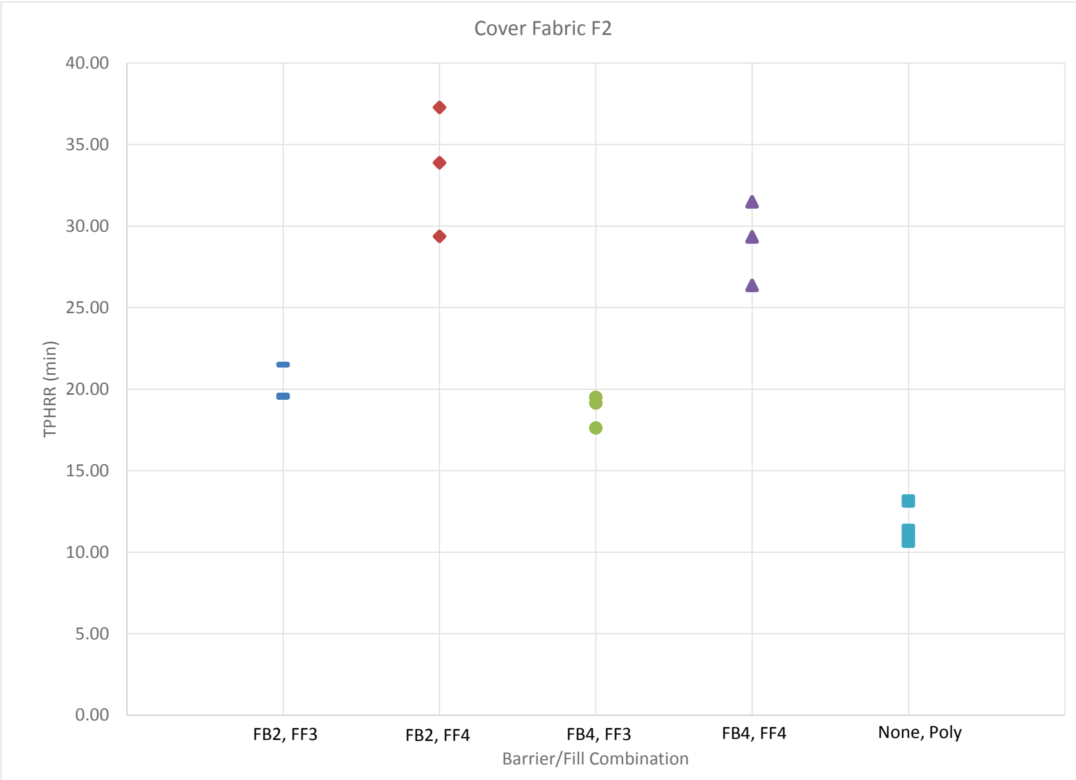

Figure 12. Time to Peak HRR (TTPHRR) for all of the chairs using cover fabric F2.

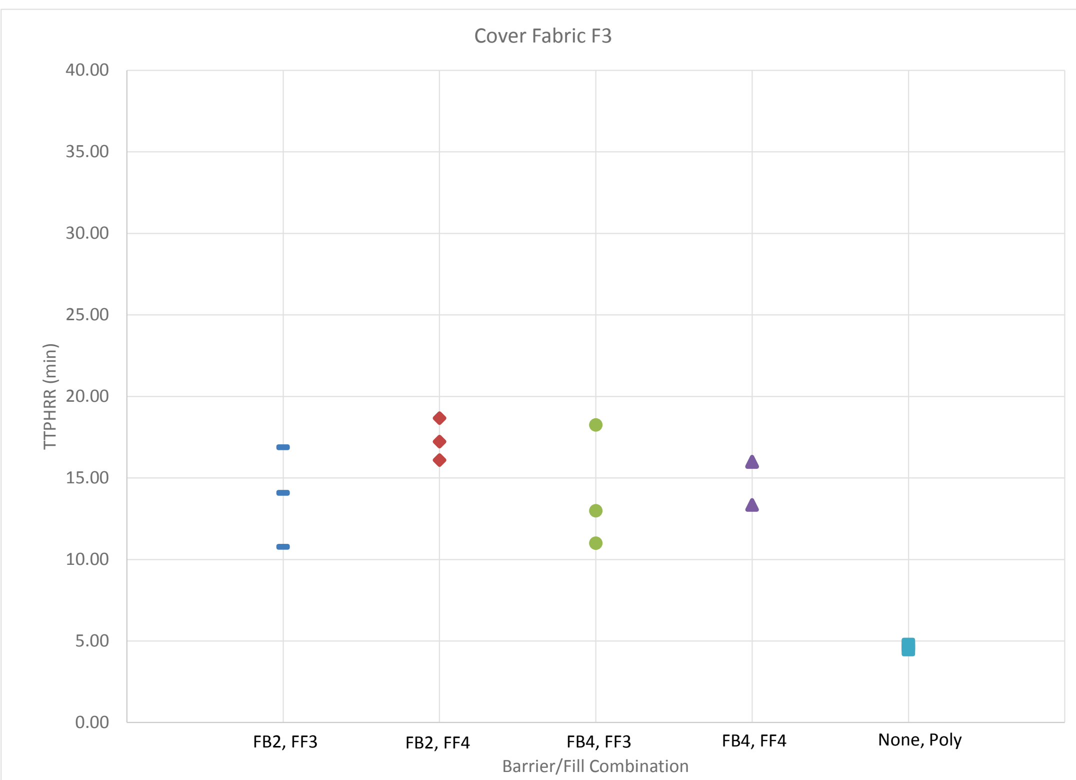

Figure 13. Time to Peak HRR (TTPHRR) for all of the chairs using cover fabric F3.

Additional Measurements

A few additional measurements were made in these tests to assist in future modeling efforts. These measurements included Heat Flux, Mass Loss, and soot measurements.

Observations

In addition to recording the HRR of the burning chairs, visual observations during testing identified qualitative differences in the burning behaviors of the chair samples. For those chairs where the fire barrier and modified loose fill offered some protection to the filling, the flames were typically smaller and less intense. For chairs with no barrier, or with less-protective barriers, the flame spread was similar on all the chairs ignited by open flame, but this progression generally took a longer time for chairs with barriers than without. The general pattern for flame spread was as follows: When the ignition flame was removed, there were flames on the seat and back cushions. Initially, the flame spread was up the back cushion and toward the corners of the seating area. Because there was no sheet barrier over the loose fill, the fire generally penetrated the cover fabric relatively quickly and began to burn the loose fill. Next, flames either reached the top of the back cushion or went around the side of the back cushion between the back cushion and the back of the chair. The flame front on the seat cushion moved outward as well. The flames increased in intensity and size and continued to burn as the back, loose fill, cushion and back of the chair became more involved in the combustion process. The back cushion burnt through first, followed by the back of the chair, which led to rapid progression with the entire chair soon engulfed in flames. As the seating area became more involved, melt dripping occurred below the chair.

Conclusion

A limited series of open-flame ignition tests was conducted at the CPSC flammability laboratory on full-scale upholstered chairs to evaluate the flammability performance when components with enhanced flammability properties, such as barriers, and modified loose fill materials, are used. The test series expanded on a previous test series, where five fire barriers were used in the construction of some upholstered chairs with foam backs. A total of 30 chairs were tested. In general, it was observed that the barriers used in this study reduced the severity of the fires and delayed the most intense burning, although to different degrees, depending on the specific barrier type. All of the chair combinations in this study burned. Generally, the cover fabric and the loose fill affected the burning behavior of the chairs. Cover fabric, F2 fire development was generally slower with slightly lower peaks, while F3 was faster with slightly higher peaks.

From the attached statistical analysis:

> Both seat cushion fire barriers tested for this study were effective at reducing the peak heat release rate (PHRR) and the time to peak heat release (time to peak) of burning chairs. The observed differences were statistically significant. Additionally, both chairs with backs made of modified loose fill materials were effective at reducing the PHRR and increasing the time to peak for burning chairs. The observed differences were statistically significant. The barriers (both seat cushion fire barriers and both chair back loose fill) each are estimated to reduce the peak heat release rate of burning chairs by more than 1,000 kilowatts. Each barrier is estimated to delay the time to peak heat release of burning chairs by at least several minutes. One of the fabrics tested was better than the other in terms of both PHRR and time to peak and the observed difference was statistically significant.

Improvements to the flammability performance of the chairs were observed with the modified materials. However, this was a limited analysis. Further study is needed to determine the costs and feasibility of this approach, and what, if any, reductions in fire losses could be achieved.

Future Work

The scope of this work was fairly limited because it looked at one chair design with a convenience sample of barriers and fills, which were not designed for upholstered furniture. The upholstered furniture market is large, with differences in design, decorative features, components, constructions, and sizes, which together present a further complication in assessing the performance needed from a fire barrier and/or modified loose fill used with upholstered furniture to address the hazard.

This preliminary study looking at several fire barriers in chair constructions showed promise for improving the flammability performance of upholstered furniture exposed to an open flame ignition source. Staff plans to continue having technical interactions with the fire safety and furniture industries so that the best performing fire safety technologies can be identified. Staff is considering additional fire barrier and loose fill upholstered furniture testing to evaluate the performance of additional materials, different furniture geometries, and different ignition scenarios.

Related Memoranda

---

[1] Memorandum to Dale R. Ray, Project Manager, Upholstered Furniture Project, from S. Mehta, Engineering Sciences, "Upholstered Furniture Full Scale Chair Tests-Open Flame Ignition Results and Analysis", May 2012.

[2] Memorandum to Andrew Lock, Project Manager, Upholstered Furniture Project, from L. Fansler and Andrew Lock, "Summary Report of Open Flame and Smoldering Tests on Chairs", January 2016.

[3] Email from David Miller, CPSC, Directorate for Epidemiology, "Full-Scale Testing Plan", June, 2013.

[4] Memorandum to Dale Ray, Project Manager, Upholstered Furniture Project, from L. Fansler, Laboratory Sciences, "Summary of Data Collected During Smoldering Chair Tests", July 2012.

[5] BS-5852, Methods of Test for Assessment of the Ignitability of Upholstered Seating by Smouldering and Flaming Ignition Sources. 1990.

Appendix A

Test Protocol – Full-Scale Chair Evaluations

Test Facilities and Instrumentation Setup

This section contains the necessary information to construct the testing environment; *i.e*., type and location of instrumentation and room design. During testing, the PIs can change the test setup conditions; however, it is the initial assumption that the information contained in this section will not be a variable in this testing study. Tests were conducted in the open calorimetry lab located in room 123A at the CPSC National Product Testing and Evaluation Center (NPTEC), instrumented as detailed in this section.

- The burn room conditions will be maintained between 15 and 27°C, with a relative humidity less than 75 percent. To achieve these conditions in the burn room, there may be a delay in starting the next test while the room recovers after it has been exhausted of smoke and heat from the prior test.
- The hood flow rate will initially be set at a minimum of 1500 CFM and adjusted as necessary to accommodate smoke and fire development.
- Heat flux gauges will be placed near the chair. Exact placement will be determined on the first day of testing.
- Heat Release Rate (HRR) will be measured by oxygen consumption calorimetry.
- Two video cameras will be used to record each test. The cameras will be placed so the front of the chair is captured by one, and the right side of the chair is captured by the other.
- One thermal imaging camera will be used, as needed, to evaluate the progress of the fire.
- The ignition source and fuel are the same as a BS5852 source 3, which is a butane flame, 270 mm in length.
- The chair will be placed in the center of the 10 ft x 10 ft canopy hood.

Sample Preparation

The upholstered chair specimens, sheeting squares, and cigarettes are required to be conditioned at a temperature of 20 ± 3°C (70° + 5°F) and a relative humidity of 50% ± 5% for 48 hours. The test will start within 10 minutes of removing the specimens from the conditioning area.
The upholstered chair samples will be removed from any packaging before conditioning.

Test Procedure

The details of the testing protocol include the following factors:

- Ignition sequence (smoldering and open flame ignition)
- Testing sequence
- Duration and termination parameters
- Data collection specifics, such as beginning and ending measurements, and sampling frequency

Data Collection

The data collected will include:

- Heat release rate vs. time. Within this measurement is data collection for CO, CO2 and O2 in the fire effluent.
- Heat flux meter data.
- Mass loss.

- Peak heat release rate.
- Time to peak heat release.
- Total energy release, as needed.

Test Setup

Open-flame ignition testing of upholstered furniture was conducted under the open calorimetry hood, instrumented as follows:

- Heat flux facing the chair back, front and sides;
- Heat release rate;
- Mass loss;
- At least two video cameras;
- At least one thermal imaging camera.

Test Protocol

Note: Have a means for extinguishing the sample. The exact chemical content of the FR foams is not known, so prepare appropriately.

1. Pretest–
    - Record the initial total mass of the sample.
    - Place sample chair in the center under the 10 ft x 10 ft canopy hood.
    - Ensure Test ID is visible on placard and within the viewing frame of the video cameras.
    - Ensure LED timer is visible and within the viewing frame of the video cameras
    - Record temperature and RH% inside the test room.
    - Clear all personnel from under the hood.
    - Turn on data acquisition system (including all sensors). Ensure appropriate readings. Begin background measurements.
    - The data should be taken in 1-second intervals.
    - Start all video and IR cameras. Ensure that chair and LED timer are clearly visible and not cropped in any camera.
    - Photograph the sample in place.
2. Ignition: Choose either open-flame or smoldering-ignition source, according to test plan.
    - Open-Flame Ignition: Lighting the igniter flame–
        i. Away from the chair, open the butane tank slowly, and light the end of the burner tube. Adjust the gas flow to the appropriate rate to achieve a 240 mm flame. Allow the flame to stabilize for at least 2 minutes.
        ii. Apply the flame for 70 ± 1 second at the center of seat/back crevice of the sample, using the bent burner tube; then immediately remove ignition source from the sample.
        iii. This is the test "Start Time." For open-flame ignition, note in data acquisition system, and start large LED timer upon removal of the ignition flame.
    - Smoldering Ignition: Placing cigarettes
        i. Light cigarettes so that no more than 4 mm (0.16 inch) is burned away,
        ii. Place one cigarette in each test location.
        iii. Immediately after placement of the lit cigarette, cover cigarettes with a cotton sheeting square, and run one finger over the sheet along the length of the covered

cigarette to ensure good contact between the sheeting square and the burning cigarette.

iv. "Start Time." For smoldering ignition, begin as soon as the last cigarette has been placed. Note in data acquisition system and start large LED timer.

3. Performing the test–
    - Make observations and notes throughout the test.
    - Periodically check on measurement readings.
    - Once Peak HRR has been observed, the operator will decide how much longer to continue test. Also, there may be multiple peaks in HRR; the PI will determine the length of test (Note: If the instantaneous HRR of a sample under test is high and the fire is observed to be growing, the test may be terminated for safety reasons.)
    - Observe the sample combustion behavior for X minutes after a Peak HRR has been reached. (Note: If the instantaneous HRR of a sample under test is X, and the fire is observed to be growing, the test may be terminated for safety reasons. This is to be determined by the PIs and safety officer.)
1. Post-Test–
    - Stop all measurements and video cameras.
    - Collect "drift measurements."

Appendix B
HRR Plots for Open-Flame Tests

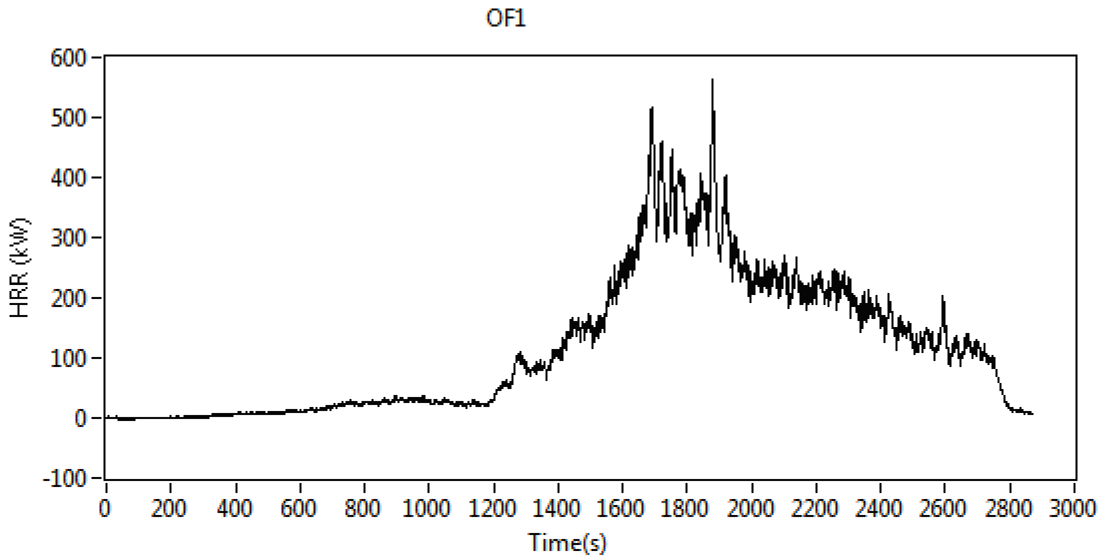

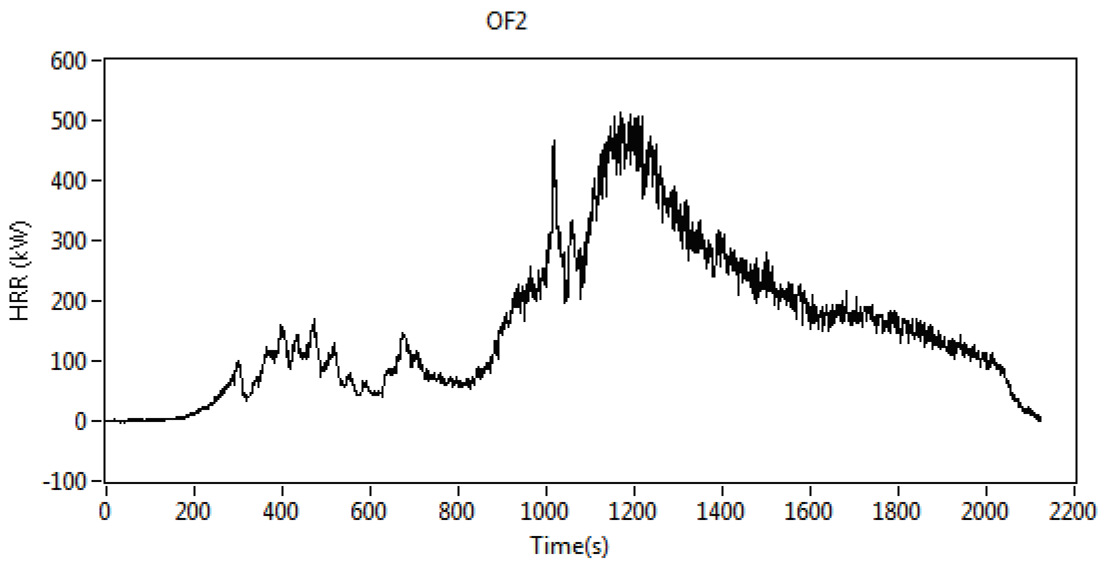

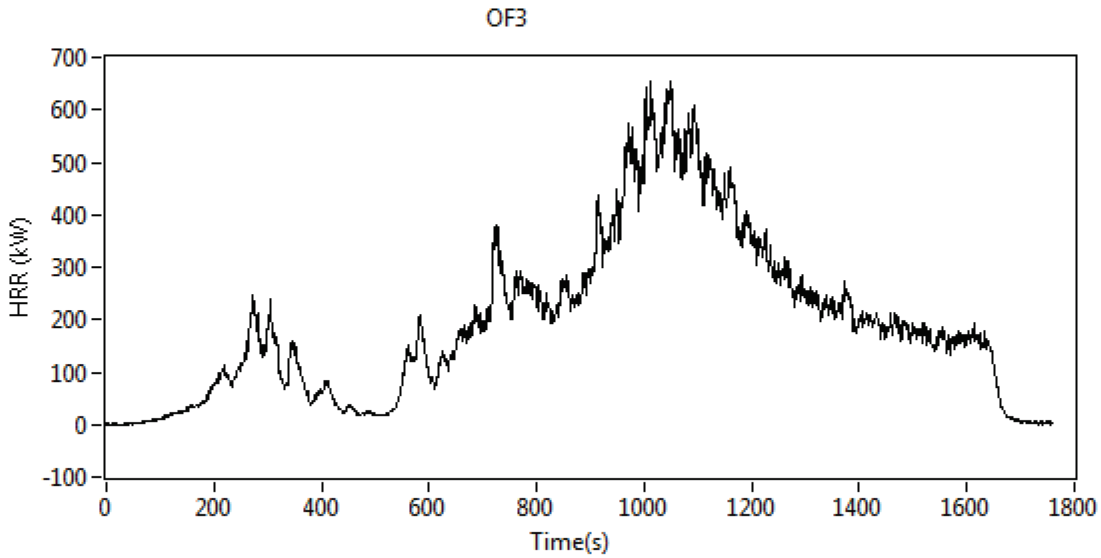
OF3
HRR (kW)
Time(s)

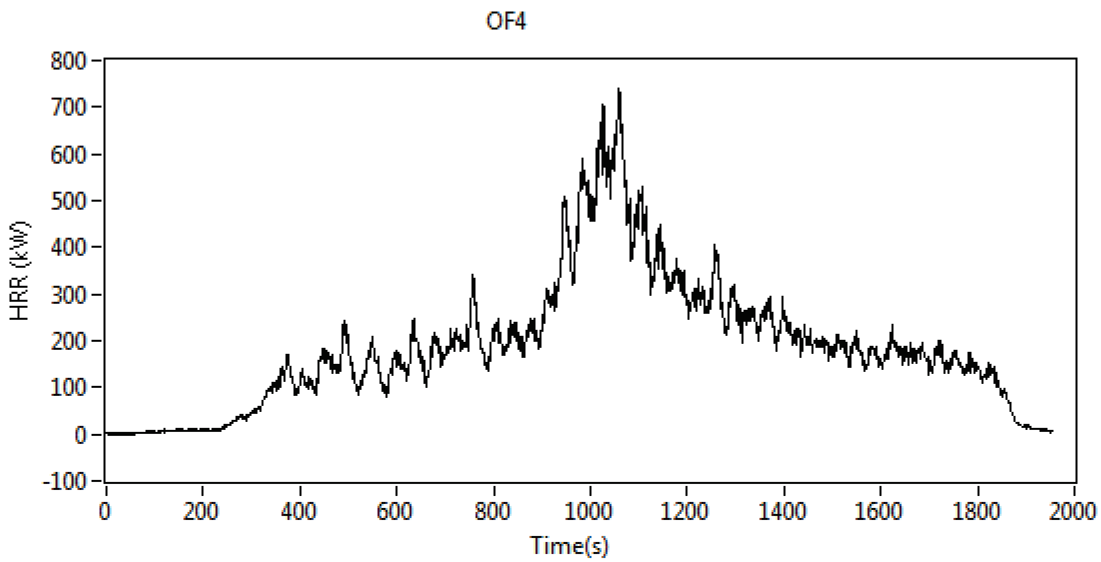
OF4
HRR (kW)
Time(s)

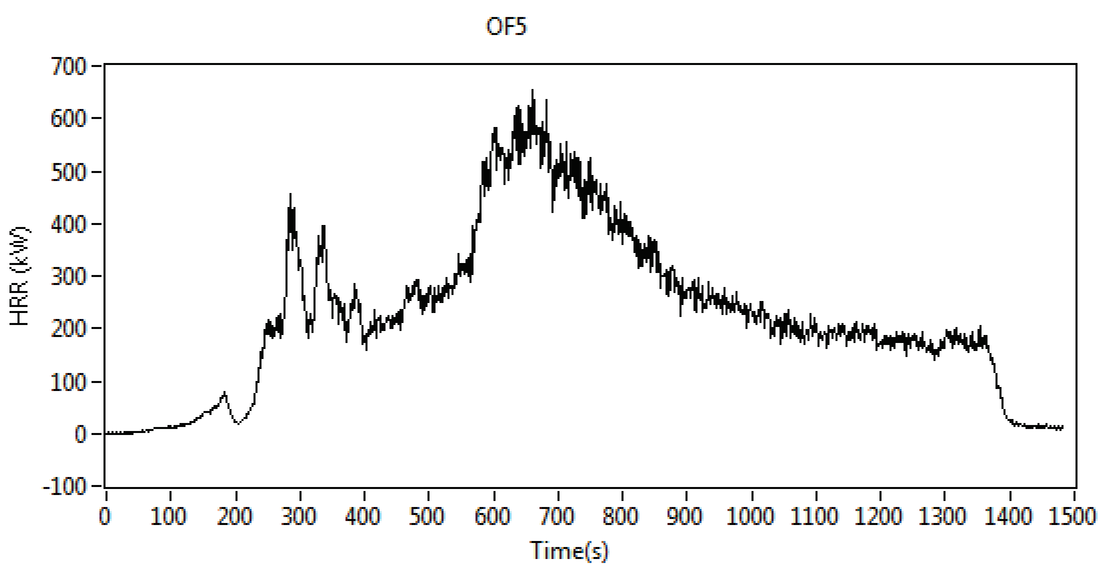
OF5
HRR (kW)
Time(s)

OF6

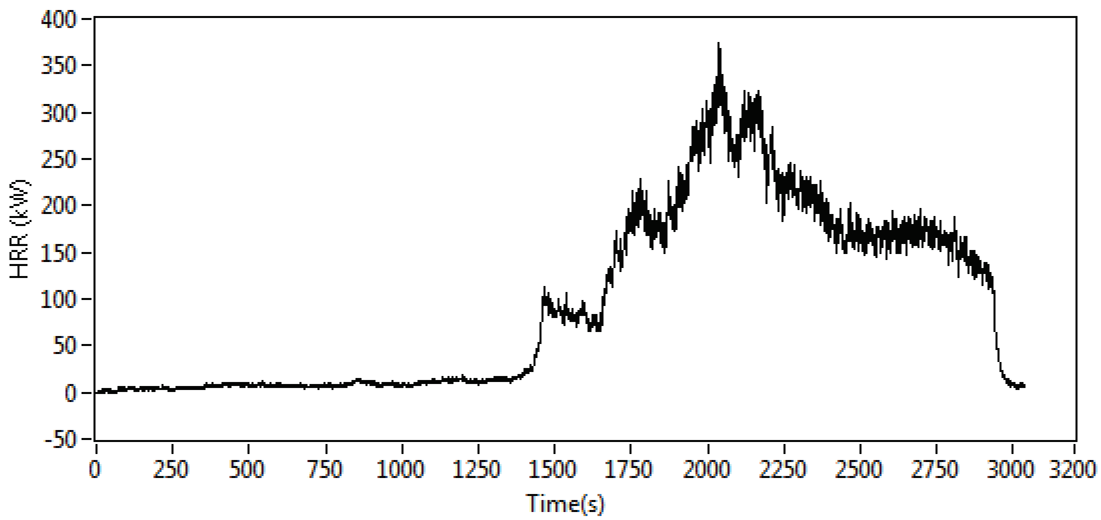

HRR (kW)
400
350
300
250
200
150
100
50
0
-50
0
250
500
750
1000
1250
1500
1750
2000
2250
2500
2750
3000
3200
Time(s)

OF7

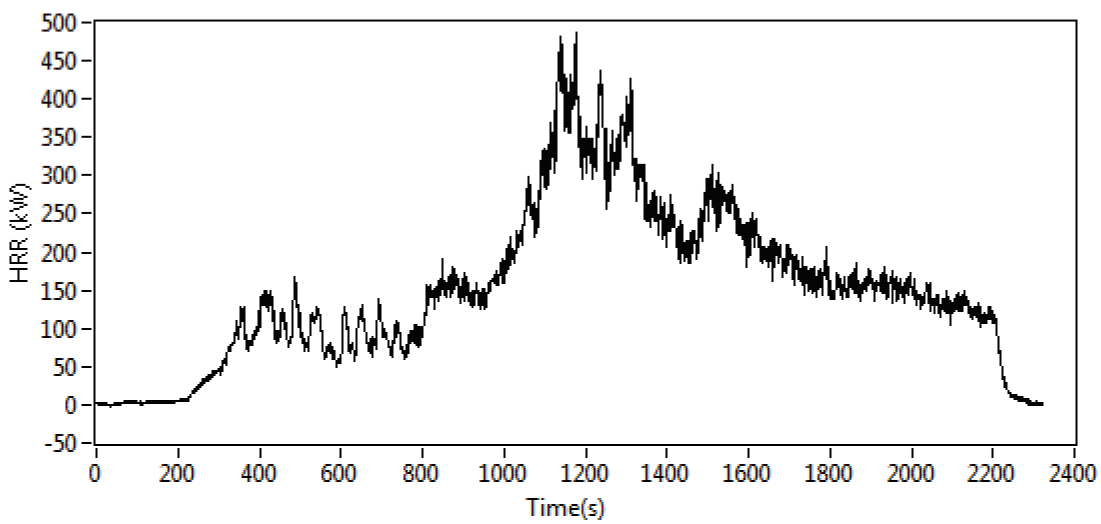

HRR (kW)
500
450
400
350
300
250
200
150
100
50
0
-50
0
200
400
600
800
1000
1200
1400
1600
1800
2000
2200
2400
Time(s)

OF8

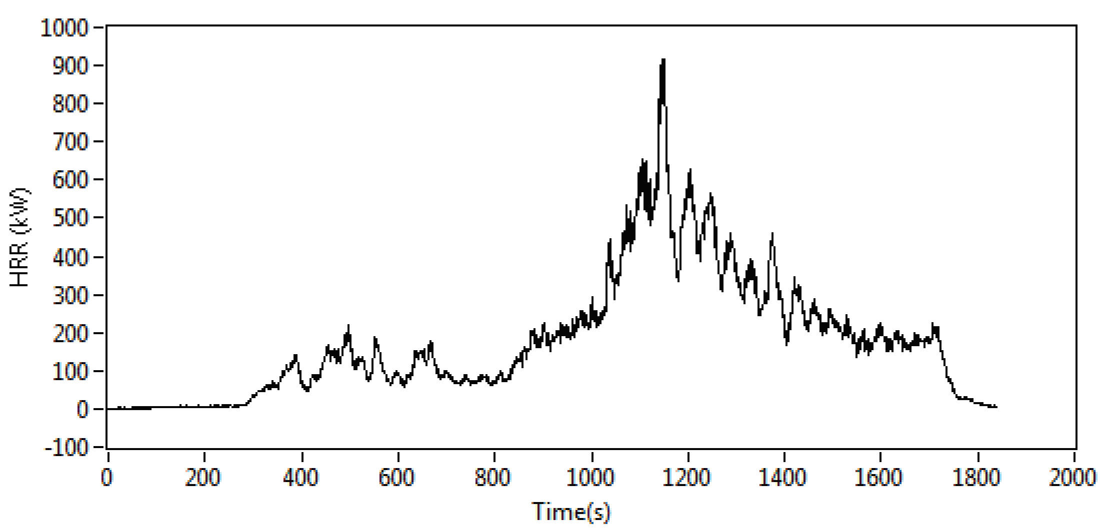

HRR (kW)
1000
900
800
700
600
500
400
300
200
100
0
-100
0
200
400
600
800
1000
1200
1400
1600
1800
2000
Time(s)

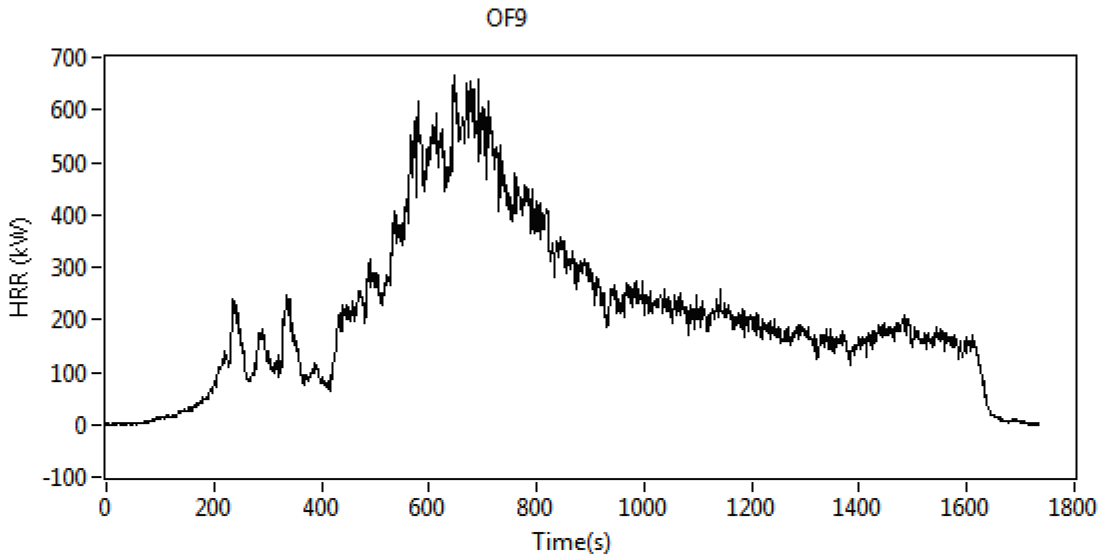
OF9
HRR (kW)
Time(s)

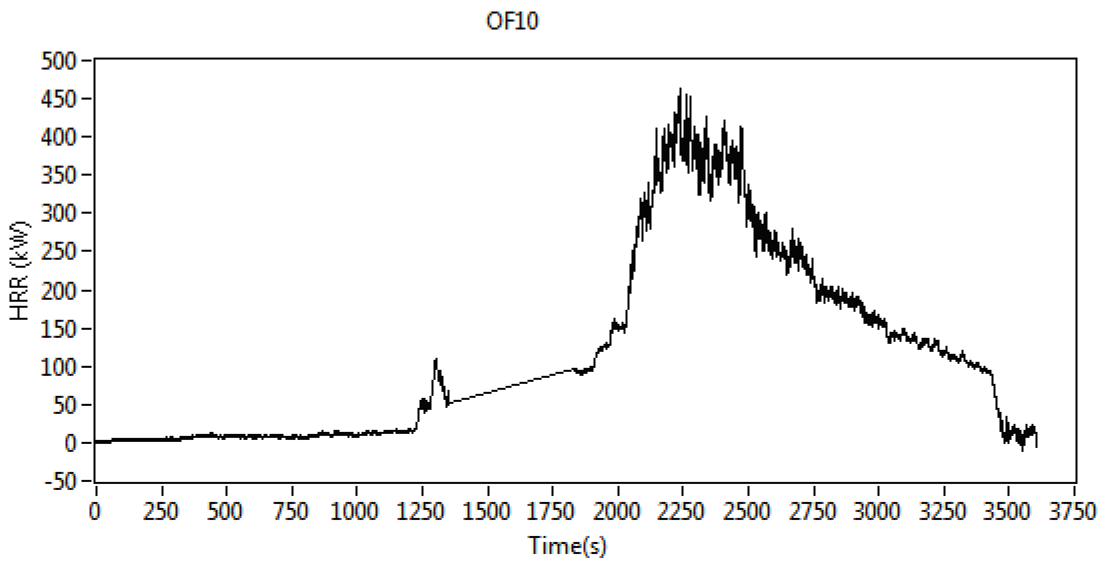
OF10
HRR (kW)
Time(s)

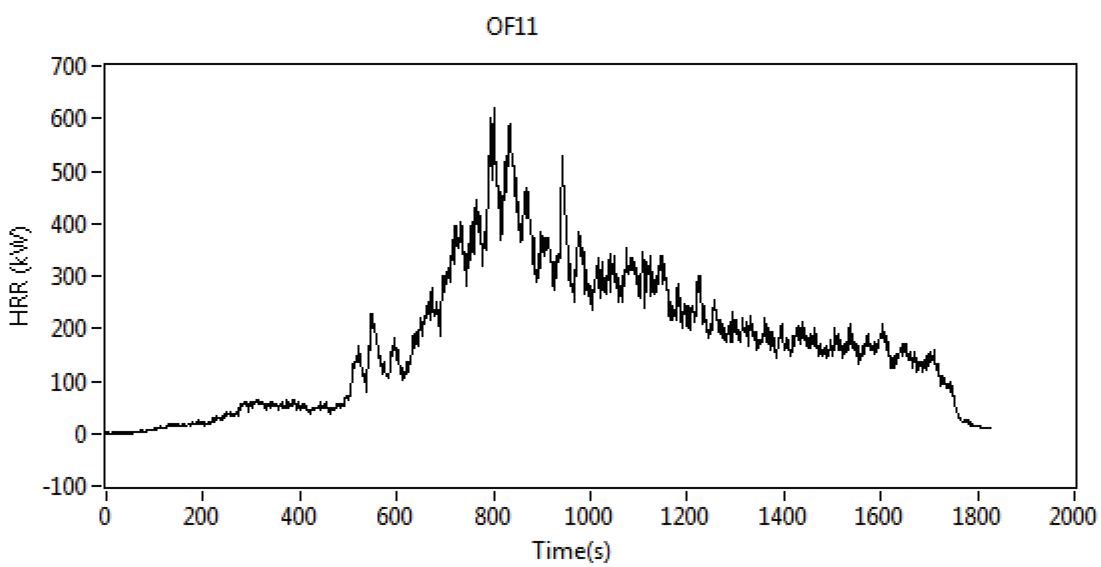
OF11
HRR (kW)
Time(s)

OF12

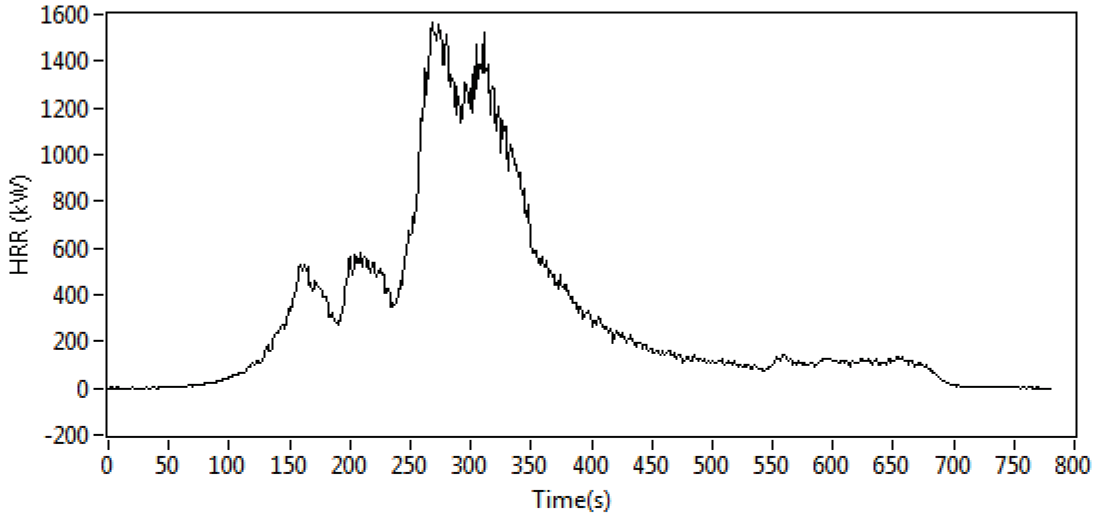

OF13

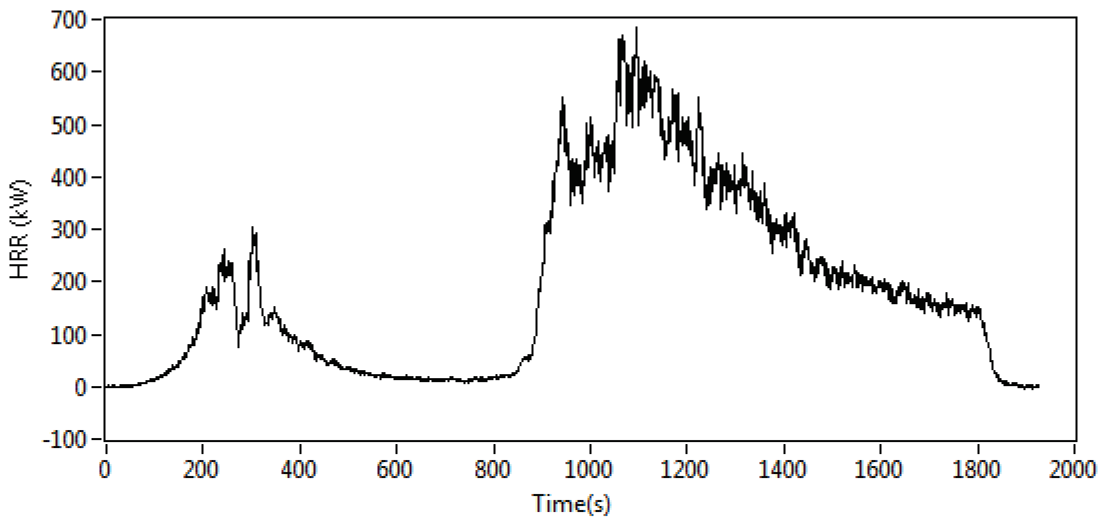

Of14

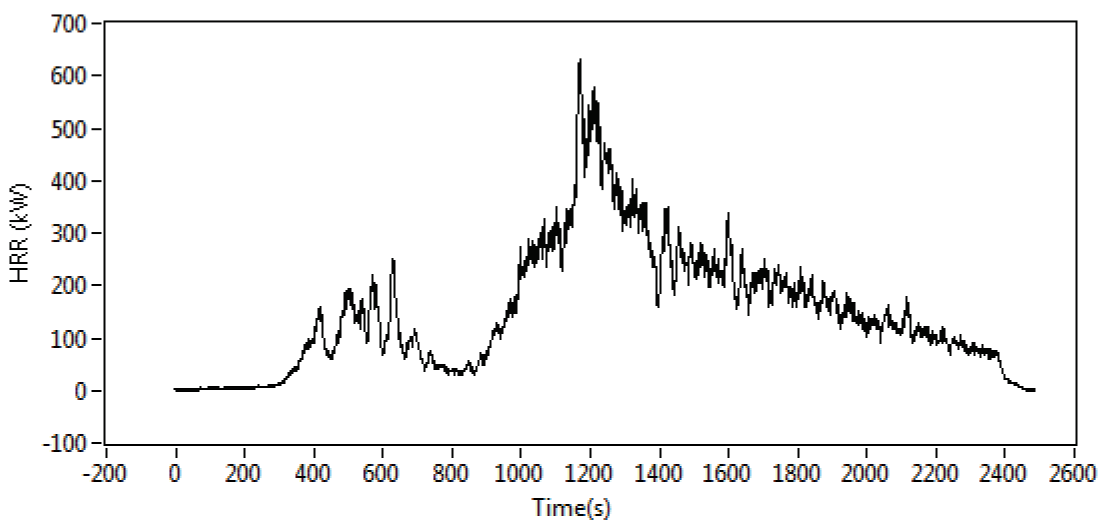

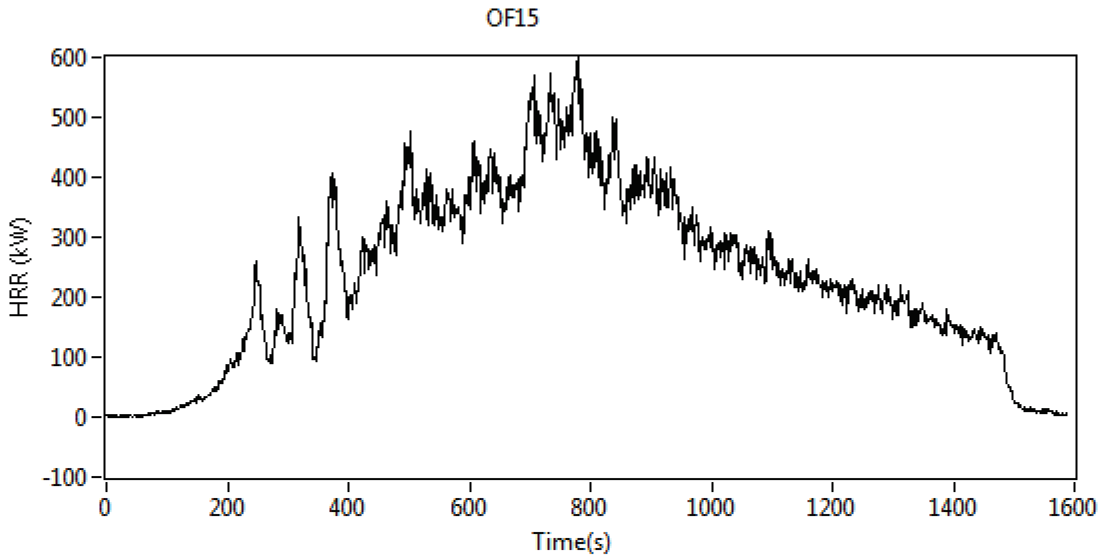
OF15
600
500
400
300
200
100
0
-100
HRR (kW)
0 200 400 600 800 1000 1200 1400 1600
Time(s)

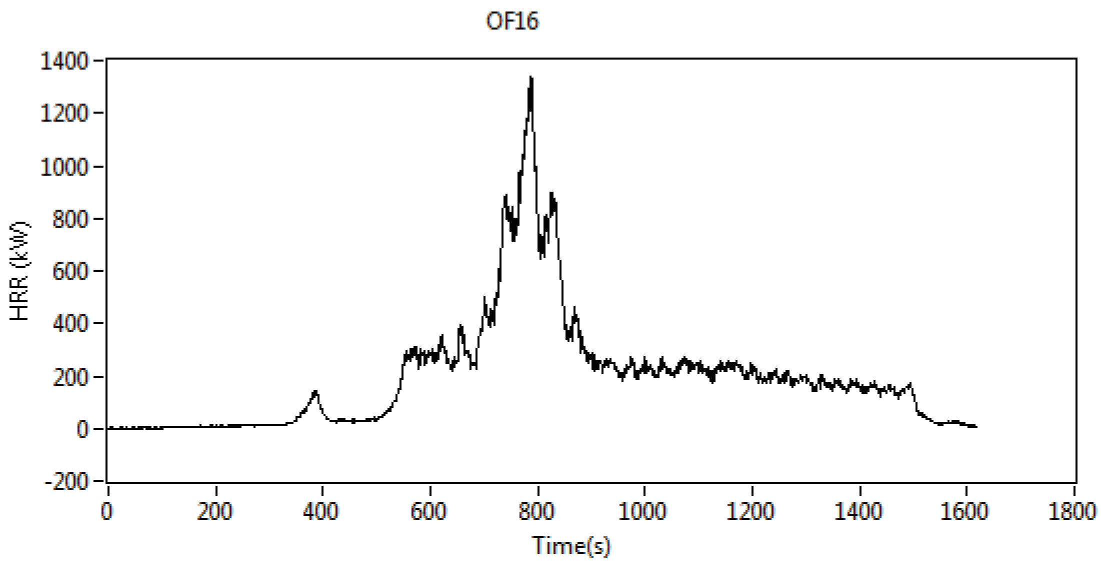
OF16
1400
1200
1000
800
600
400
200
0
-200
HRR (kW)
0 200 400 600 800 1000 1200 1400 1600 1800
Time(s)

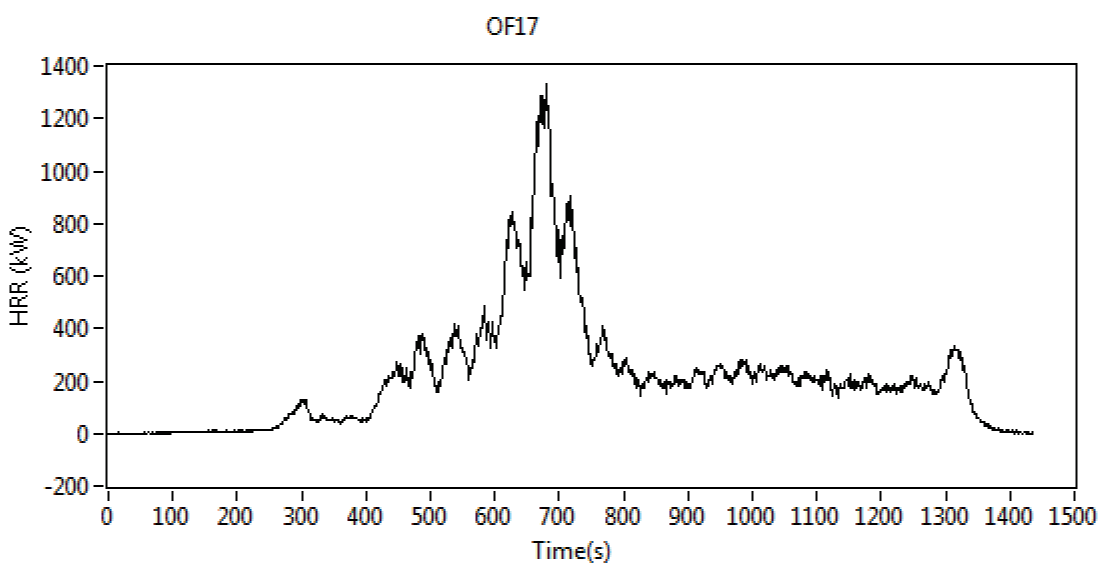
OF17
1400
1200
1000
800
600
400
200
0
-200
HRR (kW)
0 100 200 300 400 500 600 700 800 900 1000 1100 1200 1300 1400 1500
Time(s)

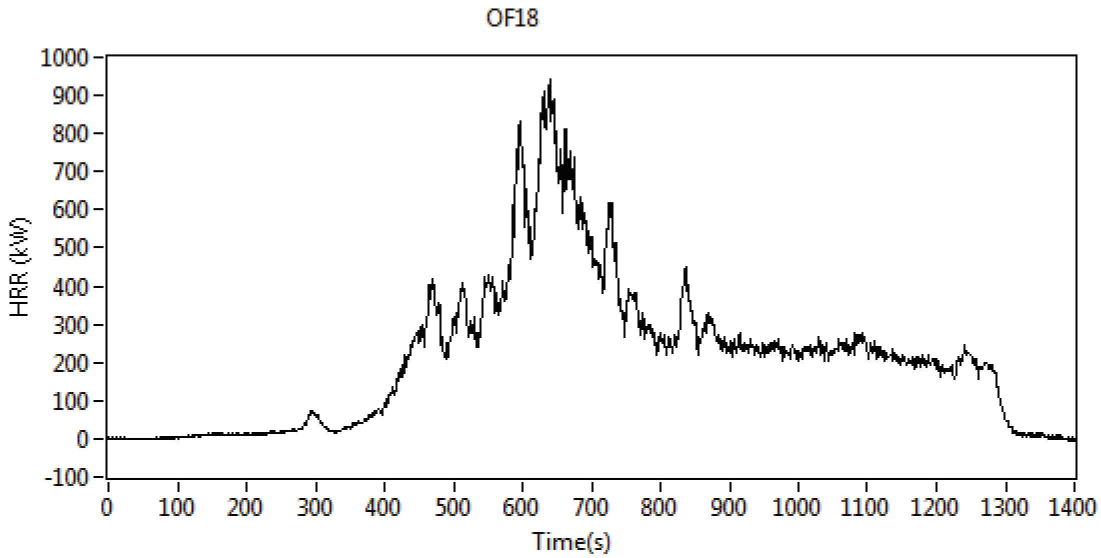
OF18
HRR (kW)
Time(s)

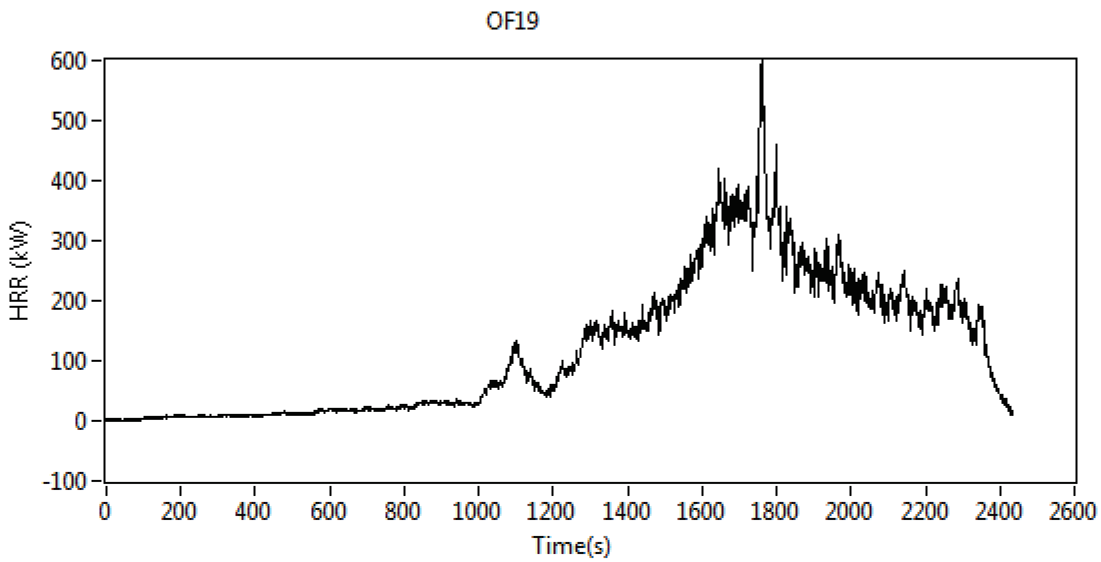
OF19
HRR (kW)
Time(s)

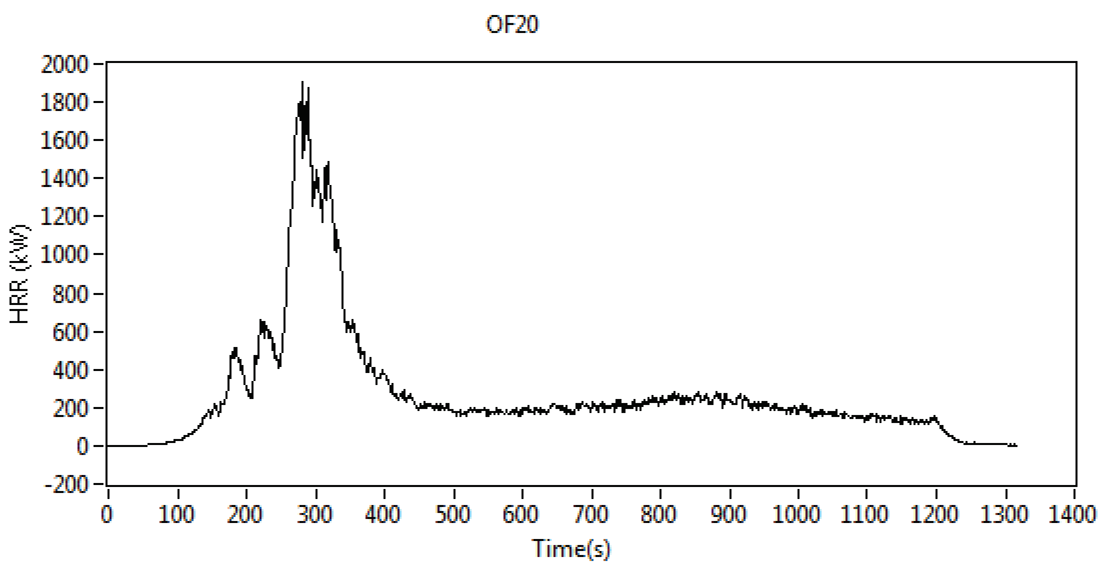
OF20
HRR (kW)
Time(s)

OF21

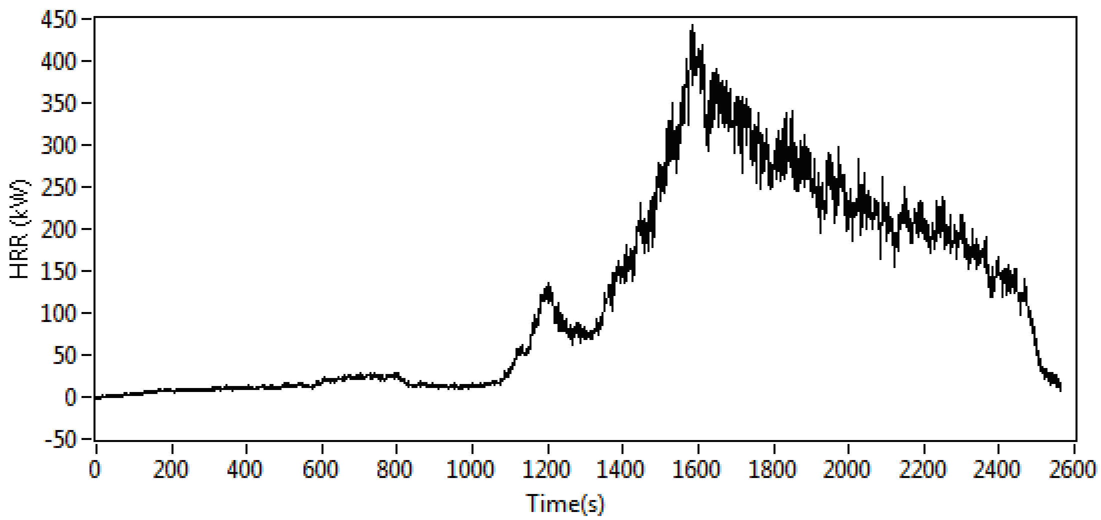

OF22

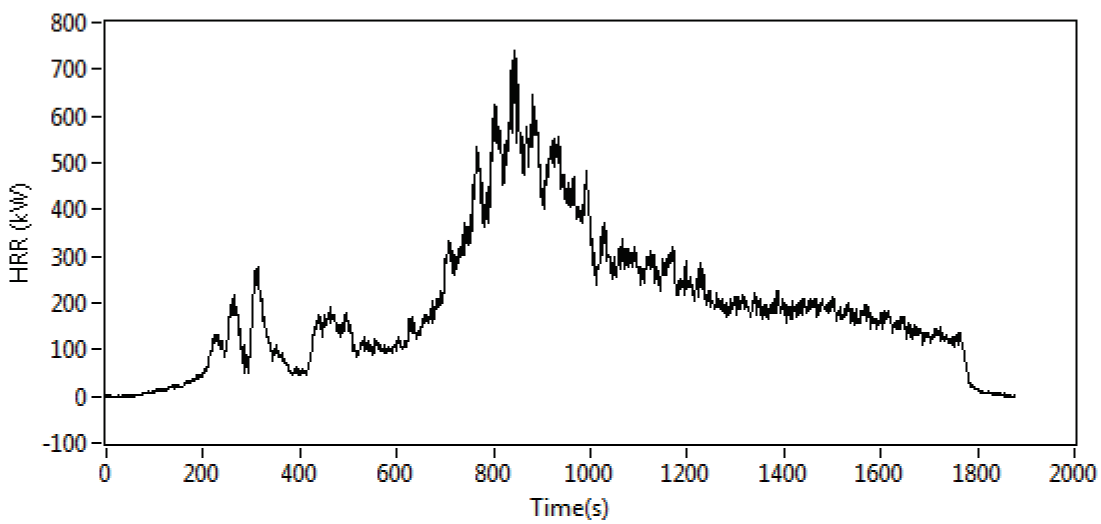

OF23

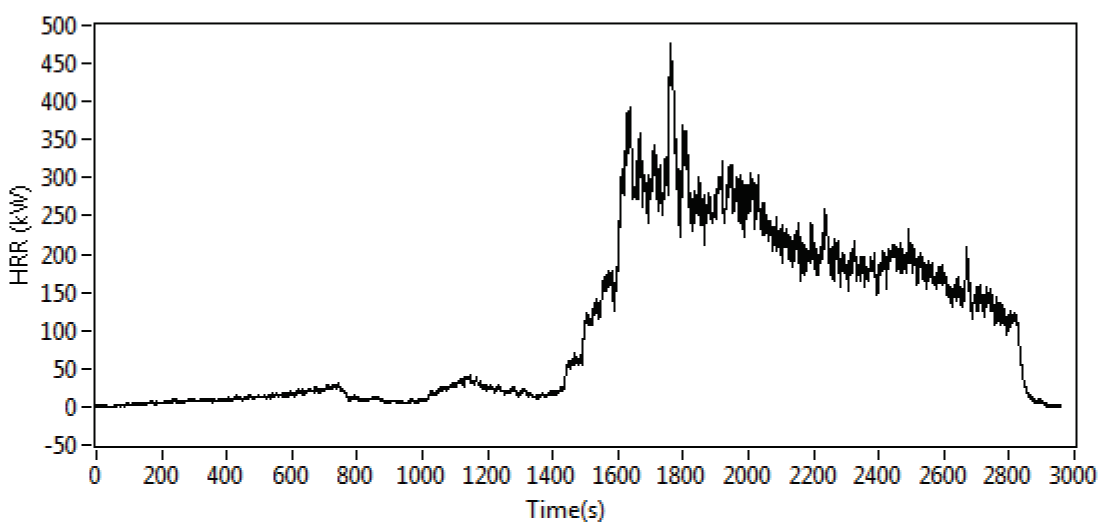

OF24

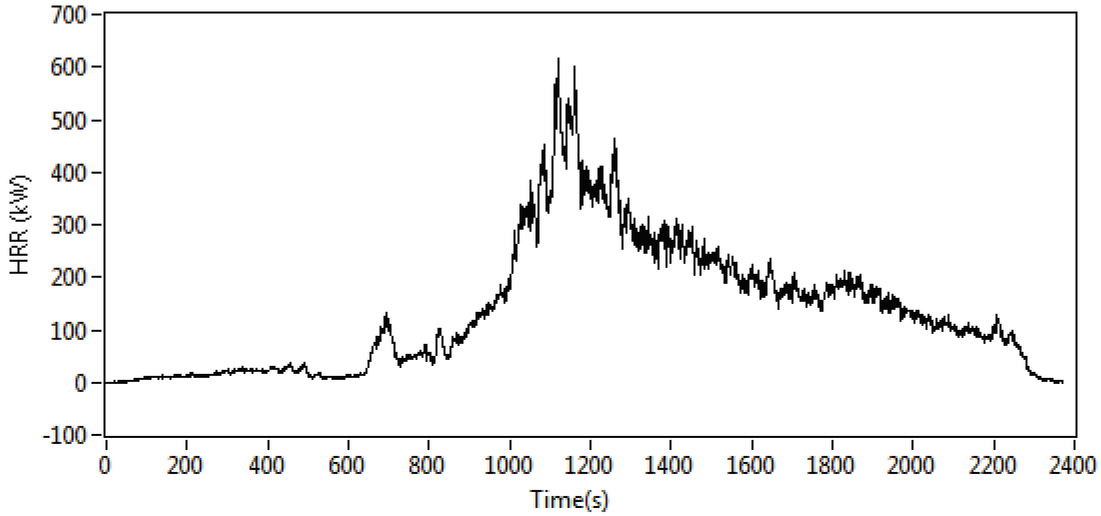

OF25

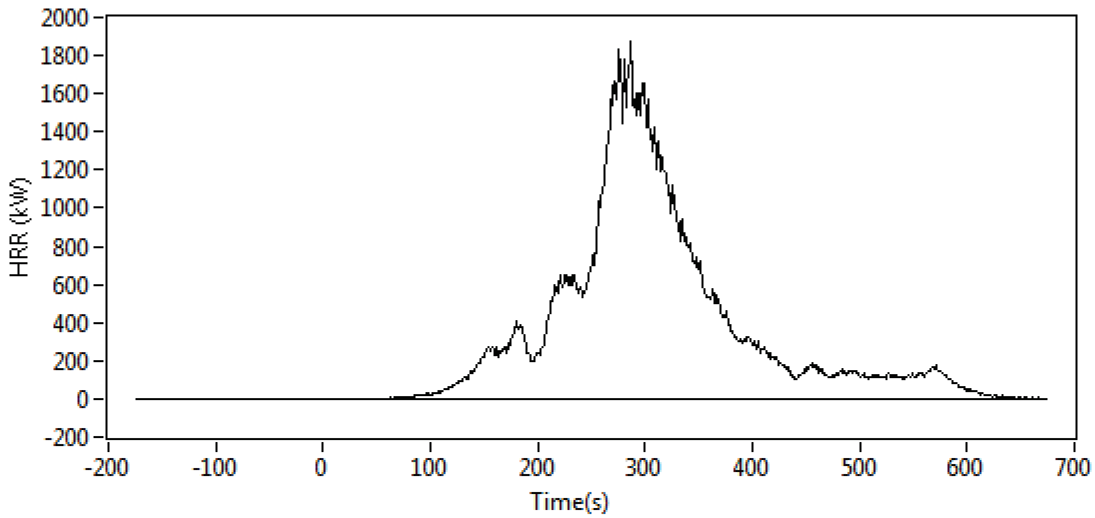

OF26

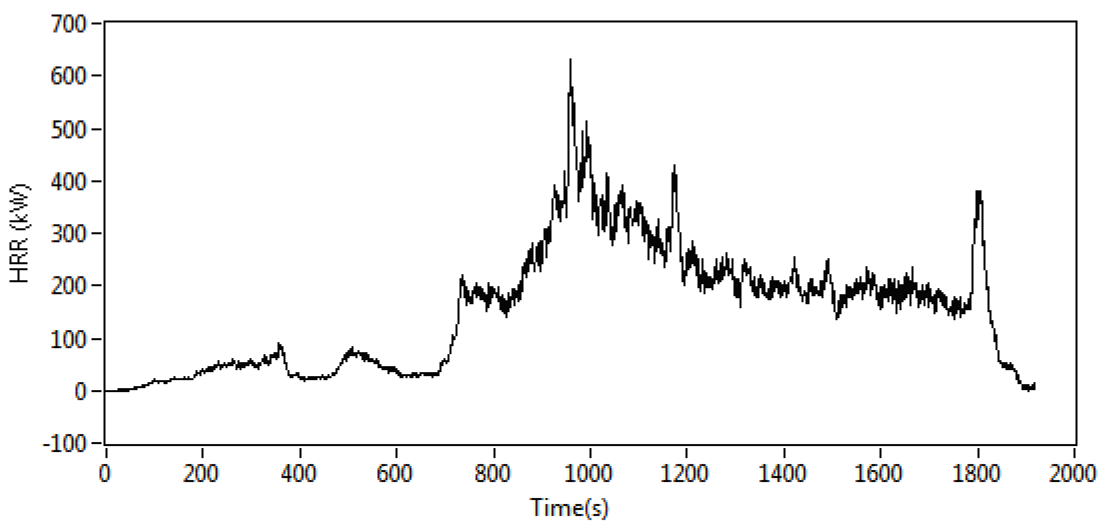

OF27

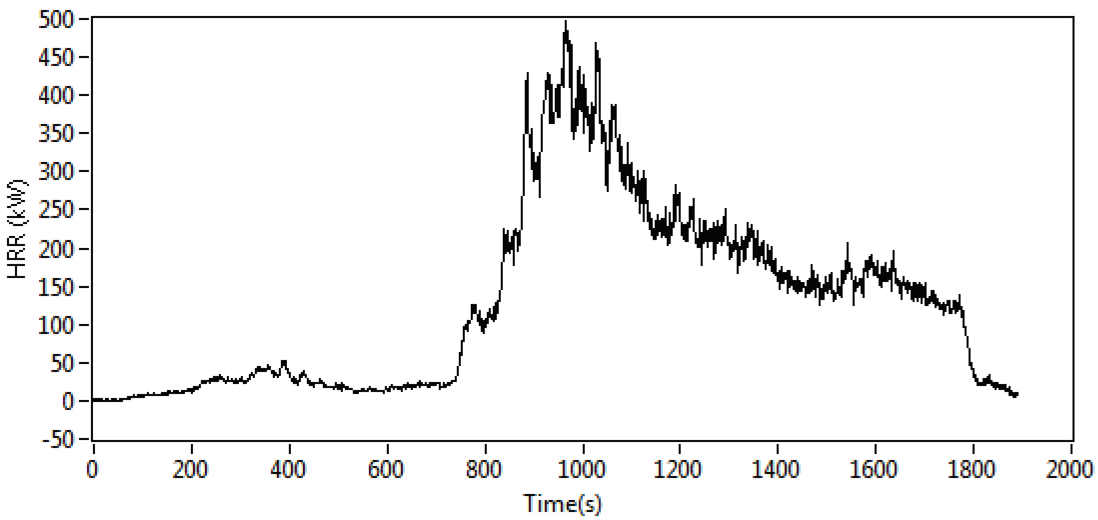

HRR (kW)
500
450
400
350
300
250
200
150
100
50
0
-50
0
200
400
600
800
1000
1200
1400
1600
1800
2000
Time(s)

OF28

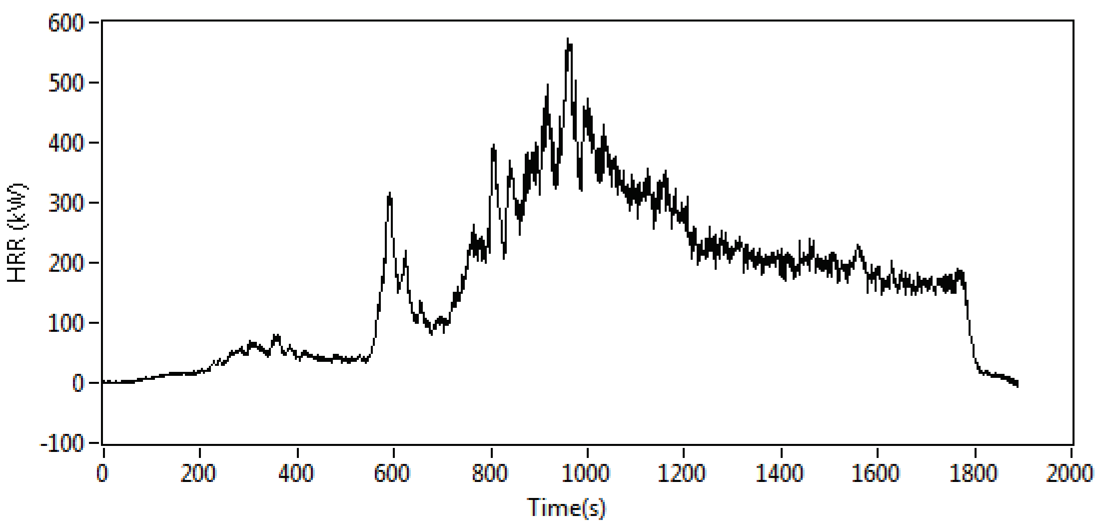

HRR (kW)
600
500
400
300
200
100
0
-100
0
200
400
600
800
1000
1200
1400
1600
1800
2000
Time(s)

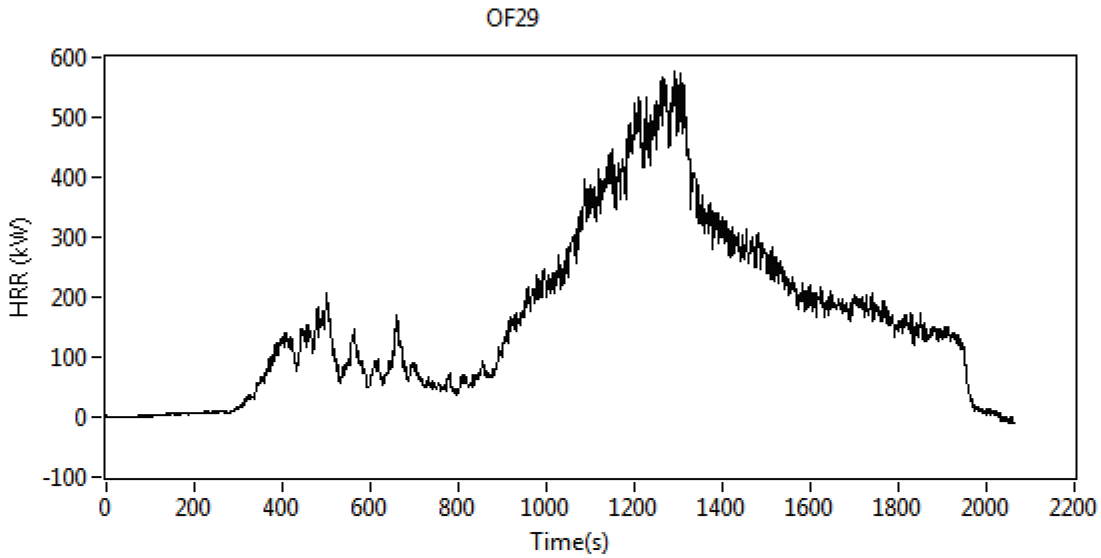
OF29
600
500
400
300
200
100
0
-100
HRR (kW)
0
200
400
600
800
1000
1200
1400
1600
1800
2000
2200
Time(s)

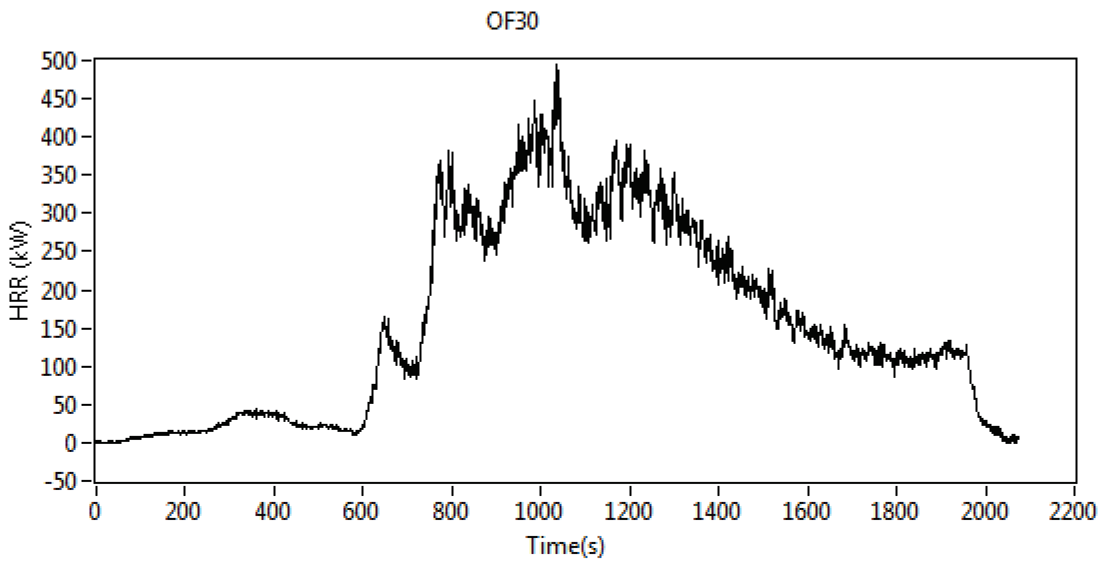
OF30
500
450
400
350
300
250
200
150
100
50
0
-50
HRR (kW)
0
200
400
600
800
1000
1200
1400
1600
1800
2000
2200
Time(s)

UNITED STATES
CONSUMER PRODUCT SAFETY COMMISSION
BETHESDA, MD 20814

Memorandum

Date: July 31, 2017

TO: Andrew Lock
Directorate for Laboratory Sciences
Upholstered Furniture Project Manager

THROUGH : Stephen J. Hanway
Division Director
Division of Hazard Analysis

FROM: David Miller
Division of Hazard Analysis

SUBJECT: Analysis of Chair Open-Flame Data

Background:

In 2014, Consumer Product Safety Commission (CPSC) staff conducted chair burn testing at CPSC's National Product Testing and Evaluation Center to assess the effectiveness of fire barriers.[1] This was part of CPSC staff's effort to evaluate various approaches to reduce the risk to consumers of upholstered furniture fires. The testing included both open-flame tests and cigarette smoldering tests. The most recent CPSC staff estimates involving upholstered furniture estimate an annual average of 440 residential structure fire deaths a year where upholstered furniture was the item first ignited by a fire. An estimated 180 of these fire deaths were ones where the heat source for the fire was smoking materials. An estimated annual average of 20 deaths occurred from fires where a candle, match, or cigarette lighter ignited the upholstered furniture. The remaining estimated 240 fire deaths where upholstered furniture was the item first ignited are attributable to other heat sources (these include space heater fires, extension cord fires, and more).

The open-flame testing demonstrated that each of the five fire barriers tested was effective at reducing the peak heat release rate of the burning chairs and increasing the time to peak heat release rate. It was not clear from the smoldering testing whether the fire barriers were effective at reducing the peak heat release rate, and the fire barriers may have (although it was not conclusive) promoted a transition to flaming fires in the chairs.

In addition to fire barriers, different fabrics were tested, as well as chairs of different simulated ages.[2] One of the two fabrics was better than the other in terms of the peak heat release rate for the open-flame fires. That fabric also proved to be better in the time to peak heat release rate. The differences in peak heat release rate and time to peak heat release rate were statistically significant. However, this fabric was ineffective at preventing a transition to flaming in smoldering fires. The age (simulated) of the chair did not have a statistically significant effect on the peak heat release or the time to peak heat release.

[1] Information about the 2014 chair testing can be found in *Analysis of Chair Open-Flame and Smoldering Data, CPSC, Miller, March, 2016.*
[2] Age was simulated by mechanical stressing of chairs.

In 2016, CPSC staff conducted more burn testing at the National Product Testing and Evaluation Center. These were small open-flame tests involving chairs with two of the same seat cushion barriers and different modified loose fill back cushion materials. Also, two different fabrics were tested.

Purpose:

The main purpose of this testing is to assess the effectiveness of a convenience sample of fire barriers in reducing the intensity and slowing the progress of full-scale, open-flame chair fires. The fire barriers tested include different barriers for the seat cushion and modified loose fill for the back of the chair. The testing was also designed to assess the effect of two different chair fabrics.

Test Program

Staff conducted open-flame testing of 30 chairs. These chairs had one of two fabrics, one of two seat cushion fire barriers (or no barrier), and o ne of two chair back modified loose fill materials (or traditional polyester). In the tests, a 240 millimeter butane flame was applied to a chair for 70 $\pm$ 1 seconds.[1] During these tests, the heat release rate was monitored throughout. CPSC staff was able to record the peak heat release rate (in kilowatts) and the time to peak heat release rate (in minutes) for each of the chairs.

Preview of Findings:

Both seat cushion fire barriers tested were effective at reducing the peak heat release rate (PHRR) and the time to peak heat release (time to peak) of burning chairs. The observed differences were statistically significant. Additionally, both chairs with backs made of modified loose fill materials were effective at reducing the PHRR and increasing the time to peak for burning chairs. The observed differences were statistically significant. The barriers (both seat cushion fire barriers and both chair back loose fill) each are estimated to reduce the peak heat release rate of burning chairs by more than 1,000 kilowatts. Each barrier is estimated to delay the time to peak heat release of burning chairs by at least several minutes. One of the fabrics tested was better than the other in terms of both PHRR and time to peak, and the observed difference was statistically significant.

Design of Experiments:

Independent Variables:

- Seat cushion fire barriers (Seat); there were two different seat cushion fire barriers (FB2, FB4) being evaluated, and some chairs had no seat cushion fire barrier. Thus, there were three different possibilities for a chair's seat cushion fire barrier.

- Chair back loose fill materials (Back); there were two different chair back loose fill materials (FF3, FF4) being evaluated, and some chairs had only traditional polyester. Thus, there were three different possibilities for a chair back's material.

[1] BS-5852, Methods of Test for Assessment of the Ignitability of Upholstered Seating by Smoldering and Flaming Ignition Sources. 1990.

- Cover fabric; there were two different cover fabrics (F2, F3) used in the chair tests.

Dependent Variables:

- Peak Heat Release Rate (PHRR)

- Time to Peak Heat Release Rate (Time to Peak)

The chairs tested were part of a convenience sample of available chairs with different seat cushion barriers, chair back materials, and fabrics. There were 30 chairs available, which broke down as described in Table 1.

Table 1. Barriers and Fabrics for Chairs Tested

Cover Fabric	Seat Cushion Barrier	Chair Back Loose Fill	Number of Chairs Tested
F2	FB2	FF3	3
F2	FB2	FF4	3
F2	FB4	FF3	3
F2	FB4	FF4	3
F2	None	None	3
F3	FB2	FF3	3
F3	FB2	FF4	3
F3	FB4	FF3	3
F3	FB4	FF4	3
F3	None	None	3

There were three chairs, each of 10 different combinations of chair components. Note that although there were two different fabrics, three different seat cushion barriers (including 'None'), and three different chair back loose fill materials (including polyester), there were not 2*3*3 = 18 combinations. This is because whenever there was no seat cushion barrier, there also was no chair loose fill material and vice versa. This reduced the number of possible combinations from 18 to 10.

After the testing, CPSC staff attempted two separate ANOVAs (analysis of variance): one with *PHRR* as the dependent variable and one with *time to peak* as the independent variable. In each ANOVA, cover fabric (*fabric*), seat cushion barrier (*seat*), and chair back loose fill material (*back*) were the independent variables. For both ANOVAs, there was the problem of a singular covariance matrix.

The underlying theory in analysis of covariance requires the covariance matrix to be nonsingular[1] because the inverse of the covariance is used in the solution to the least squares equations to obtain the parameter estimates. If the covariance matrix is singular, there is no solution to these equations.

CPSC staff used JMP 13.1[2] software to formulate a design that would enable staff to evaluate each of the independent variables (*fabric*, *seat*, and *back*) and possible interactions between fabric and seat and between fabric and back. To do this, the design called for two separate two-way ANOVAs for each dependent variable (*PHRR* and *time to peak*). This is four separate two-way ANOVAs: (1) *PHRR* is the dependent variable and *fabric* and *seat* are the independent variables; (2) *PHRR* is the dependent variable

[1] A nonsingular matrix is one that has an inverse.
[2] JMP is a statistical software package that is of particular use here in Design of Experiments (DOE).

and *fabric* and *seat* are the independent variables; (3) *time to peak* is the dependent variable and *fabric* and *seat* are the independent variables; and (4) *time to peak* is the dependent variable and *fabric* and *back* are the independent variables.

These designs involved two runs of each possible combination of *fabric* and *seat* (for the first and third ANOVA) and two runs of each possible combination of *fabric* and *back* (for the second and fourth ANOVAs). For each of the four ANOVAs there are six possible combinations of the independent variables (two cover fabrics and three levels of either *seat* or *back*). Two runs of these six combinations are 12 chairs. As an example, the details of the types and numbers of chairs involved in the first ANOVA are in Table 2.

Table 2. Chairs for PHRR Analysis of Variance for Fabric and Seat

Cover Fabric	Seat Cushion Barrier	Number of Chairs
F2	FB2	2
F2	FB4	2
F2	None	2
F3	FB2	2
F3	FB4	2
F3	None	2

The design would allow a full replicate of these 12 chairs, which would be four chairs for each combination and 24 chairs in total. It would also allow two full replicates, which would be 36 chairs. More replicates are useful for having more precise estimates and more power in hypothesis testing. However, because there were only three chairs tested with fabric F2 and no barrier and only three chairs tested with fabric F3 and no barrier, it is not possible to have a full replicate, which would require four chairs for each combination. Therefore, staff was restricted to 12 chairs for each of the four ANOVAs.

CPSC staff randomly selected 12 chairs, two for each of the six combinations of *fabric* and *seat* or *fabric* and *back*, for each of the four ANOVAs. For the ANOVAs with fabric and seat, staff randomly selected two of the six tested chairs with cover fabric F2 and seat cushion barrier FB2, two of the six tested chairs with cover fabric F2 and seat cushion barrier FB4, and two of the three tested chairs with cover fabric F2 and no seat cushion barrier, etc. See the Appendix for details about the 30 chairs tested and the 12 chairs randomly selected for each of the four ANOVA models.

Results and Analysis:

Staff decided that, for each of the four ANOVAs, the two-term interaction[1] should be included in the model if the p-value for the corresponding F-test is below 0.25. Interactions and main effects are considered statistically significant if their p-values are below 0.05.

[1] An interaction is when the effect of one independent variable differs depending on the value (or level) of another independent variable. For example, if the difference that the seat cushion barrier makes is dependent on which cover fabric is on the chair, that is a *fabric**seat* interaction.

1) Model for *PHRR* with *Fabric* and *Seat:*

The p-value for the *fabric*seat* interaction is 0.14. It is low enough to keep in the model, but is not statistically significant. Main effects are the effect that each individual variable has on *PHRR* (aside from the interaction). For the model with *PHRR* and *fabric* and *seat*, both of the main effects (*fabric* and *seat*) are statistically significant. The main effects for both *fabric* and *seat* are listed in Table 3.

Table 3. *Peak Heat Release Rate*[1] with *Fabric* and *Seat* Main Effects

Effect	**Estimate**	**95% Confidence Interval**	**p-value**
Fabric	F2 = -583.1	(-960.6, -648.8)	0.0092
Seat	FB2 = -1,026.4 FB4 = -1,065.2	(-1,403.9, -648.8) (-1,442.7, -687.6)	0.0006 0.0005

The estimates for *seat* are relative to 'No Barrier.' Another way of saying this is that 'No Barrier' is the baseline level for *seat*. For example, the model estimates that having a chair with the FB2 seat cushion barrier, means a peak heat release rate 1,026.4 kW lower than if the seat had no barrier. The model estimates that having a chair with the FB4 seat cushion barrier, would lead to a reduction of 1,065.2 kW in *PHRR*. The corresponding 95 percent confidence intervals show the range for these estimates. The estimated effect of having cover fabric F2 is a PHRR 583.1 kW lower than a chair with cover fabric F3.

The full model includes the intercept, the main effects for *fabric* and *seat*, and the *fabric*seat* interaction.

Estimated PHRR = Intercept + Fabric Effect + Seat Effect + Fabric*Seat Interaction

The intercept is the estimated *PHRR* of a chair with the baseline levels of all variables (cover fabric F3 and no seat cushion barrier). The R-squared value for this model is 0.939, which indicates a very good model that is able to explain almost all of the variation in the data. The ANOVA provides estimates for the intercept, main effects, and interaction, which are provided in Table 4. Note that the model does not take the chair back loose fill material into account.

Table 4. *Peak Heat Release Rate* with *Fabric* and *Seat* Model Parameters

Parameter	**Estimate**	**95% Confidence Interval**
Intercept	1,724.0	(1,457.1, 1,991.0)
Seat FB2	-1,026.4	(-1,403.9, -648.8)
Seat FB4	-1,065.2	(-1,442.7, -687.6)

[1] In kilowatts (kW)

Fabric F2	-583.1	(-960.6, -205.6)
Seat FB2 * Fabric F2	405.5	(-128.4, 939.4)
Seat FB4 * Fabric F2	480.1	(-53.8, 1,014.1)

So, for example, for a chair with seat cushion barrier FB4 and cover fabric F2, the model estimates a *PHRR* of 1,724.0 + (-1,065.2) + (-583.1) + (480.1) = 555.8 kW.

For perspective, a small campfire has a heat release rate of about 100 kW and a 1,000 kW fire is one where the room will likely flash over. A flashover is a catastrophic fire where the entire room is on fire.

2) Model for *PHRR* with *Fabric* and *Back:*

The p-value for the *fabric*back* interaction is 0.0003, which is statistically significant and remains in the model. This interaction tells us that the difference that the fabric makes in the *PHRR* of the burning chairs is not the same for all of the levels of loose fill material (FF3, FF4, and traditional polyester). Alternatively, it could be stated that the effect of the loose fill differs based on which cover fabric is present. Figure 1 demonstrates this interaction.

Figure 1. *Fabric*Back* Interaction for *PHRR*

Each of the lines has an upward slope, but it is much steeper for the ‘Polyester’ line than for the others, and it is also much steeper for the FF3 line than for the FF4 line, which is almost flat. It appears that the F2 cover fabric made more of a difference on the chairs with polyester. Alternatively, it can be said that the loose fill materials made more of a difference on the chairs with the F3 cover fabric.

In some cases, a statistically significant interaction can mask the main effects. But in this model, despite the significant interaction, the main effects are both statistically significant with p-values below 0.0001.

Table 5. ***Peak Heat Release Rate*** **with** ***Fabric*** **and** ***Seat*** **Main Effects**

Effect	Estimate	95% Confidence Interval	p-value
Fabric	F2 = -556.9	(-659.5, -454.4)	<.0001
Back	FF3 = -1,190.1 FF4 = -1,360.0	(-1,292.7, -1,087.6) (-1,462.6, -1,257.4)	<.0001 <.0001

The estimates for *back* are relative to 'Polyester.' The model estimates that having a chair with the FF3 loose fill material means a peak heat release rate 1,190.1 kW lower than if the chair had only polyester. The model estimates that having a chair with the FF4 loose fill material in the chair back would lead to a reduction of 1,360.0 kW in PHRR compared to chairs with only polyester. The corresponding 95 percent confidence intervals show the range for these estimates. The estimated effect in this model, of having cover fabric F2, is a PHRR 556.9 kW lower than a chair with cover fabric F3. The model does not take into account the seat cushion barrier.

The full model includes the intercept, the main effects for *fabric* and *back*, and the *fabric*back* interaction.

Estimated PHRR = Intercept + Fabric Effect + Seat Effect + Fabric*Seat Interaction.

The ANOVA provides estimates for the intercept, main effects, and interaction, which are provided in Table 6.

Table 6. ***Peak Heat Release Rate*** **with** ***Fabric*** **and** ***Back*** **Model Parameters**

Parameter	Estimate	95% Confidence Interval
Intercept	1,893.0	(1,820.5, 1,965.6)
Back FF3	-1,190.1	(-1,292.7, -1,087.6)
Back FF4	-1,360.0	(-1,462.6, -1,257.4)
Fabric F2	-556.9	(-659.5, -454.4)
Back FF3 * Fabric F2	353.4	(208.3, 498.4)
Back FF4 * Fabric F2	544.0	(399.0, 689.1)

For example, for a chair with chair back loose fill FF3 and cover fabric F2, the model estimates a PHRR of 1,893.0 + (-1,190.1) + (-556.9) + (353.4) = 555.8 kW. The R-squared value for this model is 0.997, which means that nearly 100 percent of the variability in the data is explained by the model.

<u>*Seat* and *Back* Effects on *PHRR*:</u>

The first two models examined were the models where *Peak Heat Release Rate* was the dependent variable. The first model included *fabric* and *seat*. The second model included *fabric* and *back*. Each model showed the barriers (*seat*) and loose fill materials (*back*) to be quite effective at reducing the *PHRR* of burning chairs. They are separate models, and it is important to remember that although the first model does not take the chair back loose fill into account, the 12 chairs involved had different loose fill materials. Likewise, although the second model does not take the seat cushion barrier into account, some of the 12 chairs involved had these barriers. Figure 2 details the estimated effectiveness of the seat barriers and chair back loose fill in reducing *PHRR* in burning chairs. The estimates and confidence intervals for the seat barriers come from the first model, and the ones for the loose fill come from the second model.

Figure 2. Estimated Barrier Effects – Reduction in Peak Heat Release

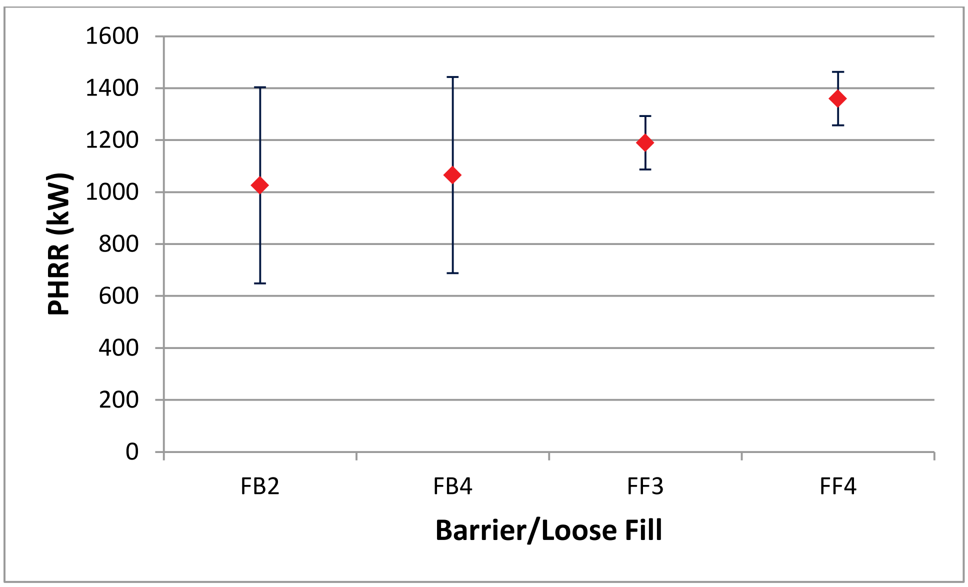

Each of the estimated effects is greater than 1,000 kilowatts. The confidence intervals are much wider for the seat cushion barriers because the standard errors for the chair back loose fill estimates were less than a third of that of the seat cushion barriers.

3) Model for *Time to Peak* with *Fabric* and *Seat:*

When staff ran the full model (including the *fabric*seat* interaction), the p-value for the *fabric*seat* interaction was 0.79. It was not statistically significant; thus, this interaction was removed from the model. Both of the main effects, *fabric* and *seat*, are statistically significant. The main effects are listed in Table 3.

Table 7. *Time to Peak*[1] with *Fabric* and *Seat* Main Effects

Effect	Estimate	95% Confidence Interval	p-value
Fabric	F2 = 9.6	(2.7, 16.5)	0.0123
Seat	FB2 = 12.1 FB4 = 10.7	(3.6, 20.5) (2.2, 19.1)	0.0111 0.0196

The estimates for *seat* are relative to 'No Barrier.' The estimates are positive, which shows that the chairs with barriers had a longer *time to peak* than the chairs without barriers. It is estimated that having a chair with the FB2 barrier in the seat will increase the *time to peak* by 12.1 minutes. The chairs with the FB4 barriers increase the *time to peak* by an estimated 10.7 minutes.

In this model, the full model is simply the intercept and the two main effects.

Estimated *Time to Peak* = Intercept + Fabric Effect + Seat Effect

The ANOVA provides estimates for the intercept and both main effects as detailed in Table 8.

Table 8. *Time to Peak* with *Fabric* and *Seat* Model Parameters

Parameter	Estimate	95% Confidence Interval
Intercept	3.5	(-3.4, 10.4)
Seat FB2	12.1	(2.7, 16.5)
Seat FB4	10.7	(3.6, 20.5)
Fabric F2	9.6	(2.2, 19.1)

For a chair with seat cushion barrier FB2 and cover fabric F3, the model estimates a time to peak heat release of 3.5 + 12.1 = 15.6 minutes. The R-squared for this model is 0.763, which indicates that the model is explaining the variation in the data well.

4) Model for *Time to Peak* with *Fabric* and *Back*:

The p-value for the *fabric*back* interaction is 0.0003, which is statistically significant. This means that the effect of the chair back loose fill materials in delaying the *time to peak* of the burning chairs differs depending on the cover fabric. It could also be said that the effect of the cover fabric in delaying the time to peak is different for the different loose fill materials (or polyester). Figure 3 helps to illustrate this interaction.

[1] In minutes.

Figure 3. ***Fabric*Back* Interaction for *Time to Peak***

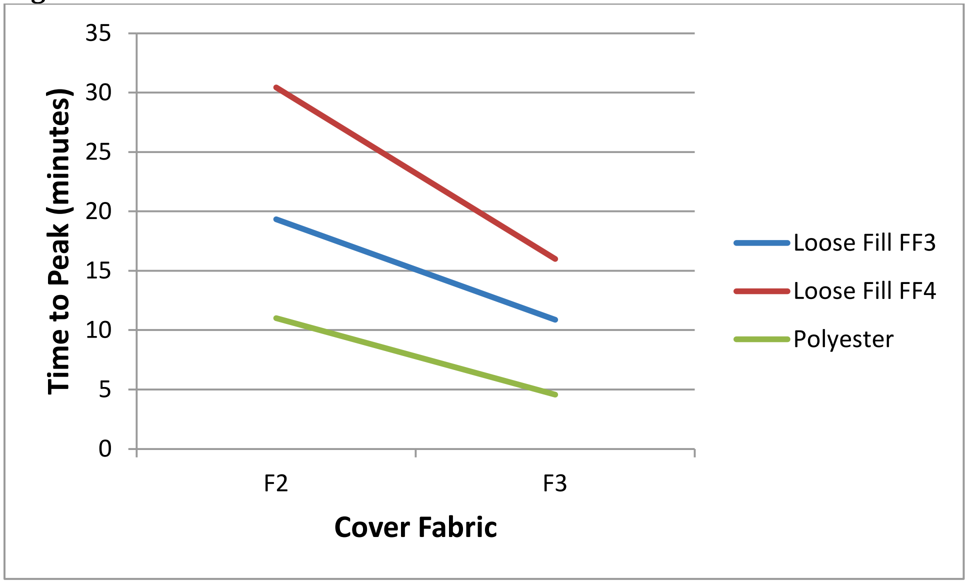

The slopes for each of the three lines are downward because the average *time to peak* of the chairs in the model was higher for chairs with cover fabric F2 for all three levels of loose fill (FF3, FF4, and polyester). The interaction can be seen in the slope of the line for loose fill FF4. The slope is considerably steeper for this line than for the other two. The F2 cover fabric made more of a difference in delaying the peak heat release for chairs with the FF4 loose fill than for chairs with the FF3 loose fill or chairs with only polyester in the chair back. Alternatively, the delaying effect of having a chair with the FF4 loose fill is larger on chairs with cover fabric F2 than on chairs with cover fabric F3.

In some instances interactions can mask main effects. However, both main effects in this model are statistically significant. The p-values for both *fabric* and *back* are below .0001.

Table 9. *Time to Peak*[1] with *Fabric* and *Back* Main Effects

Effect	Estimate	95% Confidence Interval	p-value
Fabric	F2 = 6.4	(4.8, 8.0)	<.0001
Back	FF3 = 6.3 FF4 = 11.4	(4.7, 7.9) (9.8, 13.0)	<.0001 <.0001

Again, the estimates for *back* are relative to 'polyester.' The model estimates that the chair back loose fill materials FF3 and FF4 delay the time to peak heat release of burning chairs by 6.3 and 11.4 minutes, respectively. The cover fabric F2 is estimated to provide an extra 6.4 minutes before the peak heat release, as opposed to chairs with cover fabric F3.

The full model includes both statistically significant main effects (*fabric* and *back*) and the statistically significant *fabric*back* interaction.

[1] In minutes.

Estimated *Time to Peak* = Intercept + Fabric Effect + Back Effect + Fabric*Back Interaction

Table 10 presents the estimates of the intercept, both main effects and the interaction.

Table 10. *Time to Peak* with *Fabric* and *Back* Model Parameters

Parameter	**Estimate**	**95% Confidence Interval**
Intercept	4.6	(3.4, 5.7)
Back FF3	6.3	(4.7, 7.9)
Back FF4	11.4	(9.8, 13.0)
Fabric F2	6.4	(4.8, 8.0)
Back FF3 * Fabric F2	2.0	(-0.3, 4.3)
Back FF4 * Fabric F2	8.0	(5.7, 10.3)

The model estimates that a burning chair with FF3 chair back loose fill and a F2 cover fabric would reach its peak after 4.6 + 6.3 + 6.4 + 2.0 = 19.3 minutes. As with the *PHRR* model with *fabric* and *back*, this model has an R-squared of 0.997.

<u>*Seat* and *Back* Effects on *Time to Peak*:</u>

The third and fourth models were the ones where *time to peak* was the dependent variable. The third model has *fabric* and *seat* as the independent variables. The fourth model has *fabric* and *back*. Both models showed that the barriers and loose fill involved were effective at increasing the *time to peak* for burning chairs (*i.e.*, the observed differences were statistically significant). It is important to note that, although the third model does not take the chair back loose fill into account, the 12 chairs involved had different loose fill materials. In the fourth model, the seat cushion barriers are not taken into account. Figure 4 shows the two different models estimates of barrier and loose fill effectiveness.

Figure 4. Estimated Barrier/Loose Fill Effects – Increase in *Time to Peak*

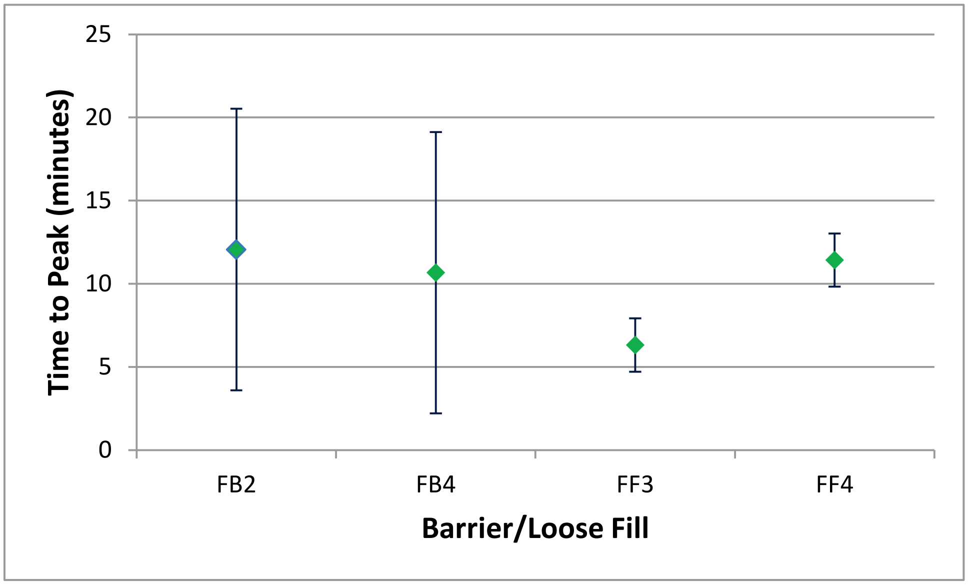

With the exception of the FF3 loose fill materials, which had an estimated increase in *time to peak* (over chairs with only polyester) of 6.3 minutes, the other three barriers/loose fill provided an estimated increase of more than 10 minutes. As with the *PHRR* models, the confidence intervals are narrower for the chair back loose fill materials because the standard errors for their estimates were much lower than for those of the seat cushion barriers.

Conclusions:

Both of the barriers and both of the loose fill materials evaluated in these open-flame tests reduced the Peak Heat Release Rate of burning chairs. The reductions were statistically significant. Statistical models found that each of the four barriers/loose fill materials had an estimated effect of reducing the *PHRR* of burning chairs by more than 1,000 kW. Also, they each proved to be effective at increasing the time to PHRR (*time to peak*) of burning chairs. All but one of the barriers/loose fill materials, provided an estimated increase *time to peak* of more than 10 minutes.

The cover fabric also showed a statistically significant difference in both *PHRR* and *time to peak*. In both of the *PHRR* models, the F2 cover fabric was estimated to have the effect of at least 500 kW lower *PHRR* than chairs with the F3 cover fabric. In the *time to peak* models, the F2 cover fabric was estimated to provide an additional 9.6 and 6.4 minutes before peak heat release, as opposed to burning chairs with the F3 cover fabric. For the models that involved cover fabric and chair back loose fill materials, there were statistically significant interactions between the cover fabric and the loose fill.

As with prior testing, the barriers proved to be effective at reducing peak heat release rate and the time to peak heat release. This time, loose fill materials were also tested, and barriers used with loose fill proved to be effective to the same degree as the seat cushion fire barriers. This round of testing did not include smoldering (*i.e*., cigarette) tests; and thus, we still do not have evidence to support that the barriers or loose fill materials would prevent or mitigate smoldering fires or perhaps even promote them.

Appendix

Burn testing was performed on 30 chairs. The appendix will provide the seat, back, cover fabric, PHRR, and time to peak information for each of these 30 chairs. It will also provide the information for the 12 chairs randomly selected for each of the four models in the analysis.

Table A1. 30 Chairs

Chair Test Name	Fabric	Seat	Back	PHRR	Time to Peak
OF7	F2	FB2	FF3	485.70	19.60
OF14	F2	FB2	FF3	630.94	19.52
OF29	F2	FB2	FF3	576.02	21.50
OF6	F2	FB2	FF4	373.74	33.88
OF10	F2	FB2	FF4	464.10	37.28
OF23	F2	FB2	FF4	477.27	29.37
OF2	F2	FB4	FF3	512.89	19.50
OF4	F2	FB4	FF3	738.97	17.62
OF8	F2	FB4	FF3	918.49	19.15
OF1	F2	FB4	FF4	563.02	31.48
OF19	F2	FB4	FF4	598.91	29.33
OF21	F2	FB4	FF4	441.71	26.37
OF16	F2	No	No	1339.99	13.13
OF17	F2	No	No	1332.18	11.33
OF18	F2	No	No	941.86	10.67
OF3	F3	FB2	FF3	653.52	16.88
OF9	F3	FB2	FF3	663.94	10.77
OF22	F3	FB2	FF3	741.81	14.08
OF24	F3	FB2	FF4	615.31	18.67
OF27	F3	FB2	FF4	496.54	16.10
OF30	F3	FB2	FF4	493.93	17.23
OF5	F3	FB4	FF3	656.14	11.00
OF13	F3	FB4	FF3	686.26	18.25
OF15	F3	FB4	FF3	599.04	12.98
OF11	F3	FB4	FF4	619.71	13.35
OF26	F3	FB4	FF4	631.50	15.98
OF28	F3	FB4	FF4	572.18	16.00
OF12	F3	No	No	1568.73	4.47
OF20	F3	No	No	1906.72	4.67
OF25	F3	No	No	1879.33	4.78

Table A2. Chairs for Model 1 – *PHRR* with *Fabric* and *Seat*

Chair Test Name	Fabric	Seat	Back	PHRR	Time to Peak
OF29	F2	FB2	FF3	576.02	21.50
OF10	F2	FB2	FF4	464.10	37.28
OF2	F2	FB4	FF3	512.89	19.50
OF19	F2	FB4	FF4	598.91	29.33
OF16	F2	No	No	1339.99	13.13
OF18	F2	No	No	941.86	10.67
OF3	F3	FB2	FF3	653.52	16.88
OF22	F3	FB2	FF3	741.81	14.08
OF13	F3	FB4	FF3	686.26	18.25
OF26	F3	FB4	FF4	631.50	15.98
OF12	F3	No	No	1568.73	4.47
OF25	F3	No	No	1879.33	4.78

Table A3. Chairs for Model 2 – *PHRR* with *Fabric* and *Back*

Chair Test Name	Fabric	Seat	Back	PHRR	Time to Peak
OF7	F2	FB2	FF3	485.70	19.60
OF23	F2	FB2	FF4	477.27	29.37
OF2	F2	FB4	FF3	512.89	19.50
OF1	F2	FB4	FF4	563.02	31.48
OF16	F2	No	No	1339.99	13.13
OF17	F2	No	No	1332.18	11.33
OF9	F3	FB2	FF3	663.94	10.77
OF22	F3	FB2	FF3	741.81	14.08
OF30	F3	FB2	FF4	493.93	17.23
OF28	F3	FB4	FF4	572.18	16.00
OF20	F3	No	No	1906.72	4.67
OF25	F3	No	No	1879.33	4.78

Table A4. Chairs for Model 2 – *Time to Peak* with *Fabric* and *Seat*

OF7	F2	FB2	FF3	485.70	19.60
OF6	F2	FB2	FF4	373.74	33.88
OF4	F2	FB4	FF3	738.97	17.62
OF19	F2	FB4	FF4	598.91	29.33
OF16	F2	No	No	1339.99	13.13
OF18	F2	No	No	941.86	10.67
OF9	F3	FB2	FF3	663.94	10.77
OF30	F3	FB2	FF4	493.93	17.23
OF15	F3	FB4	FF3	599.04	12.98
OF28	F3	FB4	FF4	572.18	16.00
OF20	F3	No	No	1906.72	4.67
OF25	F3	No	No	1879.33	4.78

Table A5. Chairs for Model 2 – *Time to Peak* with *Fabric* and *Back*

Chair Test Name	Fabric	Seat	Back	PHRR	Time to Peak
OF14	F2	FB2	FF3	630.94	19.52
OF23	F2	FB2	FF4	477.27	29.37
OF8	F2	FB4	FF3	918.49	19.15
OF1	F2	FB4	FF4	563.02	31.48
OF17	F2	No	No	1332.18	11.33
OF18	F2	No	No	941.86	10.67
OF9	F3	FB2	FF3	663.94	10.77
OF5	F3	FB4	FF3	656.14	11.00
OF26	F3	FB4	FF4	631.50	15.98
OF28	F3	FB4	FF4	572.18	16.00
OF12	F3	No	No	1568.73	4.47
OF20	F3	No	No	1906.72	4.67

SUBJECT: **NIST Technical Note 1920 -- "*Predicting the Effects of Barrier Fabrics on Residential Upholstered Furniture Fire Hazard*"** [1]

The attached report is **NIST Technical Note 1920 -- "*Predicting the Effects of Barrier Fabrics on Residential Upholstered Furniture Fire Hazard.*"** The work was conducted under Inter-Agency Agreement CPSC-I-13-0022, and is the final deliverable. NIST was contracted by the Consumer Product Safety Commission (CPSC) to use CPSC data to predict how the chair fires would affect tenability in a variety of residential living area configurations. The same barriers were used in a study of upholstered furniture flammability conducted by CPSC staff.[2]

CPSC has published a proposed rule to reduce the fire hazards associated with upholstered furniture. In 2013, CPSC staff held an Upholstered Furniture Fire Safety Technology Meeting to promote a discussion of fire barrier technologies and the potential benefits barriers could provide toward improving or reducing furniture flammability. After that meeting, staff conducted a test program at CPSC's National Product Testing and Evaluation Center involving full-scale chairs exposed to open-flame and cigarette-ignition sources to evaluate the potential effectiveness of five selected fire barriers. The results of the full-scale testing, chemistry analysis and a toxicity analysis of the barrier materials are the subjects of separate reports by CPSC staff.[2]

The objectives of the study conducted by NIST were to predict the fire hazard and tenability in various residential configurations based on test data obtained by CPSC staff on the performance of various pieces of upholstered furniture using fire barriers. The NIST report includes a summary of predicted performance characteristics of each barrier and cover fabric combination. NIST evaluated a variety of different residence configurations and evaluated the probability of flashover and the probability of a lethal thermal Fractional Effective Dose (FED) would be experienced in an adjacent room. The results show how different barriers had varying performance, depending on the specific configurations and room geometries. NIST found that barrier fabrics can reduce the probability of lethal conditions occurring in less than 30 min by at least 50 percent, and that further work is needed to consider the hazard produced by larger furniture and the effects of secondary fuel sources becoming involved in the fire.

[1] This statement was prepared by the CPSC staff, and the attached report was produced by NIST for CPSC staff. The statement and report have not been reviewed or approved by, and do not necessarily represent the views of, the Commission.

[2] Memorandum to Andrew Lock, Project Manager, Upholstered Furniture Project, from L. Fansler and Andrew Lock, "Summary Report of Open Flame and Smoldering Tests on Chairs", January 2016.

NIST Technical Note 1920

Predicting the Effects of Barrier Fabrics on Residential Upholstered Furniture Fire Hazard

Morgan C. Bruns

This publication is available free of charge from:
http://dx.doi.org/10.6028/NIST.TN.1920

National Institute of
Standards and Technology
U.S. Department of Commerce

NIST Technical Note 1920

Predicting the Effects of Barrier Fabrics on Residential Upholstered Furniture Fire Hazard

Morgan C. Bruns
Fire Research Division
Engineering Laboratory

This publication is available free of charge from:
http://dx.doi.org/10.6028/NIST.TN.1920

June 2016

U.S. Department of Commerce
Penny Pritzker, Secretary

National Institute of Standards and Technology
Willie May, Under Secretary of Commerce for Standards and Technology and Acting Director

National Institute of Standards and Technology Technical Note 1920
Natl. Inst. Stand. Technol. Tech. Note 1920, 46 pages (June 2016)
CODEN: NTNOEF

This publication is available free of charge from:
http://dx.doi.org/10.6028/NIST.TN.1920

Contents

List of Figures

List of Tables

List of Acronyms

BF	Barrier Fabric
CBUF	Combustion Behaviour of Upholstered Furniture
CDF	Cumulative Distribution Function
CF	Cover Fabric
CFAST	Consolidated Model of Fire and Smoke Transport
CPSC	Consumer Product Safety Commission
FED	Fractional Effective Dose
HGL	Hot Gas Layer
HRR	Heat Release Rate
MQH	McCaffrey, Quintiere, and Harkleroad
NFPA	National Fire Protection Association
NIST	National Institute of Standards and Technology
PDF	Probability Density Function
RUF	Residential Upholstered Furniture

List of Symbols

a	fabric combination label
c_p	specific heat
f_X	probability density function of X
g	gravitational constant
h_w	effective heat transfer coefficient in wall
k	thermal conductivity
l	loss parameters
x	building parameters
A_1	living room area
A_2	bedroom area
A_o	total ventilation area in MQH
F	thermal FED
H	ceiling height
K_x	fire location correction factor
L	random variable for loss parameters
N	number of Monte Carlo samples
T	temperature
T_c	flashover temperature
W_i	width of room i
$\dot{Q}$	heat release rate
X	random variable for building parameters
$\mathscr{D}_{ij}$	switch for door between rooms i and j
$\mathscr{H}$	Heaviside step function
$\mathscr{X}$	fire location parameter
γ	HRR curve
η_1	living room aspect ratio
θ	controlled parameters
ρ	density
ϕ	indicator function

Abstract

A probabilistic methodology is presented for estimating building fire hazard in the presence of significant scenario uncertainty. This methodology is applied to the specific case of residential upholstered furniture (RUF) fires. The objective of this application is to assess the fire losses associated with different cover fabric and barrier fabric combinations. Several RUF chairs with different fabric combinations are considered. Open furniture calorimeter heat release rate (HRR) data for these chairs was provided by the Consumer Product Safety Commission (CPSC). Residential building statistics are compiled to generate a probabilisitic description of typical residential fire scenarios. A correlation and a zone model are used to predict the hazard conditions resulting from these chair fires in an ensemble of residential fire scenarios. Hazard is quantified in terms of the probability of flashover in the room of fire origin and the probability that the thermal fractional effective dose (FED) in an adjacent bedroom is greater than one. It is seen that the predictions of hot gas layer (HGL) temperature using the correlation are significantly higher than those predicted by the zone model. The more accurate zone model indicates that a single RUF chair fire is too small to flashover nearly all rooms considered. However, the zone model results indicate that the choice of barrier fabric significantly affects the HGL temperature. A reduction in the peak HGL temperature of at least least 100 $^\circ$ C was achieved for cases with barrier fabrics other than the worst performer. Even in the absence of flashover, it is possible to produce fatal conditions in an adjacent room for typical RUF chair fires. Barrier fabrics can reduce the probability of lethal conditions occurring in less than 30 min by at least 50 %. Further work is needed to consider the hazard produced by larger furniture and the effects of secondary fuel sources becoming involved in the fire.

Section 1

Introduction

1.1 Objective and Technical Approach

Despite advances in fire protection engineering and flammability standards, residential fire losses remain significant. According to the National Fire Protection Association (NFPA) [1], in the period between years 2009 and 2013, an average of 2470 civilians die each year in home fires. Efforts to reduce the residential fire problem should be focused on the ignition and fuel sources that are most hazardous. Of the fatalities from residential fires, an average of 420 or 17 % resulted from upholstered furniture being the first item ignited [1]. A more detailed analysis of the fire data between years 2006 and 2010 revealed that an additional average of 130 deaths could be attributed to fires in which upholstered furniture was the "primary item contributing to fire spread" [2]. It is clear that residential upholstered furniture (RUF) is a significant part of the national fire problem.

Many technologies have been introduced for reducing the flammability of RUF. Such technologies are effective either by decreasing the probability of ignition or limiting the intensity of an ignited piece of RUF. The goal of reduced flammability is to reduce fire losses—typically thought of in terms of deaths and monetary costs. Introduction of these technologies coincide with industrial, commercial, and environmental costs. It is therefore important to estimate the relative costs and benefits of any proposed flammability reduction technology. One approach for reducing RUF flammability is the addition of a barrier fabric between the upholstery and the padding material. Such barriers act by limiting heat and mass transfer between the padding material and the flame. Barrier fabrics can reduce heat release rate (HRR) of RUF, but it is uncertain to what extent this reduction in HRR affects life safety in typical residential fire scenarios. This report presents some preliminary research on a methodology for estimating the reductions in fire losses corresponding to the use of barrier fabrics in RUF.

The consequences of a fire may be predicted using a fire model. Several classes of fire models are available including simple algebraic correlations, computational two-layer zone models, and computational fluid dynamics (CFD) codes. The choice of model depends on what predictions are necessary, but in all cases some information about the fire scenario is needed. Relevant fire scenario information includes the building geometry (e.g., floor area, ceiling height, ventilation, etc.), construction materials, and the fire burning rate. For many applications such as fire protection engineering or fire scene reconstruction, the scenario parameters are known and can be directly applied as inputs to the model. However, in assessing the overall hazard facing a community, it is necessary to consider a broad range of scenarios. Two approaches are possible for accounting for the variability in fire scenarios. First, a select number of representative cases could be considered. If these cases are reasonably selected, then the model predictions could be used to estimate the fire hazard in the community. The weakness of this first approach is that it not always clear what cases are representative of realistic fire scenarios in the community. A second approach, and the approach taken in this report, is to estimate probability distributions describing the uncertain parameters in an RUF fire scenario. This method is more challenging because it requires statistics on the various scenario parameters used as inputs to the fire model. A key element of this research then is to gather and analyze the available data on residences in the community. Note that the methodology is general, and can be applied to estimating the effects of other actions intended to reduce fire losses.

Gathering residential building statistics is the first step in estimating fire losses. The second crucial step is a methodology for propagating this variability through the fire model. In almost all realistic applications it is necessary to use a numerical approach for uncertainty propagation. In this report, Monte Carlo (MC) simulation is suggested as robust method for propagating the uncertainty in building parameters through fire models. Because of the large number of simulations required to obtain accurate MC results, an efficient fire model is necessary.

A complete analysis of the potential benefits of a flammability technology should include a consideration of the causes and locations of deaths in residential fires. Gann et al. [3] analyzed the fire statistics between years 1986 and 1990 and found that around 10 times as many deaths outside the room of fire origin were attributed to smoke inhalation as compared to burns. Such data may be used in conjunction with the results presented in this paper to estimate the potential reduction in fatalities associated with the widespread use of an effective barrier fabric.

In this report, the methodology sketched above is described in detail and applied to the case of a single RUF chair with several different cover and barrier fabric combinations. Future work should include the effects of secondary combustible items on the predicted fire losses. Additionally, hazard was quantified exclusively by either the occurence of flashover or a thermal fractional effective dose (FED), and so a more complete analysis should include the hazard due to toxic gases. The research presented in this report is primarily devoted to developing a methodology for estimating fire losses. The implementation of this methodology is currently in a prototype form, and therefore the emphasis will not be on the predicted results. Future work is necessary to study and improve the data and models, which are essentially inputs into the methodology. It is hoped that improvements to the present prototypical methodology will be suggested and even implemented by a variety of experts interested in reducing the fire problem. In the remainder of this section, a brief survey of the relevant literature is presented, and the remainder of the report is outlined.

1.2 Literature Review

Several similar studies have been reported in the literature. In this section, a brief overview of related work is provided.

Bukowski [4] used a zone model to predict the hazard of various RUF fires in a three room layout. The varied parameters were floor plan geometry, wall materials, heat of combustion of the fuel, the smoke fraction produced, the RUF burning rate, and the presence of an open door. These parameters were typically varied to one or two values other than the nominal values. Hazard was quantified in terms of gas temperatures, hot gas layer (HGL) height, optical density, and thermal FED. It was found that the hazard criteria are most sensitive to the burning rate of the fuel. The results of this analysis are qualitative due to the limited number of cases considered and the fact that these cases are not rigorously connected to real fire scenarios through well-characterized building data.

The methodology described in the preceding paragraph was implemented in the software HAZARD I [5]. HAZARD I was designed with a focus towards single-family residential structures. The zone model FAST in conjunction with evacuation models were used to predict fire losses. The authors cautioned that the results should only be used for comparisons between products as the models were not developed enough to make precise predictions. The HAZARD I model was applied to a typical ranch home kitchen fire with multiple occupants.

An approach very similar to that of the present report was developed by Clarke et al. [6]. The objective of the referenced research was to use fire and egress models in conjunction with fire data to estimate the change in hazard associated with a change in product. Several applications were studied including the hazard of RUF [7]. The weightings of the specific fire scenario parameters (e.g., time of day, mobility, house size, etc.) were mostly based on data from the national fire statistics. Some of the weightings for RUF were provided by an expert panel. For the furniture application, the modeled fires were assumed to take place in a prototypical ranch home. Fire dynamics and egress were modeled using HAZARD I. The predicted fire deaths compared well with the deaths recorded in the available fire statistics. The research examined the sensitivity of the results to such factors as the locations of the occupants, the potential for occupant rescue, occupant delay in evacuating the house, duration of pre-flamming smoldering, thermal window breakage, and the home size.

The hazard of a single room scenario was explored by Babrauskas [8]. HAZARD I was used to predict the hazard for several cases in which the HRR, toxicity, and ignition time of the RUF fire were varied. Hazard was quantified in terms of gas temperature exceeding 100 °C and the toxicity concentration-time product exceeding 900 g min/m^3. It was concluded that life safety is much more strongly dependent on HRR as compared to toxicity. This is primarily a consequence of the fact that only pre-flashover cases were considered in which the toxicity of gases is relatively low.

Peacock et al. [9] studied flashover using several correlations in addition to the Consolidated Model of Fire and Smoke Transport (CFAST). Flashover is typically defined in terms of the conditions needed to ignite certain target materials within the room of fire origin. Flashover is relevant to hazard in that a post-flashover compartment is certainly untenable and will produce much toxic gas that may be transported to other rooms within the home. Recommended flashover criteria are temperatures exceeding 600 °C and floor heat fluxes greater than 20 kW/m^2. It was found that correlations such as those of Thomas [10] and McCaffrey et al. [11] are able to predict flashover just as well as CFAST for the scenarios considered. In a continuation of this work, Babrauskas et al. [12] found that there was considerable variability in the occurrence of flashover as a function of HRR in rooms of similar geometry. This variability was attributed to differences in the dynamic behavior of HRR versus time curves. Such behavior is not accounted for in typical correlations. CFAST simulations were used to show that there is a broad range of critical HRRs needed for flashover. Although the critical HRR was found to depend strongly on the time at which flashover occurs, simulations indicate that the results are relatively insensitive to the shape of the HRR curve.

In order to assess the reduction in fire losses associated with a changed mattress flammability standard, Ohlemiller and Gann [13] used CFAST to predict the spread of smoke throughout a four room structure. This structure was similar to that used by Bukowski [4], but with an additional large compartment to account for the rest of the house. Variations were made to the size of the room of fire origin as well as the door opening fraction. It was found that a reduction in HRR did not eliminate all risk to the occupants, but that it did lead to a much reduced probability that a nearby item would be ignited. From an investigation of fire statistics, it was determined that a significant reduction in HRR would result in a significant reduction in the number of flashovers. Consequently, fire losses would be significantly reduced.

The potential for sublethal incapacitation in fires was studied by Peacock et al. [14] using CFAST. In this work it was noted that a significant limitation of CFAST is an inability to account for the toxicity associated with under-ventilated fires. Three scenarios were simulated: a ranch house, a hotel, and an office. Tenability was accounted for using a thermal FED based on heat and incapacitating asphyxiant gases. Calculation of this FED was based on the models given in ISO 13571 [15]. It was found that time to incapacitation due to heat was much smaller than the time to incapacitation due to asphyxiant gases except for cases of smoldering. Fire deaths due to toxic gas inhalation mostly occur post-flashover.

Several papers have demonstrated methods for propagating uncertainty through fire models. Upadhyay and Ezekoye used the Quadrature Method of Moments (QMOM) to propagate HRR uncertainty through CFAST and an algebraic model for layer height [16]. Layer height cumulative distribution functions (CDFs) were reconstructed using a generalized lambda distribution. The results of the QMOM simulations compared favorably with those obtained by more thorough Monte Carlo simulations. This indicates that efficient methods such as QMOM could be used to adequately propagate uncertainty through fire models.

Monte Carlo simulation of CFAST was used to determine the effects of HRR curve uncertainty on the Available Safe Egress Time (ASET) by Kong et al. [17]. Latin hypercube sampling was used to improve efficiency. Two uncertain parameters, peak HRR and fire growth rate, were considered as random model inputs and modeled as normal or log-normal probability distributions. An extremely large single compartment, representing a commercial building was considered, and the results were presented along with a sensitivity analysis.

From the above discussion, it is clear that both fire hazard analysis and uncertainty propagation are important technical problems. Furthermore, these issues have been studied extensively individually, but relatively little work has been done on the convergence of these two problems. A major contribution of the research presented in this report is a method to use rigorous uncertainty propagation techniques for the analysis of fire hazard in residential scenarios.

1.3 Outline of Report

The objective of this research is to use modeling and simulation to estimate the fire safety benefits of using barrier fabrics in RUF. In the next section, the probabilistic method used to achieve this goal is described. Section 3 presents the data needed to apply the methodology to the problem of RUF fires. The two fire models used to predict fire hazard from the uncertain inputs are discussed in Sec. 4. Results are presented in Sec. 5, and summarized in Sec. 6. Note that confidence in the estimated fire losses depends on the quality of both the models and the data, and future work will be directed towards increasing this confidence.

Section 2

Predicting Fire Losses

2.1 Models for Fire Losses

To investigate the potential benefits of using barrier fabrics in residential upholstered furniture (RUF), it is necessary to have a method for using available data to predict these benefits. In fire safety, the benefit of an action is typically measured by the resultant reduction in fatalities or property loss. Thus, the most beneficial action is the one with the smallest estimated *fire losses*. In this section, a probabilistic approach is presented for using fire models to estimate fire losses.

It is helpful to begin by developing a mathematical formalism for describing the loss due to a fire and its relationship to the relevant details of the home in which that fire takes place. That relationship is essentially a fire model. For example, there are several algebraic correlations used to predict the temperature in a compartment as a function of the heat release rate (HRR) of a fire. In addition to the HRR, such correlations will require some information on the size and shape of the compartment. So in this case, the temperature is the loss metric (as a surrogate since higher temperatures are more likely to result in deaths and structural damage), the correlation is the fire model, and the HRR and compartment geometry are the scenario parameters. For this report, the situation is complicated because the scenario parameters and, consequently, the loss metric are uncertain. In order to avoid ambiguity, the preceding discussion is now described mathematically.

The fire losses may be quantified as l, representing monetary costs, deaths, resources, or any other appropriate measure. The loss metric l can be applied to a building, community, state, nation, or any other system susceptible to fire. To evaluate the effectiveness of an action (e.g., the selection of a barrier fabric), the action must be parameterized through a set of *controlled parameters*, θ. It is important to emphasize that the controlled parameters are chosen by an engineer or decision maker. For example, in the case of barrier fabrics, θ could denote different types of barriers, and the RUF manufacturer has complete freedom to select whatever barrier fabric that most satisfies their design and safety requirements.

Fire scenarios can vary considerably, and so it is necessary to approach the problem probabilistically. In the field of probability and statistics, it is common to distinguish the value actually taken by a random variable and the random variable itself. This is accomplished notationally by using an upper case letter for the random variable, and the lower case equivalent for the value of a particular instantiation of that variable. The random variable for loss is thus denoted as L. The appropriate representation of a random variable is a probability distribution. The remainder of this section will involve describing how to use fire models in conjunction with relevant data to estimate the probability distribution for fire losses given a choice of the controlled parameters. This probability distribution will be denoted as $f_L(l|\theta)$ if l is a continuous variable, or $\Pr(L=l|\theta)$ if l is a discretely distributed variable.

Determination of a probability distribution for L in terms of the controlled parameters, requires a model relating the loss metric, l, to θ. Such a loss model will typically consist of a fire model component that relates the physical parameters describing the scenario, x, to the resultant environmental conditions in a structure as a consequence of a fire. Fire models can range from simple empirical correlations to sophisticated computational fluid dynamics (CFD) software.

A complete loss model requires additional considerations beyond the purely physical nature of a fire model. Loss models may be extremely complicated, especially if the loss metric involves human life. Such loss models require knowledge of physiology, human mobility, as well as fire detection and suppression technologies. In the present work, evacuation, detection, and suppression are not considered.

Conceptually, a loss model can be thought of as a map of the scenario parameters to the loss metric:

$$l = g(x) \tag{2.1}$$

In words, the loss model, g, takes the input scenario parameters, x, and predicts the loss metric, l. Equation (2.1) gives a single deterministic result for a single specified scenario. Therefore, Eq. (2.1) requires that the scenario described by x is known. It is further assumed that the scenario parameters are dependent on the controlled parameters, θ, in some way. That is, in order for the effect of the controlled parameter to be evaluated, it is necessary that θ have some effect on the scenario as it is described by the loss model. The simplest relationship would just be that one of the scenario parameters *is* the controlled parameter. For example, the scenario parameters could be the set $x = \{a, b, \theta\}$.

In general, the scenario is not precisely known and must be characterized as a set of random variables, X. The uncertainty of the scenario must be characterized from relevant statistics. The procedure of determining and applying these statistics is demonstrated in Sec. 3, but first it is appropriate to discuss how such information may be used to estimate fire loss probabilities.

2.2 Estimating Fire Loss Probabilities

The problem is to determine the uncertainty in fire losses from the uncertainty in the scenario. The approach taken to solve this problem is to use Monte Carlo simulation. In the context of uncertainty propagation, Monte Carlo simulation is the procedure of running a model many times for many different scenarios and then using the results to characterize the uncertainty in the outputs. The simulated scenarios are sampled from probability distributions describing the uncertainty in these parameters. For the example of a compartment temperature correlation, one would simply randomly select many values of HRR and compartment sizes to get a large number of predicted compartment temperatures. If the sampled values of HRR and the compartment sizes are representative of the uncertainty in these parameters, then the set of predicted values will be representative of the compartment temperature uncertainties. The process is straightforward, but a more mathematical description is given in the following for the sake of precision.

It is assumed that probability distributions for the scenario parameters are known. These parameters may be continuous or discrete and the uncertainty will be characterized by a mixed joint density function conditional on the controlled parameters, $f_X(x|\theta)$. In the following, it will be assumed that the loss metric is discretely distributed, but the continuous case is analogous. The relationship between the probability distribution for L and the probability distribution for X is

$$\Pr(L = l|\,\theta) = \int dx\; f_X(x|\theta)\phi\,[l = g(x)] \tag{2.2}$$

where $\phi\,[l = g(x)]$ is the indicator function that evaluates to one if $g(x) = l$ and is otherwise zero.

The integral in Eq. (2.2) is usually impossible to evaluate analytically. Fortunately, the problem is readily amenable to Monte Carlo simulation where the integral is approximated as

$$\Pr(L = l|\,\theta) \approx \frac{1}{N}\sum_{i=1}^{N}\phi\,[l = g(x_i)] \tag{2.3}$$

where the x_i are N samples from X. In practice, this requires a large number of samples, especially as the dimensionality of X increases. It is therefore necessary to have relatively efficient fire and loss models. An additional use of the Monte Carlo samples is to compute the expected value of L. This approximation is made from the samples using

$$\langle L(\theta)\rangle = \frac{1}{N}\sum_{i=1}^{N} g(x_i) \tag{2.4}$$

It will typically take fewer samples to accurately estimate $\langle L\rangle$ than it will to approximate $\Pr(L = l)$.

An more efficient alternative to Monte Carlo simulations is the quadrature method of moments (QMOM), which has been used to propagate uncertainty through fire models [16]. Although this procedure will not be used in the following, it is a potential tool for use in future extensions of this work.

Generally, there will be multiple scenario parameters, and $f_X(x|\theta)$ will be multivariate. Sampling from a multivariate function is not straightforward. For many cases, the random variables composing X will be independent. In such cases, the marginal distributions may be sampled separately. For cases in which the statistical model may be represented by a directed graph, it is possible to decompose the joint probability distribution into a product of conditional distributions. The set of model parameters is first partitioned into M subsets denoted x_i for $i = 1, \ldots, M$. The joint distribution function is then written as

$$f_X(x) = \prod_{i}^{M} f_{X_i}(x_i|x_i^*) \tag{2.5}$$

where x_i^* represent all variables upon which the set x_i depends. This representation makes it possible to do ancestral sampling of the joint distribution. For the simple case of one variable, X_2 having a known probability distribution conditional on the values of another variable, X_1, the joint distribution is sampled by taking random samples, $x_{1,i}$, from f_{X_1} and subsequently obtaining the samples $x_{2,i}$ by sampling from $f_{X_2}(x_2|x_{1,i})$.

The next section will discuss characterizing f_X for residential structures in the United States. This will involve collecting data for residential building geometries. Additionally, data is presented relating the controlled parameter, θ, which in this case is a label for a particular cover and barrier fabric combination, to one of the uncertain model parameters, which in this case is a HRR curve.

Section 3

Data

3.1 Overview

In order to analyze the consequences of a change in some controllable parameter θ, it is necessary to determine both the relationship of θ to the fire model and the probability distribution of the scenario parameters, X. In this section, the relevant data is compiled. The controllable parameter is the cover and barrier fabric combination used in an residential upholstered furniture (RUF) chair. The relationship between a particular fabric combination and the fire model is provided by experimental heat release rate (HRR) data for several chairs. A generic residential fire scenario is presented, and relevant building statistics for that scenario are collected, and summarized as probability distributions.

3.2 Chair Fire Data

The chair fire data were provided by the Consumer Products Safety Commission (CPSC). Experiments were performed in an open furniture calorimeter, and the relevant data is the HRR as a function of time. The HRR associated with these tests will tend to be different than that experienced by an identical chair burning in a compartment due to decreased ventilation and heat feedback from the walls. A decrease in ventilation can reduce the oxygen supply enough to reduce the gas phase combustion, but the available oxygen is not typically reduced significantly prior to flashover. Heat feedback from compartment walls and the hot gas layer (HGL) can cause the HRR to increase [18]. The CPSC tests were performed on chairs with the same geometry, foam, and construction. Three variables distinguished the tests: the cover fabric, the barrier fabric, and whether the chair had been repeatedly stressed. Note that the terminology “cover fabric” is used here to denote the outer layer of upholstery fabric. In cigarette smoldering tests, “cover fabric” typically refers to a small piece of fabric placed on top of the smoldering cigarette. For the purposes of this analysis, only the fabric combination was considered since the degree of stress a piece of furniture has experienced cannot be controlled in residential settings. Two cover fabrics were used. Both of these cover fabrics were tested four to seven times with one of six different barrier fabrics.

A total of 68 tests were analyzed. The HRR curves for all of these tests are plotted in Fig. 3.1 where the results have been separated into (a) cover fabrid 2 and (b) cover fabric (3). In many of

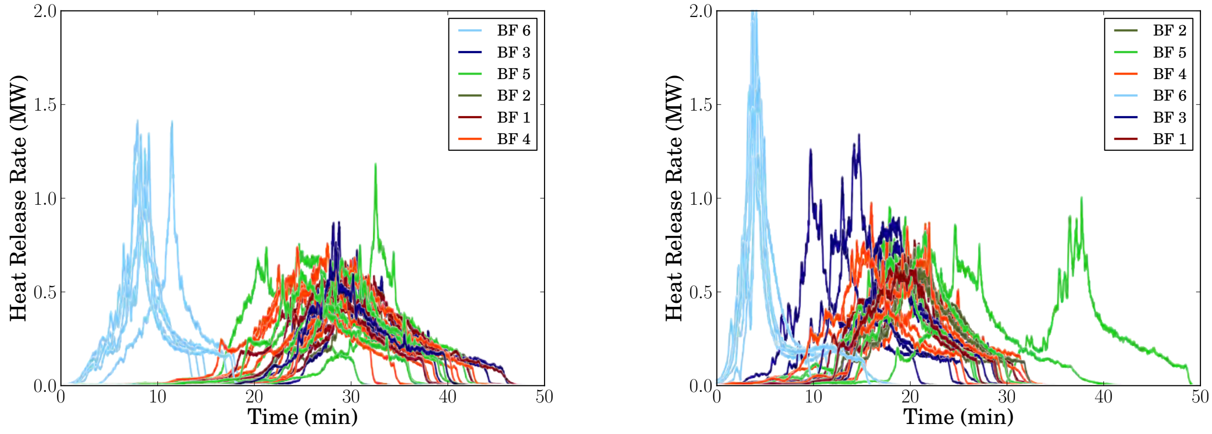

(a) (b)

Figure 3.1: CPSC chair fire HRR versus time curves for (a) cover fabric 2 and (b) cover fabric 3. "BF" denotes "Barrier Fabric".

the figures in this report, "CF" and "BF" will be used as shorthand for "Cover Fabric" and "Barrier Fabric", respectively. It is clear from Fig. 3.1 that the choice of cover and barrier fabric can have a significant influence on the time and value of the HRR peak. For cover fabric 2, the difference between barrier fabric 6 and the other barrier fabrics is significant.

To see these trends more clearly, a summary of the data in terms of the HRR peak is presented as a scatter plot in Fig. 3.2. The error bars Fig. 3.2 represent one standard deviation of the experimental data. The mean and standard deviation of the peak HRR data are tabulated in Table 3.1. Clearly, chairs using barrier fabric 6 have the highest peak HRR by a significant amount for both cover fabrics. It is also apparent that use of cover fabric 3 typically results in more intense fires. At the other end of the spectrum barrier fabric 2 seems to provide a significant amount of flammability reduction when coupled with either cover fabric. In general, it is seen that as the peak HRR decreases, the time until that peak is reached increases. This is explained by the fact that all chairs have about the same total heat release (integrated HRR), and so extending the fire over greater time results in a lower peak HRR.

The data presented above will be used as input into the loss models described in Sec. 4. These models predict the effects of a given fire in a compartment. It will be assumed that the burning rate of the chairs will be the same in the compartments as it was in the open calorimeter. This is not strictly valid because of heat feedback and potential ventilation effects that are absent in the furniture calorimeter. Some research has suggested that for fires with peak HRRs greater than around 2 MW, the HRR is relatively insensitive to enclosure effects [19]. A more recent and comprehensive research project, The Combustion Behaviour of Upholstered Furniture (CBUF) programme [18] compared peak HRRs measured in a furniture calorimeter to those measured in a room calorimeter. For peak HRRs less than 100 kW, there is little disparity between the room and open calorimeter results. Most of the data correspond to furniture that produced peak HRRs in the range of 400 kW to 1 MW in the furniture calorimeter. For most of this data, the furniture calorimeter tends to underpredict the corresponding room value. For some cases, the underprediction can be up to nearly

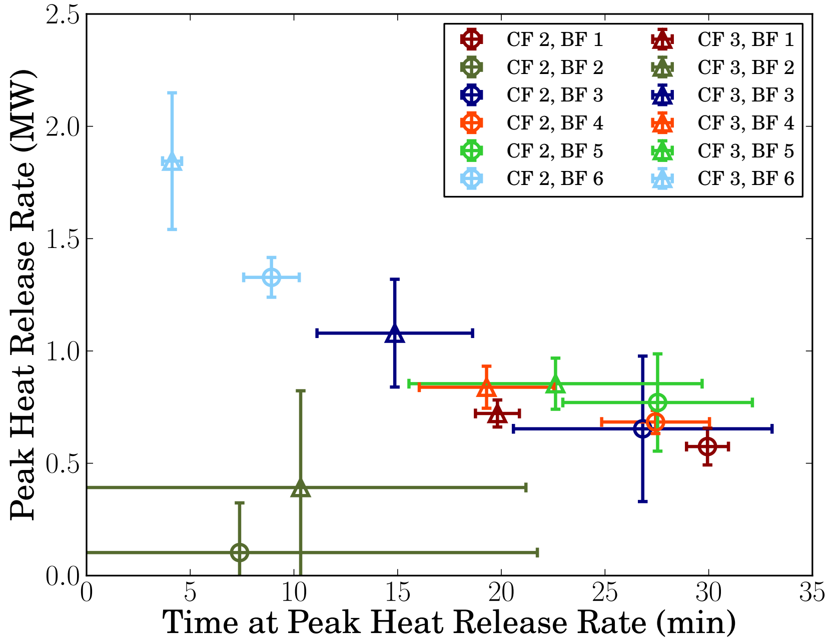

Figure 3.2: Average CPSC chair fire peak HRR versus average time to peak HRR.

Table 3.1: CPSC chair fire peak HRR mean and standard deviation.

Cover Fabric	Barrier Fabric	Replicates	Time of Peak HRR (min)	Peak HRR (MW)
2	1	4	29.9 ± 1.0	0.57 ± 0.08
2	2	5	7.4 ± 14.4	0.10 ± 0.22
2	3	6	26.8 ± 6.2	0.65 ± 0.32
2	4	7	27.4 ± 2.6	0.68 ± 0.05
2	5	6	27.5 ± 4.6	0.77 ± 0.22
2	6	6	8.9 ± 1.3	1.33 ± 0.09
3	1	4	19.8 ± 1.1	0.72 ± 0.06
3	2	6	10.3 ± 10.9	0.39 ± 0.43
3	3	5	14.9 ± 3.8	1.08 ± 0.24
3	4	6	19.3 ± 3.2	0.84 ± 0.09
3	5	7	22.6 ± 7.1	0.85 ± 0.11
3	6	6	4.1 ± 0.5	1.85 ± 0.30

600 kW. Since many of the chair fires considered in this report have peak HRRs in this range (see Table 3.1), it is necessary to note that the fire hazard might be underpredicted.

As an aid to relating the RUF HRR data to the loss models, it is helpful to make reference to some of the theory of Sec. 2. The controlled parameter for all cases is the fabric combination, and so it is appropriate to define θ as the tuple of $a \equiv (\mathrm{cf}, \mathrm{bf})$ where cf and bf are the cover and barrier fabric labels, respectively. This ordered pair influences the fire model through the HRR, $\dot{Q}$, which will be treated as an uncertain scenario parameter, $\dot{Q}^*$—here the superscripted asterisk denotes that the variable is a random variable. Three approaches are taken for the two loss models. The first two approaches are for sampling just the peak HRR, while the third approach is for sampling the entire HRR versus time curve. The first and second sampling approaches are distinguished by the underlying distribution. In the first approach, the sampled values are taken to be one of the experimentally measured peak HRRs for a particular fabric combination. The second approach is based on sampling from a continuous probability density function (PDF) that was fit to the experimental data. The first and third approaches utilize discrete probability distributions, while the second approach utilizes a continuous probability distribution. The choice of approach for modeling the HRR uncertainty will depend on the model and the method used. In the analysis of this report, all three approaches will be used. These approaches are described formally in the following paragraphs.

In some cases, only the peak HRR, $\dot{Q}_p$ is necessary. So the first approach is to just sample from the available experimental peak HRR values for a given fabric combination. Assuming a uniform distribution among the measured values, the appropriate probability distribution is

$$\Pr\left(\dot{Q}_p^* = \dot{Q}_{p,j} | a\right) = \frac{1}{N_a}, \quad j = 1, \ldots, N_a \tag{3.1}$$

where $\dot{Q}_{p,j}$ is one of the measured peak HRRs for fabric combination a, and N_a is the number of replicate experiments for fabric combination a (see the third column in Table 3.1).

A second approach is possible when only the peak HRR is needed. In this approach, the statistics listed in Table 3.1 are used to define a probability density function (PDF) for the peak HRR. In many physical processes, a normal distribution is a reasonable model of stochastic behavior. However, the requirement that $\dot{Q} > 0$ necessitates the use of a truncated normal distribution. For distributions truncated at zero, this PDF assumes the form

$$f_{\dot{Q}_p^*}\left(\dot{Q}_p | a\right) = \frac{\exp\left[-\left(\dot{Q}_p - \mu_a\right)^2 / 2\sigma_a^2\right]}{\sigma_a\sqrt{2\pi}\left\{1 - \frac{1}{2}\left[1 + \operatorname{erf}\left(-\mu_a/\sigma_a\sqrt{2}\right)\right]\right\}} \tag{3.2}$$

where μ_a and σ_a are the mean and standard deviation for the peak HRR of combination a as listed in the last column of Table 3.1.

A third approach is needed for cases in which the entire HRR versus time curve is needed. In such scenarios, it is appropriate to sample the experimental curves directly. Since the full HRR curve must be represented by a large number of points, it is not straightforward to develop statistical models for each point in the curve. Therefore, a sample will be an entire experimental HRR curve represented as a set of time-HRR pairs: $\gamma \equiv \left\{\left(t, \dot{Q}\right)\right\}_i$. Each experiment corresponds to a set of time-HRR pairs, and the probability of sampling a single γ will be uniform across the available HRR curves for a given fabric combination, a. That is, if γ_j denotes a time-HRR curve corresponding to fabric combination a, then

$$\Pr\left(\Gamma = \gamma_j | a\right) = \frac{1}{N_a}, \quad j = 1, \ldots, N_a \tag{3.3}$$

The choice of using Eq. (3.1), Eq. (3.2), or Eq. (3.3) will depend primarily on what information is required by the model. As will be seen in Sec. 4, the MQH correlation requires that only a single value of $\dot{Q}$ be given. For all of the MQH calculations then, either Eq. (3.1) or Eq. (3.2) will be used. Conversely, for the CFAST model, a time dependent HRR curve is required, and so Eq. (3.3) must be used.

3.3 Building Statistics

The consequences of a RUF fire depend on the scenario. The scenario is defined by the building, its contents, and the people present at the time of the fire. Residential buildings are exceptionally varied in construction so not all potential scenarios can be analyzed. However, it is possible to design a representative set of residential structures by reference to the appropriate building statistics. A generic three room building section is presented. This building section is characterized by several variables. Some of these parameters are assumed to be known. Other building parameters are uncertain. These uncertain variables are characterized by the probability distributions presented in this section.

Previous researchers have used three room models to analyze the effects of furniture fires (e.g., in [4]). Such models allow for the examination of fire hazard in both the room of origin as well as in connected rooms. The generic model used in the present research is sketched in Fig. 3.3. In this set of scenarios, it is assumed that the fire occurs in the living room, which has a floor area of A_1. The geometry of this room influences heat losses, and so the aspect ratio of the room, $\eta_1 \equiv L_1/W_1$, must be considered. Since the location of the fire with respect to the walls can have a significant effect on the development of the hot gas layer (HGL), it is necessary to introduce a fire location parameter, $\mathscr{X}$, that specifies whether the fire is in the center of the room, against a wall, or in a corner. Hot gases from the fire can spread through the doors, $\mathscr{D}_{12}$, $\mathscr{D}_{13}$, and $\mathscr{D}_{23}$, which may or may not be open. Hot gases can spread down the hall, which has a variable width of W_3, but the length of the hallway is determined by A_1, η_1, and the area of the bedroom, A_2. The ceiling height, H, is assumed to be the same throughout the home. Note that the generic home model of Fig. 3.3 will have a limited supply of oxygen due to the assumption that all ventilation to the remainder of the house is closed. No data was found on whether this assumption is typical of U.S. homes, but future work should examine the sensitivity of the hazard assessments to the availability of additional air from non-participating compartments.

A list of all of the variable building parameters is provided in Table 3.2. For each of these parameters, a probability distribution must be determined. Before discussing this, however, a few constant parameters will be introduced.

Several of the building parameters required by the models are assumed to be constant. Based on minimum requirements from the International Residential Code (IRC) [20], the door heights

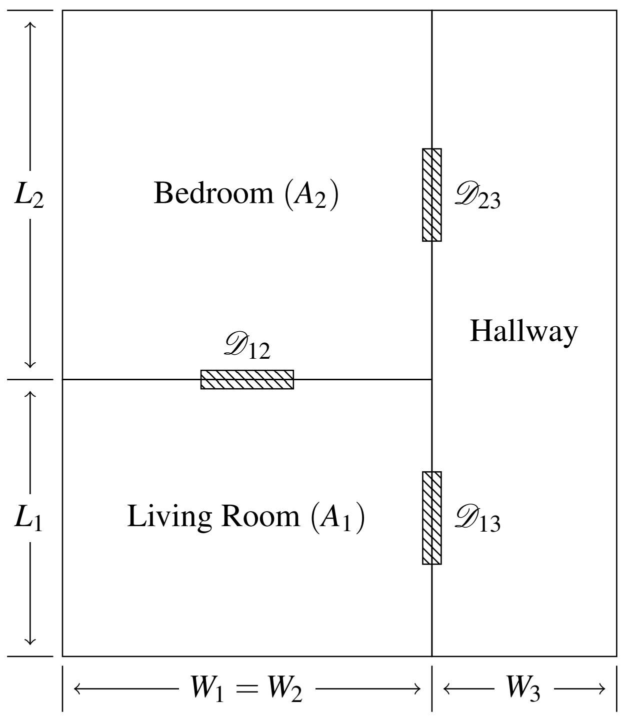

Figure 3.3: Schematic of three-room layout for residential fire scenarios.

Table 3.2: Random variable building parameters considered in analysis.

Parameter	Notation (units)
Living Room Area	A_1 (m^2)
Bedroom Area	A_2 (m^2)
Living Room Aspect Ratio	η_1 (-)
Ceiling Height	H (m)
Door Openings	$\mathscr{D}_{ij}$ (-)
Hall Width	W_3 (m)
Fire Location	$\mathscr{X}$ (-)

Table 3.3: Constant building parameters used in models.

Parameter	Notation (units)	Value
Door Height	H_d (m)	1.98
Door Width	W_d (m)	0.81
Wall Thickness	L_w (m)	0.0127
Wall Thermal Conductivity	k_w (W/m·K)	0.28
Wall Density	ρ_w (kg/m^3)	810
Wall Specific Heat Capacity	c_w (J/kg·K)	1000
Ambient Temperature	T_∞ (K)	295.15

are held constant at 78 in (1.98 m), and the door widths are always 32 in (0.81 m). The walls are assumed to be made of standard 0.5 in (0.0127 m) gypsum wallboard. Thermophysical properties of the gypsum were taken from reference [21]. An ambient temperature of 22 °C (295.15 K) is in all simulations. A summary of the constant parameters is provided in Table 3.3.

In the remainder of this section, probability distributions are specified for each of the uncertain building parameters. These distributions are based on available data as much as possible. In cases where the data were unavailable, the minimal assumption about the variable was assumed—in most cases, the minimal assumption is that of a uniform probability for all possible values. Improvements to the analysis can be made by the application of better data to the stochastic representation of the scenario.

As a preliminary to developing realistic probability distributions for the living room and bedroom areas (A_1 and A_2, respectively), data on the total square footage of residential units was sought. Such data were obtained from the United States Census Bureau's 2013 American Housing Survey (AHS) [22]. The results of this survey include information on the number of residential units in a given range of floor area. The data from the AHS does not include explicit lower and upper bounds. That is, the lower bin is given as including all homes with square footage less than 500 ft^2, and the upper bin is given as including all homes with square footage greater than 4000 ft^2 (371.6 m^2). Therefore, it was necessary to make assumptions on the lower and upper bounds of the data. An assumed minimum of 400 ft^2 (37.2 m^2) and a maximum of 6000 ft^2 (557.4 m^2) were selected. The results should not be too sensitive to this choice of bounds since they represent a small portion of the total probability mass. This data is represented as a cumulative distribution function (CDF) in Fig. 3.4.

The data on total home area was used in conjunction with results from the National Association of Home Builders (NAHB) [23] to arrive at estimates on the distributions of living room and bedroom floor areas. The NAHB report [23] surveyed builders of single-family homes on the distribution of total home area between the various rooms in the house. In particular, the average area of the master bedroom and the living room were reported for homes of "small", "average", and "large" sizes. This data is provided in Table 3.4.

Lines were fit to this data to give relationships for the average room floor areas, A_1 and A_2, as functions of the total home area, A_T. These lines could be used to obtain samples of A_1 and A_2 given a sampled value of A_T in accordance with the ancestral sampling procedure described

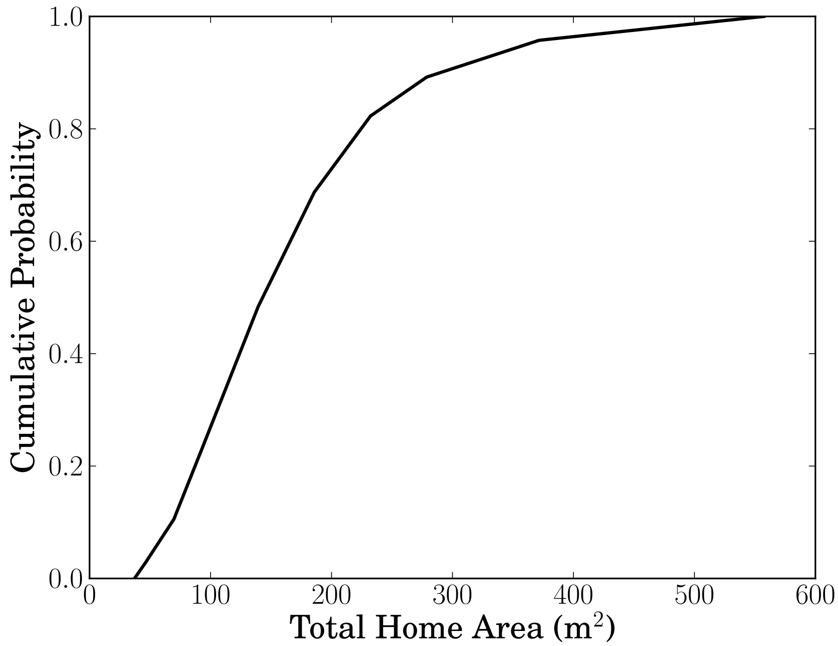

Figure 3.4: Cumulative distribution function (CDF) of total residential floor area.

Table 3.4: Average room floor area from NAHB data [23]

Home Size	Total Home (m^2)	Living Room (m^2)	Bedroom (m^2)
Small	151	17.9	21.4
Average	240	20.7	28.7
Large	351	26.2	38.2

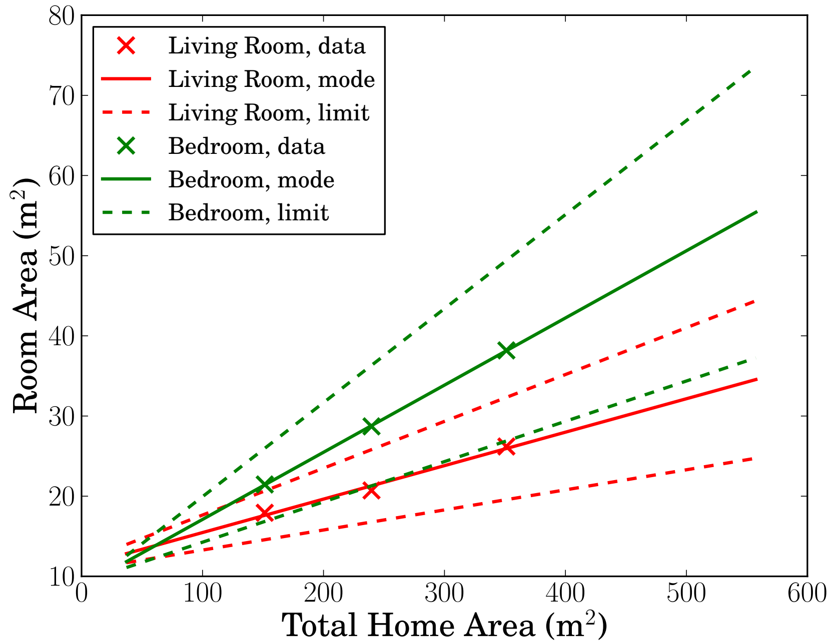

Figure 3.5: Room area triangular PDF parameters as a function of total home area.

at the end of Sec. 2. However, there is likely to be some variability in the relationship between the room floor areas and the total home floor area. Such variability was allowed for by assuming triangular probability distributions about the average values for the living room and bedroom areas. Triangular distributions are three parameter PDFs requiring lower and upper bounds in addition to the peak value. Symmetric distributions are assumed so that the peak value, $A_{i,p}$ is just the average value predicted from the correlation between the room and total areas. The lower and upper bounds were determined as $A_{i,p} \pm \delta\,(A_{i,p} - A_{\min})$ for $i = 1,2$ where δ was chosen to be 0.4 and $A_{\min} = 10$ m^2. These parameter values are somewhat arbitrary, but they reasonably represent the large uncertainty in room area variation. A plot of the three triangular distribution parameters along with the NAHB data is provided in Fig. 3.5.

Samples for the living room and bedroom areas were obtained from ancestral sampling as follows. A sample of the total home area, $A_{T,i}$ was obtained from the CDF plotted in Fig. 3.4. Corresponding samples for $A_{1,i}$ and $A_{2,i}$ were taken from the triangular distributions with parameters corresponding to the lines plotted in Fig. 3.5. The resultant CDFs for the room areas are shown in Fig. 3.6. It is seen that the median room areas are around 20 m^2.

The next uncertain parameter to be considered is the living room aspect ratio, η_1. No data was found on this parameter, and so a uniform distribution was assumed between the bounds of 0.5 and 1. Note that it is not necessary to extend this distribution above 1 since this would just replicate a room geometry below 1. For example, two rooms of the same floor area and with aspect ratios of 3/4 and 4/3 are equivalent.

Ceiling height data was obtained from the U.S. Energy Information Administration's Residential Energy Consumption Survey (RECS) [24]. In response to the question of whether they had

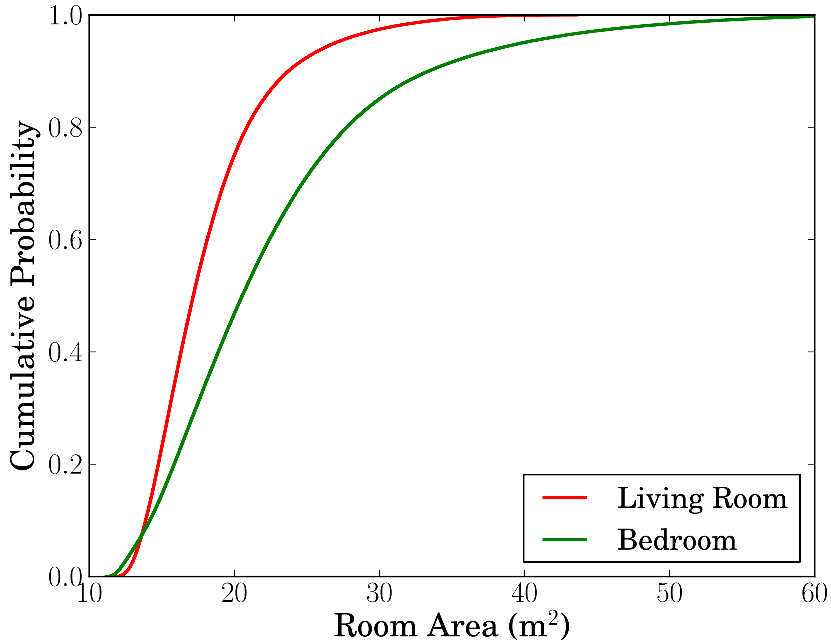

Figure 3.6: Cumulative distribution functions (CDFs) for room floor areas.

“unusually high ceilings” (defined as greater than 8 ft (2.44 m), 27 % of respondents replied “yes”. A piecewise linear CDF was assumed since no other information was found. A lower bound was chosen of 7 ft (2.13 m) based on the minimum height in the IRC [20]. The upper bound on ceiling height was estimated to be 10 ft (3.05 m). The resultant CDF for ceiling height is plotted in Fig. 3.7.

It is significantly more difficult to estimate the likelihood that any of the doors shown in Fig. 3.3 will be open. The state of the doors will be represented by the 3-tuple $\mathscr{D} \equiv (\mathscr{D}_{12}, \mathscr{D}_{13}, \mathscr{D}_{23})$, where the elements of $\mathscr{D}$ assume values of 1 if that door is open and zero if that door is closed. For scenarios in which both living room doors are closed, it is impossible for occupants in other rooms to be at risk (at least under the assumptions of the model). Furthermore, flashover is not really well-defined for under-ventilated compartments. In order to avoid the case with no ventilation, it is assumed that at least one of the living room doors is opened. This results in a total of six possible cases for the door state tuple: (1,0,0), (0,1,0), (1,1,0), (1,0,1), (1,1,1), and (0,1,1). It is assumed that the probabilities of these six states are the same and therefore equal 1/6.

The width of the hall, W_3, is uncertain. A lower bound of 3 ft (0.91 m) is chosen based on the requirement of the IRC [20]. The upper bound was assumed to be equal to 6 ft (1.83 m). A uniform PDF was assumed between these two values. It is likely that there is a strong correlation between W_3 and the total area of the home, A_T. However, this correlation is unknown at present, and so W_3 is allowed to be independent of A_T.

The final uncertain parameter that must be characterized is the fire location parameter, $\mathscr{X}$. The necessity of including this parameter is due to the fact that the HGL temperatures are significantly increased if the fire is next to a wall or in a corner. Therefore, $\mathscr{X}$ is allowed to be discretely

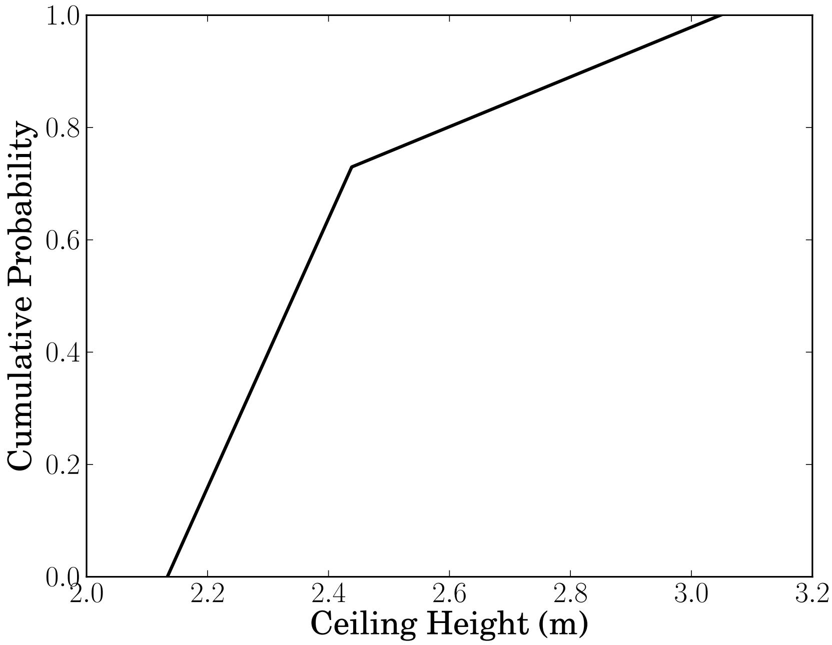

Figure 3.7: Cumulative distribution function (CDF) for ceiling height.

distributed between locations in the center of the room, against a wall, or in a corner. No data is available on how people actually distribute furniture in their homes, and so the minimal assumption of uniform probability is required once again. In particular, it is reasonable that the furniture be at any location in the room with equal probability. It is more likely that a piece of RUF will be in a corner or against a wall in a smaller room as compared to a larger room. Thus, the probability of the furniture being in one of the three possible locations is assumed to be proportional to the relative area of that location for the given room. It is apparent that these probabilities are

$$\Pr(\mathscr{X} = \text{Corner}) = \frac{4L_f^2}{A_1} \tag{3.4}$$

$$\Pr(\mathscr{X} = \text{Wall}) = \frac{2L_f(W_1 + L_1) - 4L_f^2}{A_1} \tag{3.5}$$

$$\Pr(\mathscr{X} = \text{Center}) = 1 - \Pr(\mathscr{X} = \text{Corner}) - \Pr(\mathscr{X} = \text{Wall}) \tag{3.6}$$

where L_f is the characteristic dimension of the furniture. Note that this model assumes that the furniture is approximately square, and that furniture can be located in front of open doors. The first assumption is acceptable for the purposes of this research as square RUF chairs are the fuel source. The second assumption will have little effect for most rooms as the door width is much less than the perimeter of the living room. Because the probabilities in Eqs. (3.4)-(3.6) are conditional upon the area and aspect ratio of the living room, it is necessary to use the ancestral sampling procedure described at the end of Sec. 2 in which samples for A_1 and η_1 are generated and then used to generate a sampled value of $\mathscr{X}$.

All of the uncertain parameters listed in Table 3.2 have been characterized in terms of probability distributions. In general, samples are produced through random number generation and the inverse CDFs of the building parameters. In some cases, the SciPy "stats" module [25] is used to draw samples from discretely distributed random variables. The samples must be drawn in a specific order due to the dependencies discussed above. Specifically, a total room area sample must precede the room area samples, and the living room area and aspect ratio samples must precede the fire location sample.

The probability distributions presented in this section were used to estimate fire losses. This is achieved by Monte Carlo simulations in which samples from these probability distributions are used as inputs to one of two fire models. In the next section, these fire models are discussed.

Section 4

Model Descriptions

4.1 Overview and Selection of Loss Metrics

The selection of an appropriate loss model is a coupled process. First, the appropriate loss metric, l, must be selected, and then a model must be found that predicts l. That model will depend on some set of environmental parameters, and a fire model must be chosen that predicts these quantities. The controlled parameters, θ, must have some influence on the fire model or its input parameters so that the effects of varying these parameters can be studied.

In this section, two loss models are described. The first is based on an empirical correlation for the hot gas layer temperature (HGL) in the room of fire origin—in this case, the living room. The second model is based on a zone model used to predict HGL temperature and height in all three rooms of the test home described in the previous chapter. In both cases, the loss metric is assumed to be the occurrence of fatal conditions in the house during the course of the fire. This definition for l does not equate to the number of fatalities since no assumptions have been made with regard to the presence of people in the home. Future work should incorporate a statistical description of the presence of people throughout the home. Such a description would extend the results of the present work beyond a rough measure of the potential for fatalities to the actual expected number of fatalities.

Predicting fatalities depends on many different factors such as the number and age of building occupants as well as the presence of smoke detectors or sprinklers. While consideration of evacuation, detection, and suppression is a possible avenue for future work, such factors are beyond the scope of the present research. In this report, two criteria are used to evaluate tenability: transition to flashover and thermal fractional effective dose (FED).

After a compartment has transitioned to flashover, most combustibles in the room will be burning, and the fire will be under-ventilated. In all cases, the compartment will be uninhabitable, and hot, toxic gases will be transported throughout the residence. Therefore, occupants in connecting rooms are at considerable risk in a post-flashover scenario. It has been suggested that compartment fires transition to flashover once the HGL temperature exceeds 500 °C to 600 °C [10]. For cases in which the ambient temperature is 22 °C, this results in a range of flashover temperature rises of ΔT between 478 °C and 578 °C. In the analysis of Sec. 5, it will be assumed that a temperature rise of 500 °C results in flashover. Using a temperature from the lower end of the flashover range is a conservative estimate as it will tend to over-predict the frequency of flashover. Future work should consider the sensitivity of the results to the choice of flashover temperature.

The second loss model is based on the concept of a thermal FED. The thermal FED is the ratio of the dose received to a critical dose usually associated with lethality or incapacitation [26]. The dose is typically associated with a toxic gas (e.g., carbon monoxide or hydrogen cyanide) or heat exposure. In this case, only the hazard associate with heat is considered, since the production of toxic gases is relatively small for well-ventilated, pre-flashover fires. There is some literature to indicate that, indeed, heat exposure represents a significantly greater threat to life safety as compared to toxic gases in residential fires [14]. It is recommended [15] that the thermal FED be computed as

$$F(t) = \int_0^t \left(\frac{(q''(t'))^{1.33}}{r} + \frac{(T(t'))^{3.4}}{5 \times 10^7} \right) dt' \tag{4.1}$$

where q'' is the radiant heat flux in kW/m^2, r is the radiant exposure dose, and T is the temperature in °C. All times are in minutes. Equation 4.1 accounts for both exposure of skin to radiant and convective heat. The choice of r depends on what threshold is appropriate. For the analysis of this report, a value of $r = 16.7$ will be used as representative of a dose resulting in 50 % fatalities for the average population. Note that incapacitations could occur at thresholds much lower than this, especially for vulnerable populations. The choice of r was made in order to consider the most serious risks to the occupants and is therefore not conservative. Future analysis should take into account a range of critical radiation threshold values.

Fatal conditions are predicted by both the transition to flashover of the room of fire origin and the thermal FED in the living room. The application of these models in conjunction with the data presented in Sec. 3 will be used in Sec. 5 to predict the probability of lethal conditions in a fire associated with a given fabric combination.

4.2 Empirical Correlation

Several correlations have been developed for estimating temperatures in compartment fires [27]. Such correlations are typically based on an energy balance where unknown parameters are lumped together and then calibrated to experimental data. A widely used correlation for hot gas layer (HGL) temperature in naturally ventilated compartments was developed by McCaffrey, Quintiere, and Harkleroad [11]. This so-called MQH correlation was fit to data from over 100 experimental sets, and has been validated against several sets of additional data [28]. The basic form of the MQH correlation is

$$\frac{\Delta T}{T_\infty} = 1.63 K_x \left(\frac{\dot{Q}}{\rho_\infty c_{p,\infty} A_o \sqrt{g H_o} T_\infty} \right)^{2/3} \left(\frac{h_w A_w}{\rho_\infty c_{p,\infty} A_o \sqrt{g H_o}} \right)^{-1/3} \tag{4.2}$$

where $\Delta T \equiv T - T_\infty$, T is the HGL temperature, T_∞ is the ambient temperature, K_x is a factor to account for the location of the fire within the room, $\dot{Q}$ is the HRR of the fire, ρ_∞ is the density of ambient air, $c_{p,\infty}$ is the specific heat of ambient air, A_o is the area of the vent opening, H_o is the top height of the vent opening, g is the gravitational acceleration, h_w is the effective heat transfer coefficient of the walls, and A_w is the total wall area. The factor K_x is used to correct for whether the chair is in the center of the room ($K_x = 1$), against a wall ($K_x = 1.3$), or in a corner ($K_x = 1.7$). The values of these coefficients are based upon the empirical results of Mowrer and Williamson [29].

The effective heat transfer coefficient is typically modeled by assuming that the walls are thermally thick or thermally thin. The characteristic penetration time of the wall, t_w, is calculated as

$$t_w \equiv \left(\frac{\rho_w c_w}{k_w}\right)\left(\frac{L_w}{2}\right)^2 \tag{4.3}$$

where ρ_w is wall density, c_w is the wall specific heat, k_w is the wall thermal conductivity, and L_w is the thickness of the wall. For times less than t_w, the wall is assumed to be thermally thick, and the effective heat transfer coefficient is computed as

$$h_w = \sqrt{\frac{k_w \rho_w c_w}{t}} \tag{4.4}$$

At times greater than t_w, it is typically assumed that the wall is thermally thin so that $h_w = k_w/L_w$. For standard 1/2 in gypsum wall board with the properties listed in Table 3.3, the penetration time is found to be less than about two minutes. Examination of the chair fires in Fig. 3.1 reveals that the widths of the heat release rate (HRR) peaks at half-height is approximately 3 to 6 minutes. Because of the sharpness of the peaks, though, it is difficult to say whether or not either a thermally thick or a thermally thin approximation is valid. In any case, the MQH simulations presented in Sec. 5 were performed using a switch between thermally thick and thin at the penetration time. This ended up being a conservative estimate, since the times at the peak HRR were in the thermally thin regime for all cases. A thermally thin model will tend to set a lower bound on heat losses from the room, and so the results are conservative with respect to the upper layer temperature—that is, the HGL temperature will tend to be overestimated.

The parameters in Eq. (4.2) may be expressed in terms of the parameters discussed in Sec. 3. The total wall area may be computed as

$$A_w = 2H(\eta_1 + 1)\sqrt{\frac{A_1}{\eta_1}} + 2A_1 - (\mathscr{D}_{12} + \mathscr{D}_{13})H_d W_d \tag{4.5}$$

The vent opening area is the total open door area $A_o = (\mathscr{D}_{12} + \mathscr{D}_{13})H_d W_d$, and the vent opening height is the door height, $H_o = H_d$.

It is straightforward to rearrange the MQH correlation to compute the HRR necessary to achieve a critical temperature rise for flashover. Mathematically, this relationship is

$$\dot{Q}_c = (1.63K_x)^{-3/2}\left(k_w A_w \rho_\infty c_{p,\infty} A_o \sqrt{gH_o}/L_w T_\infty\right)^{1/2} \Delta T_c^{3/2} \tag{4.6}$$

where it is has been assumed that the walls are thermally thin. The thermally thin assumption follows from the discussion of the previous paragraph, and results in a lower bound estimate for the critical HRR. Equation (4.6) is useful for determining the largest fire that a given room can contain without proceeding to flashover.

There are two approaches for computing the probability of flashover. The most straightforward approach is based on forward MQH model, Eq. (2.3). For the MQH-based loss model the uncertain scenario parameters are $x = \{t_p, \dot{Q}_p, A_1, \eta_1, H, \mathscr{D}, \mathscr{X}\}$, which are used in Eq. (4.2) along with Eq. (4.5) to predict the HGL temperature. Note that the peak HRR, $\dot{Q}_p$, and the time of the peak HRR, t_p, are dependent on the choice of the fabric combination, a. Using N samples from the probability distributions for the uncertain parameters in provided in Sec. 3, a set of N temperatures is found using Eq. (4.2). The resultant temperature samples, T_i for $i = 1, \ldots, N$ can be used to build a histogram representative of the probability distribution for the uncertain HGL temperature. Additionally, the probability of flashover is obtained by counting the number of temperature samples greater than the flashover temperature and dividing by N. More formally, let $l = 1$ correspond to flashover and $l = 0$ correspond to no flashover. Then the loss model may be expressed as $l = \mathscr{H}\left[T\left(x|a\right) - T_c\right]$, where $\mathscr{H}\left(\cdot\right)$ is the Heaviside step function and $T\left(x|a\right)$ is computed using Eq. (4.2). Substitution of this information into Eq. (2.3) gives the equation for computing the probability of flashover for a given fabric combination:

$$\Pr\left(L = 1|a\right) = \frac{1}{N}\sum_{i=1}^{N} \mathscr{H}\left[T\left(x_i|a\right) - T_c\right] \tag{4.7}$$

An alternative approach for computing the flashover probability is based on the inverse MQH correlation, Eq. (4.6). Beginning with Eq. (2.2) and using the notation of the preceding paragraph gives an alternative equation for computing the probability of flashover

$$\Pr\left(L = 1|a\right) = \int_0^\infty d\dot{Q}_p \int dx_0\, f_{\dot{Q}_p^*}\left(\dot{Q}_p|a\right) f_{X_0}\left(x_0\right) \mathscr{H}\left[\dot{Q}_p - \dot{Q}_c\left(x_0\right)\right] \tag{4.8}$$

where $f_{\dot{Q}_p^*}\left(\dot{Q}_p|a\right)$ is the PDF for the peak HRR of chairs with fabric combination a as computed by Eq. (3.2), x_0 is just x excluding the peak HRR parameters, and $f_{X_0}\left(x_0\right)$ is the joint probability distribution built from the various probability distributions discussed in Sec. 3. It has been assumed that the walls of the room are thermally thin and so the time of the peak HRR drops out of consideration. It is apparent that the second integral in Eq. (4.8) can evaluated separately resulting in

$$\Pr\left(L = 1|a\right) = \int_0^\infty d\dot{Q}_p\, f_{\dot{Q}_p^*}\left(\dot{Q}_p|a\right) \Pr\left(\dot{Q}_p \geq \dot{Q}_c\right) \tag{4.9}$$

This casting of the problem has the advantage that the CDF $\Pr\left(\dot{Q}_p \geq \dot{Q}_c\right)$ may be generated using Monte Carlo simulations and then reused for each HRR peak PDF for a given fabric combination. Both Eqs. (4.7) and (4.9) will be used in Sec. 5.

It is important to note that the MQH correlation was derived by fitting data to experiments in which the compartment opened into a large well-ventilated volume. Thus, there was little feedback from the exterior of the fire room. Such scenarios do not correspond exactly with the three room home scenario sketched in Fig. 3.3. The extent of this discrepancy was unknown for typical residential fire scenarios, and so an objective of this research is to develop a quantitative understanding of the difference in predictions from the single-compartment MQH model and the multi-compartment predictions from CFAST.

4.3 Zone Model

Zone models are a class of fire models in which compartments are split into a small number of zones (usually one or two). Within each zone, the state variables are assumed to be constant with respect to spatial location. That is, the thermodynamic state variables are assumed to be lumped with respect to space into a set of average values that are representative of the entire zone. As the

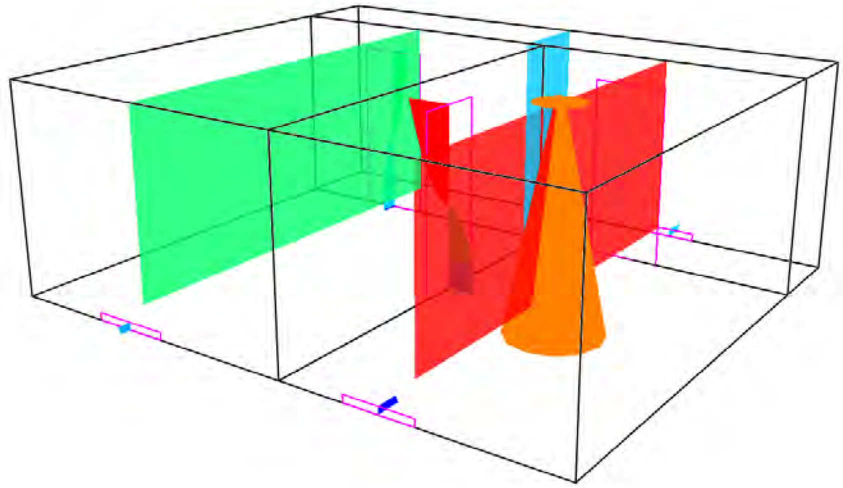

Figure 4.1: Visualization of a typical CFAST simulation.

fire develops, the volume, temperature, and composition of each zone is evolved according to a set of ordinary differential equations derived from conservation of mass and energy principles. In this report, the two-zone Consolidated Model of Fire and Smoke Transport (CFAST) [30] is used to predict the state of the gas throughout the three room structure sketched in Fig. 3.3. CFAST was first released in 1990, but it is based on zone models in development for several years prior. It includes various sub-models and is validated against a significant number of fire experiments [31]. It has been observed that CFAST does tend to over-predict HGL temperature [28], but this is generally a conservative propensity with respect to life safety.

A visualization of a typical CFAST simulation of the generic home is provided in Fig. 4.1. The black lines in Fig. 4.1 represent the edges of compartment walls, and the pink lines are the boundaries of doors or vents. The orange cone-shaped feature represents the fire plume at the peak HRR. The colored rectangles bisecting each room represent the HGL. In this scenario, the HGL in the living room is very close to the floor. The HGL in the bedroom is still relatively hot, but it not quite as low as the living room HGL. The hallway temperature is significantly lower than that in the bedroom because, in this case, the door between the hallway and the living room is closed. Note the vents at the floors in each compartment. These were inserted to account for pressure-induced leakage from the compartments.

There are many advantages of using CFAST for the prediction of fire losses. First, CFAST more accurately models the scenario than empirical correlations. Multiple rooms are allowed, transient heat losses to the walls are taken into account, and the reduction in HRR associated with oxygen depletion is modeled. Second, CFAST provides sufficient information to predict tenability in any of the compartments. In particular, an estimate of thermal FED is possible in addition to HGL temperature-based predictions of flashover. Third, CFAST is relatively efficient. Although much slower than an evaluation of the MQH correlation, CFAST takes orders of magnitude less time than a detailed CFD model. A single run of a typical scenario takes on the order of 3 s on a typical workstation. This makes it possible to run, for instance, 10 000 simulations over the course of a workday.

Table 4.1: Concrete floor thermophysical properties.

Floor Thickness	L_f (m)	0.15
Floor Thermal Conductivity	k_f (W/m·K)	1.75
Floor Density	ρ_f (kg/m^3)	2200
Floor Specific Heat Capacity	c_f (J/kg·K)	1000

Details on the governing equations and implementation of CFAST may be found in the CFAST Technical Reference Guide [30] and so will not be discussed here. However, a few words are appropriate on the model specifics used for the simulations presented in Sec. 5. The floor was assumed to be 0.15 m concrete, and the assumed thermophysical properties are listed in Table 4.1. The assumption of concrete floors is not necessary, and other floor materials are common. Future work should incorporate additional floor materials into the analysis. The walls were chosen to be gypsum with the same properties used in the MQH calculations and listed in Table 3.3.

Another issue that was considered was air leakage from the compartments. This is typically handled in CFAST by creating additional vents areas equal to a typical effective leakage area. Leakage areas are typically quantified as area ratios defined as the equivalent leakage area divided by the total surface area. For typical surfaces, this ratio can range from 10^{-5} to 10^{-2} [32]. For all of the CFAST simulations, a leakage area ratio of 10^{-3} was chosen as appropriate relative to the total compartment surface area. Thus, the equivalent leakage area for room i was computed to be $10^{-3}\left[2A_i + 2H\left(L_i + W_i\right)\right]$. Leakage was implemented using a 0.08 m high vent at the floor of each compartment where the width was varied to obtain the required effective leakage area.

A couple of assumptions were made concerning the fire. First, the fire was assumed to be at the floor of the compartment. This is a conservative estimate with respect to the HGL temperature. Second, the horizontal area of the base of the fire was assumed to be 0.8 m^2. This is representative of a typical RUF chair.

Two loss metric were considered: flashover in the living room, and thermally fatal conditions in the bedroom. The first of these loss metrics is a function of HGL temperature in the living room. The flashover probability is calculated using Eq. (4.7) only with an extended uncertain parameter set. Instead of only peak HRR values being used, an entire time-HRR curve, γ, was used—as sampled with Eq. (3.3).

The thermal FED defined in Eq. (4.1) will be used to determine the occurrence of fatal conditions in the bedroom. The integral was approximated using a simple rectangular rule integration of the CFAST outputs at 10 s intervals. The heat flux was computed by defining a CFAST target at the floor of the bedroom. Following Peacock et al. [14], the following algorithm is used for determining which temperature to apply in Eq. (4.1) in terms of the height of the HGL interface, z_l, and the HGL temperature:

- if $z_l > 1.5$ m, use the lower layer temperature;
- if 1 m $< z_l <$ 1.5 m and HGL temperature is greater than 50 °C, use the lower layer temperature;
- if 1 m $< z_l <$ 1.5 m and HGL temperature is less than 50 °C, use the HGL temperature; or
- if $z_l < 1$ m, use the HGL temperature.

This algorithm is intended to model the response of a typical occupant to the height and temperature of the HGL. The first case accounts for situations in which the HGL is high enough that most occupants would be able to stay in the cooler air below. The second two cases correspond to scenarios in which a typical occupant would choose to stand upright or squat based on the temperature of the HGL. That is, if the HGL is cool enough (i.e., less that 50 °C), then the occupant would be able to stand. If, however, the HGL temperature is too uncomfortable, most people would choose to squat. Finally, for HGLs descended lower than 1 m, it is assumed that occupants would not be able to avoid exposure to the HGL gases.

Section 5

Results

5.1 Overview

The loss models described in the previous section may be simulated with inputs sampled from the building statistics provided in Sec. 3 to estimate losses in typical residences in the United States. These results allow for a comparison of the effectiveness of the different barrier fabrics used in the chair fire tests performed by the CPSC.

The quality of the loss estimates depends on several factors including the accuracy of the input data, the number of Monte Carlo (MC) simulations performed, and the accuracy of the fire models. The accuracy of the output probability distributions depends on the accuracy of the input probability distributions. The discussion in Sec. 3 is largely a justification for probability distributions used to describe the uncertain building and fire scenario parameters. In all cases in which there was a lack of relevant information, the minimal assumption of a uniform distribution was made. Assuming uniform distributions will result in conservative estimates of the uncertainty in the loss metric, provided that the extent of the bounds is not underestimated. This possible over-prediction in uncertainty is not generally a problem since it is consistent with what is known about the potential fire scenarios. Of greater concern with regards to the input data is the potential that the data used is not truly representative. Again, this is not necessarily a problem in that it means that the estimated loss probabilities are the best that can be predicted based on the information available, but it also means that the results could change significantly if better data become available.

A sufficient number of simulations must be performed in order to sufficiently sample from the input probability space. The variance of a MC approximation decreases as $N^{-1/2}$, but it is unknown *a priori* how many samples are needed to achieve the desired precision. There are various techniques for reducing the number of required samples such as Latin hypercube and importance sampling. In the following, it was found that more advance sampling techniques were not required. Instead, comparing results with increasing N revealed that convergence was achieved with a reasonable number of samples.

Finally, the quality of the results depends on the model uncertainty. Fortunately, the models used in this report have been well-validated against experimental data. McGrattan et al. [28] compared MQH and CFAST model predictions with experimental data from a number of diverse scenarios. Of particular importance for the analysis of this research are the hot gas layer (HGL) temperature, HGL height, and surface heat flux since these quantities are used to predict flashover and the thermal fractional effective dose (FED). McGrattan et al. [28] found that MQH over predicts HGL temperature by 17 % on average. Note tht this bias percentage was determined from cases in which the compartment was ventilated to a large exterior, and so the uncertainty is not necessarily representative of the fire scenarios considered in this report. Similarly, McGrattan et al. [28] found that CFAST over predicts, on average, the HGL temperature by 20 %, under predicts the HGL height by 5 %, and, and over predicts surface heat fluxes by 5 %. These numbers give an idea of the accuracy of the models, but since they are only average quantities, it is not generally possible to apply them as corrections to the model results. An improvement in existing models, or the development of new models could improve the results presented below.

5.2 Predicting Hazard with the MQH Correlation

The MQH correlation provides a link between the size of a fire and the temperature in the hot gas layer (HGL). As discussed in Sec. 4, the correlation is useful for estimating fire losses both in its forward form, predicting flashover, and its inverse form, predicting the size of a fire resulting in flashover. In this section, both of these forms are applied using the building and fire statistics as inputs.

Sampling and evaluating a single MQH case takes on the order of 0.001 s on a typical desktop workstation. Consequently, it takes about 16 min to perform 1 million MC simulations.

5.2.1 Inverse MQH

The inverse mode of the MQH correlation was used to generate a probability distribution for the critical heat release rate (HRR) required to produce flashover in the range of typical living rooms characterized by the building statistics. Essentially, Eq. (4.6) was simulated N times with each simulation corresponding to a sampled living room. It was first necessary to determine if a sufficient number of samples were taken. This may be investigated by plotting a statistic of the critical HRR, $\dot{Q}_c$ as a function of N. Such a convergence plot is provided for the median value of $\dot{Q}_c$ in Fig. 5.1. It is seen that the variability in the estimate of the median flashover HRR is small after around 100 000 samples. Furthermore, even with only 1 000 samples, a reasonable estimate of the median value of $\dot{Q}_c$ is obtained.

The probability density function (PDF) of $\dot{Q}_c$ is provided in Fig. 5.2. This PDF was generated by a normed histogram of 512 000 MC samples. Four distinct peaks are observed. These peaks are a consequence of the discretely distributed building parameters—namely, the fire location and the door opening combination. Fires smaller than 0.5 MW are seen to have a very low probability of causing flashover in the living room, assuming that no other fuel sources become involved. The lower bound of this data is 440 kW implying that, within the uncertainty of the building statistics and the model, fires that remain smaller than this value will not flashover any living room in an ensemble of rooms sampled from the building parameter probability distributions. The 5th percentile of this data is 510 kW. That is, fires smaller than 510 kW will flashover 5 % of living rooms sampled from the input probability distributions. The median critical HRR is 850 kW as seen in Fig. 5.2.

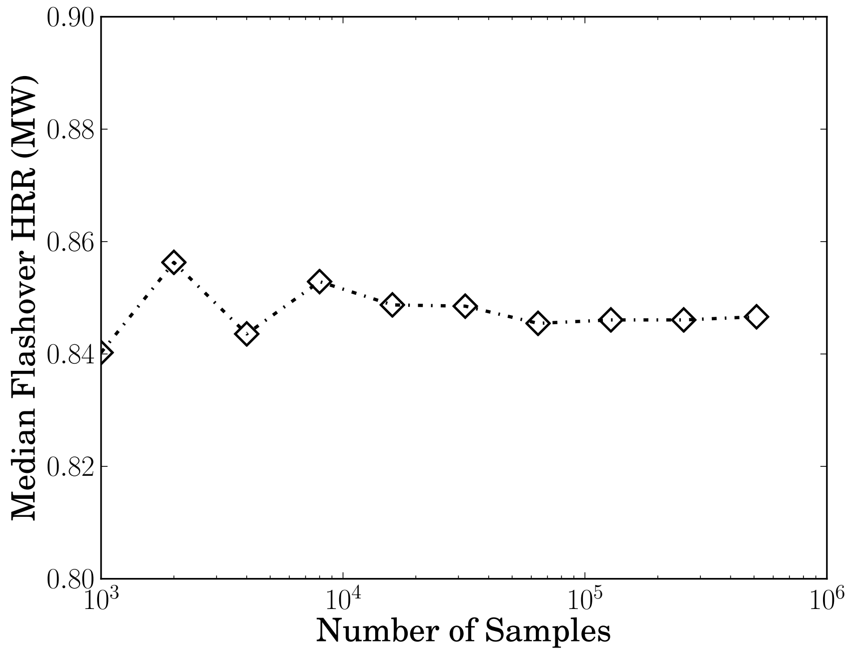

Figure 5.1: Median flashover HRR, as computed by the inverse MQH correlation, versus number of samples.

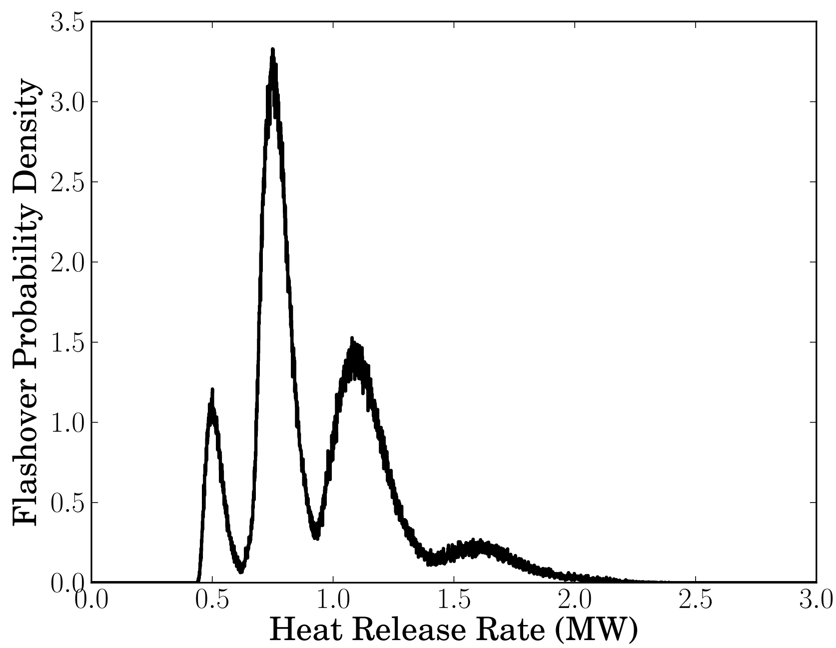

Figure 5.2: Probability density function (PDF) of the critical flashover HRR obtained using the inverse MQH correlation.

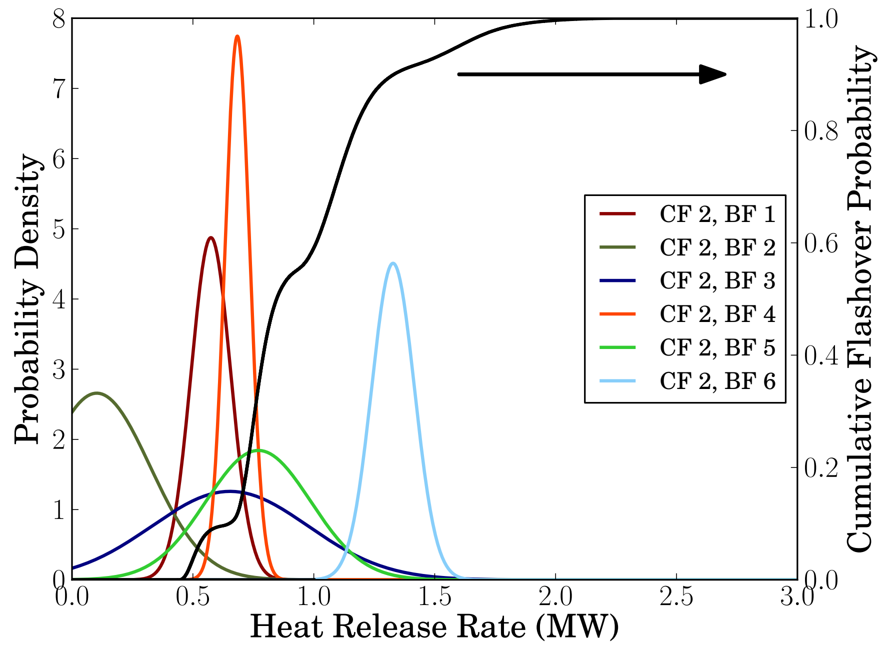

Figure 5.3: Heat release rate PDFs for cover fabric two compared to flashover probability for chairs.

In addition to helping quantify a critical HRR for flashover, the inverse MQH correlation, Eq. (4.6), may also be used to estimate flashover probabilities. This is accomplished using the flashover probability distribution plotted in Fig. 5.2 as a cumulative distribution function (CDF), $\Pr\left(\dot{Q}_p \geq \dot{Q}_c\right)$. The CDF is substituted into Eq. (4.9) along with the peak HRR PDF in the form of Eq. (3.2). Both the CDF and peak HRR PDFs for the RUF fires with cover fabric two are plotted in Fig. 5.3. An equivalent plot for cover fabric three is provided in Fig. 5.4. The degree to which the colored PDFs overlap with the CDF (black line) corresponds to the probability of flashover. As was noted in Sec. 3, cover fabric three tends to produce more intense fires. Thus the peak HRR PDFs in Fig. 5.4 overlap with the critical HRR CDF to a greater extent than those in Fig. 5.3, and thus chairs wrapped with cover fabric three are more likely to result in flashover of the living room. Similarly, barrier fabric six is seen to produce a much greater likelihood of flashover according to the MQH correlation.

The probabilities of flashover for the various fabric combinations computed using the inverse MQH correlation and 512 000 samples from the building data probability distributions are provided in Table 5.1. These values were computed using Eq. (4.9). Evaluation of Eq. (4.9) may be visualized with the aid of Figs. 5.3 and 5.4. The flashover probability is computed as the integrated product of the colored lines with the black line. As previously mentioned, cover fabric three and barrier fabric six are the most likely to cause flashover. Barrier fabric two is seen to reduce the flashover probability to less than 1 % if used with cover fabric two. On the other end of the severity spectrum, chairs with barrier fabric six are, on average, more than 90 % likely to lead to flashover of living rooms.

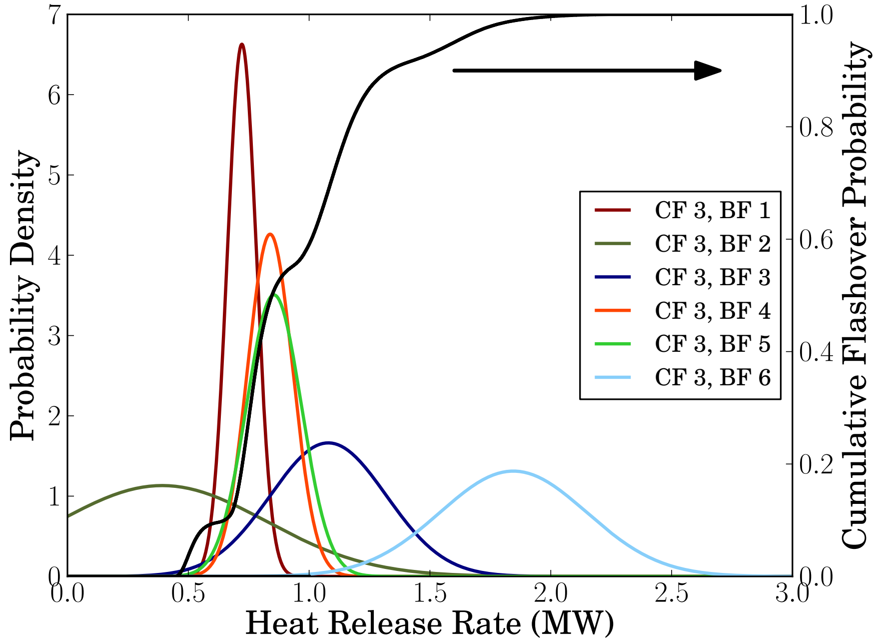

Figure 5.4: Heat release rate PDFs for cover fabric three compared to flashover probability for chairs.

Table 5.1: Flashover probabilities of all fabric combinations using the inverse MQH method.

Cover Fabric	Barrier Fabric	Flashover Probability
2	1	8.2 %
2	2	0.6 %
2	3	26.5 %
2	4	15.6 %
2	5	33.8 %
2	6	88.9 %
3	1	22.8 %
3	2	17.4 %
3	3	66.2 %
3	4	43.6 %
3	5	44.8 %
3	6	97.0 %

5.2.2 Forward MQH

The results of the previous section provide useful information on the allowable size of RUF fires in a statistical ensemble of rooms that is to some extent representative of living rooms across the United States. The inverse MQH correlation does not provide information about the HGL temperature, however. In this section, the forward MQH correlation is used to predict a distribution HGL temperatures, which is in turn used to compute flashover probabilities. This approach is equivalent with the approach taken using the CFAST model in the next section. Also, in contrast to the previous section, the flashover probability calculations will be based on a discrete distribution of peak HRR values so the estimates will be slightly different than those of Table 5.1. Specifically, peak HRR values will be sampled using Eq. (3.1) rather than Eq. (3.2). It is of interest to see how much of an effect this choice of models has on the predicted flashover probabilities.

The basic approach is to generate samples of living room parameters from the probability distributions of Sec. 3 and then use these samples to compute an ensemble of HGL temperatures for the different fabric combinations. A plot of the CDFs of the peak living room HGL temperature grouped by barrier fabric is shown in Fig. 5.5. These CDFs were created as normed histograms of 131 584 samples for each fabric combination. After the grouping by barrier fabric, each CDF in Fig. 5.5 is based on 263 168 samples. The vertical dotted line at 522 °C represents the assumed value of the flashover temperature. The point at which the CDF curves intersect this critical line correspond to the flashover probability. There is a greater than 60 % probability that chairs with barrier fabric two will not result in HGL temperatures greater than about 10 °C higher than the ambient temperature of 22 °C. This is due to the fact that a number of the chairs with barrier fabric two did not ignite. On the other hand, there are almost no chairs with barrier fabric six that do not result in a HGL temperature exceeding 400 °C. The four remaining barrier fabrics result in peak HGL living room temperatures distributed between these two extremes.

It is also helpful to look at the distribution of temperatures with respect to the two cover fabrics. A plot of the living room temperature CDFs for cover fabrics two and three is shown in Fig. 5.6. Each of these CDFs is a normed histogram generated from 789 504 samples after combining the samples from each of the six barrier fabrics combined with the corresponding cover fabric. It is apparent that the choice of cover fabric has much less influence on the potential for flashover than does the choice of barrier fabric—at least for those materials considered in this report. The change in flashover probability between the two cover fabrics is about 20 % as compared to about 90 % for the change between barrier fabric 2 and barrier fabric 6 as seen in Fig. 5.5.

As with the inverse MQH simulations discussed in the previous section, the convergence of the simulations was checked by plotting the flashover probability versus the number of samples for each fabric combination in Fig. 5.7. As with the inverse MQH simulations, the flashover probabilities vary little after around 100 000 samples. Also, it is observed that fairly accurate estimates of the flashover probabilities is obtained with even around 1000 samples.

The flashover probabilities computed using the forward MQH correlation and the discrete distribution for the HRR peaks are compiled in Table 5.2. There is little difference with the values in Table 5.1. The greatest difference in terms of probabilities is for the cover fabric two, barrier fabric five combination in which the probability of flashover is 3.4 % higher for the inverse MQH

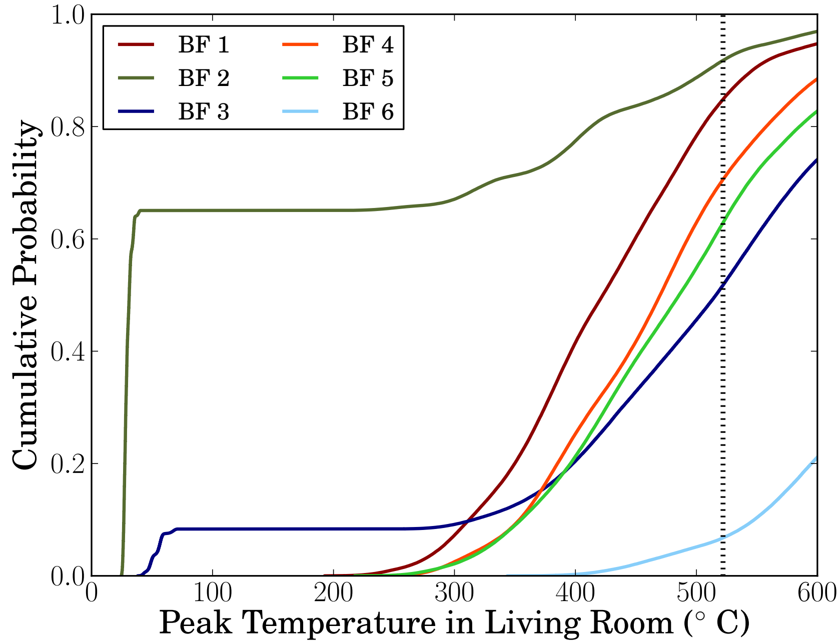

Figure 5.5: Cumulative probability distribution for hot gas layer temperature in living room for all barrier fabrics as predicted by the MQH correlation.

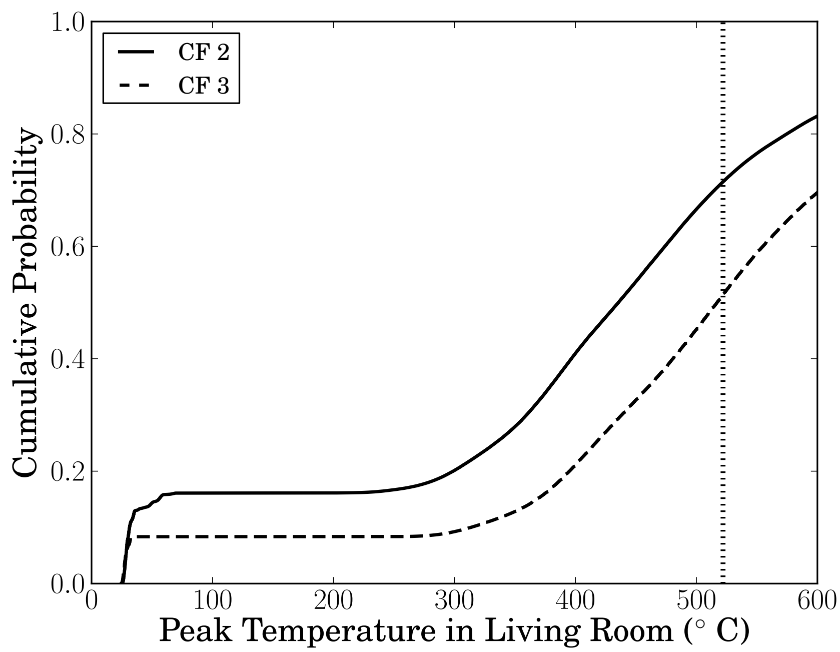

Figure 5.6: Cumulative probability distribution for hot gas layer temperature in living room for both cover fabrics as predicted by the MQH correlation.

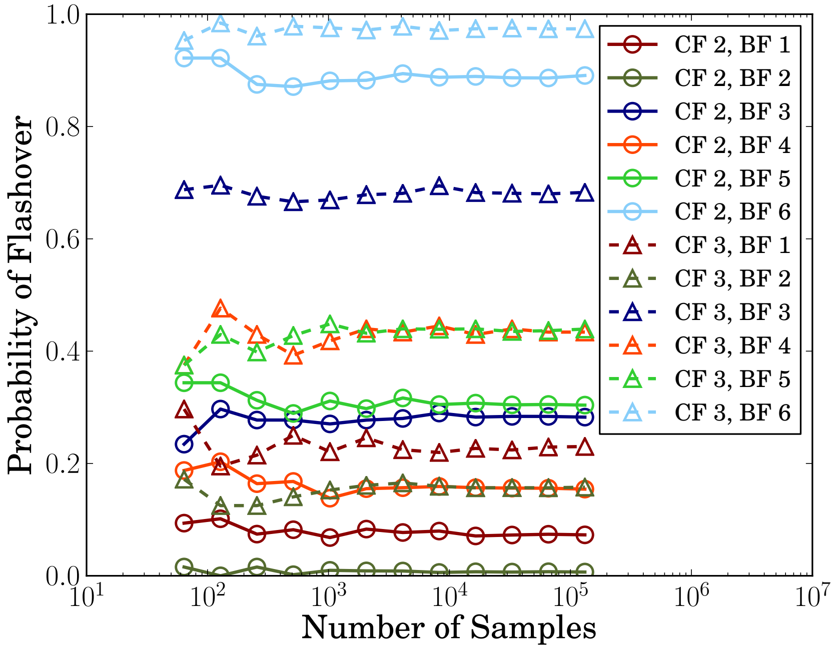

Figure 5.7: Convergence of flashover probabilities using MQH based model.

Table 5.2: Flashover probabilities of all fabric combinations using MQH based model.

Cover Fabric	Barrier Fabric	Flashover Probability
2	1	7 %
2	2	1 %
2	3	28 %
2	4	15 %
2	5	30 %
2	6	89 %
3	1	23 %
3	2	16 %
3	3	68 %
3	4	43 %
3	5	44 %
3	6	97 %

calculation. This discrepancy is due to the fact that the PDF for that fabric combination straddles the rapidly increasing region of the critical flashover CDF. Thus, small variations in the probability distribution for the cover fabric 2, barrier fabric 5 combination will result in large variations in the flashover probability.

It is helpful to group the flashover probabilities in terms of the barrier fabrics since the objective of this report is to assess the impact that barrier fabrics have on RUF fire hazard. The probabilities

Table 5.3: Flashover probabilities from barrier fabrics using forward MQH model.

Barrier Fabric	Flashover Probability
1	15 %
2	8 %
3	48 %
4	29 %
5	37 %
6	93 %

that a chair with one of the six barrier fabrics will cause a living room to flashover are listed in Table 5.3. The effectiveness of several of the barrier fabrics in reducing the flashover probability is clear. Compared with the worst performing barrier fabric (barrier fabric six), all of the other barriers have reduce the flashover probability by at least about 45 %. The best performing barrier fabric reduces the flashover risk to only 8.2 %.

The MQH results show a clear distinction in the performance of the several barrier fabrics. These results are limited for several reasons, though. The only loss metric considered is the transition to flashover. Therefore, it is impossible to make any predictions concerning life safety in adjoining rooms. Perhaps of greater importance, however, is that the MQH correlation is based on data for compartments venting to an arbitrarily large exterior. Because of this, it is likely that the flashover probabilities will be over-predicted. In the next section, similar simulations are performed using CFAST as the fire model. The CFAST results will not be subject to these limitations.

5.3 Predicting Hazard with CFAST

Hazardous conditions in both the living room and the bedroom were estimated for all 12 fabric combinations using CFAST. Specifically, transition to flashover and the thermal FED were computed. Up to 10 000 MC simulations for each fabric combination were performed. A typical CFAST scenario took approximately 3 s of CPU time on a typical desktop workstation.

It was found that for almost all of the fabric combinations, the RUF chair fires were insufficiently large to flashover the living room. The only exception was for chairs covered with cover fabric three and barrier fabric six. These chairs had only a 0.1 % chance of causing flashover. The discrepancy between this result and that obtained using the MQH correlation is due to the previously mentioned fact that the MQH correlation was developed using data in which the compartment vents were connected to a large open space rather than an adjacent compartment. It was observed that the HGL temperatures in CFAST were considerably lower for cases in which the door openings were defined to be connected to the exterior of the home rather than to the adjacent bedroom and hallway. It was observed that for otherwise identical cases, the peak HRR was almost halved in scenarios in which the living room doors opened to the other interior rooms. This decrease in HRR was seen to correspond to a near halving in the available oxygen in the living room.

Since the flashover probabilities were all effectively zero, convergence of the simulations were checked by considering another statistic—namely, the probability that the bedroom thermal FED

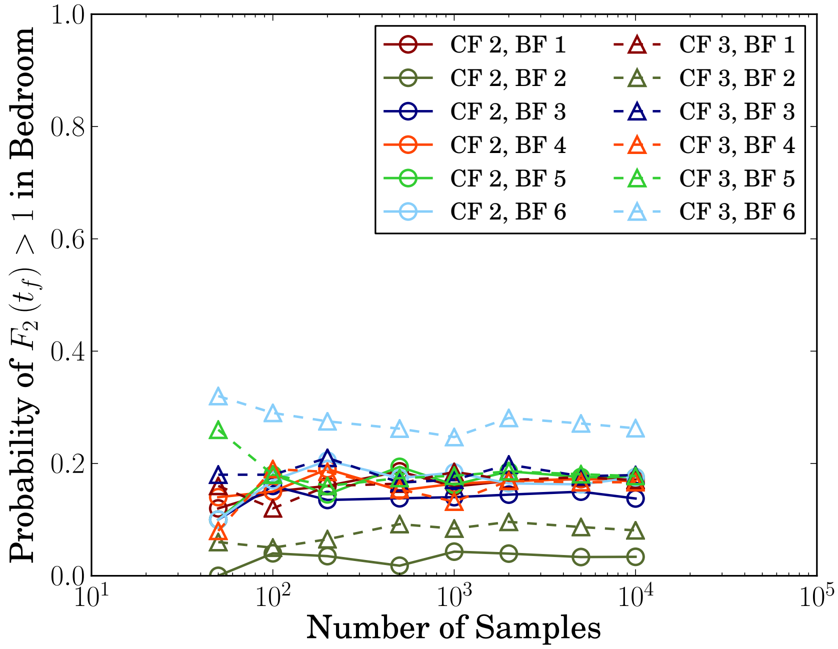

Figure 5.8: Convergence of the probability of the living room fractional effective dose exceeding one.

exceeded one at any point in the simulation time. A thermal FED greater than one corresponds to lethal conditions for 50 % of the population in the bedroom. A plot of the probability of lethal conditions in the bedroom versus the number of MC simulations is shown in Fig. 5.8. It appears that the variability in the failure probability is small for results based on more than 2 000 simulations. More simulations could be performed to confirm this, but it would take approximately 42 days to run 100 000 simulations for each of the 12 fabric combinations. Such a calculations would be possible utilizing multiple processors, but the variability apparent in Fig. 5.8 is sufficiently small that such an effort is not necessary.

The probabilities that the final thermal FED in the bedroom, $F_2\left(t_f\right)$ exceeds one are listed in Table 5.4 for each of the six barrier fabrics. Note that these probabilities correspond to 20 000 simulations for each barrier fabric. Clearly, none of the barrier fabrics completely eliminate the hazard in the bedroom. However, a substantial reduction in hazard is seen between barrier fabrics six and two. The remaining four barrier fabrics are seen to have intermediate and relatively similar hazard potential for occupants in the bedroom.

More information on the bedroom thermal FED is presented in Fig. 5.9 in which the full CDFs for each barrier fabric are plotted. For all cases, there is a probability of at least about 20 % that the bedroom thermal FED is effectively zero. These cases of near zero thermal FED correspond to scenarios in which the bedroom is not connected to the living room because the doors are closed. The thermal FED is never exactly zero since the integral written in Eq. (4.1) is always nonzero. Barrier fabric two has about a 70 % probability of the FED being approximately zero as

Table 5.4: Probability of lethal condition in the bedroom for each barrier fabric base on the thermal FED.

Barrier Fabric	Probability of FED > 1
1	17 %
2	6 %
3	16 %
4	17 %
5	18 %
6	22 %

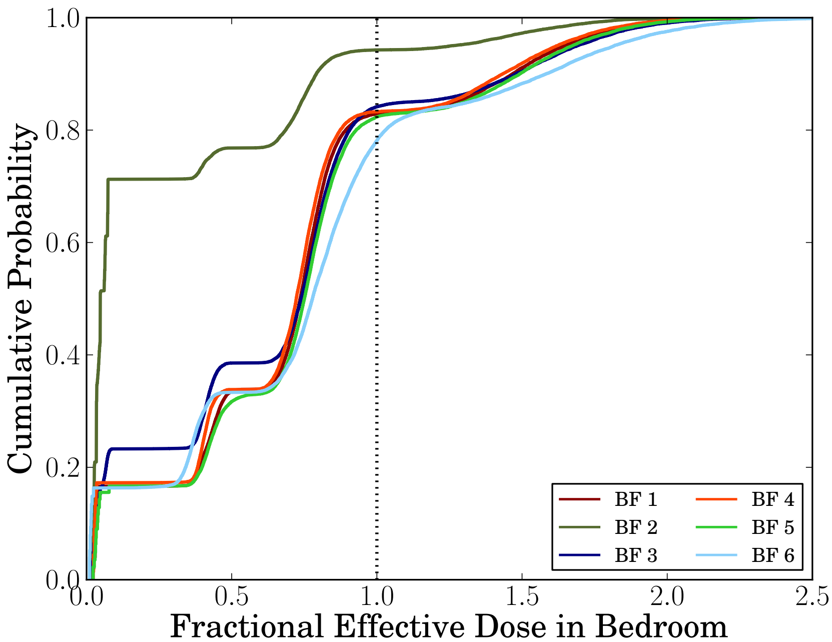

Figure 5.9: Cumulative distribution function for bedroom thermal FED in bedroom for all barrier fabrics as predicted using CFAST.

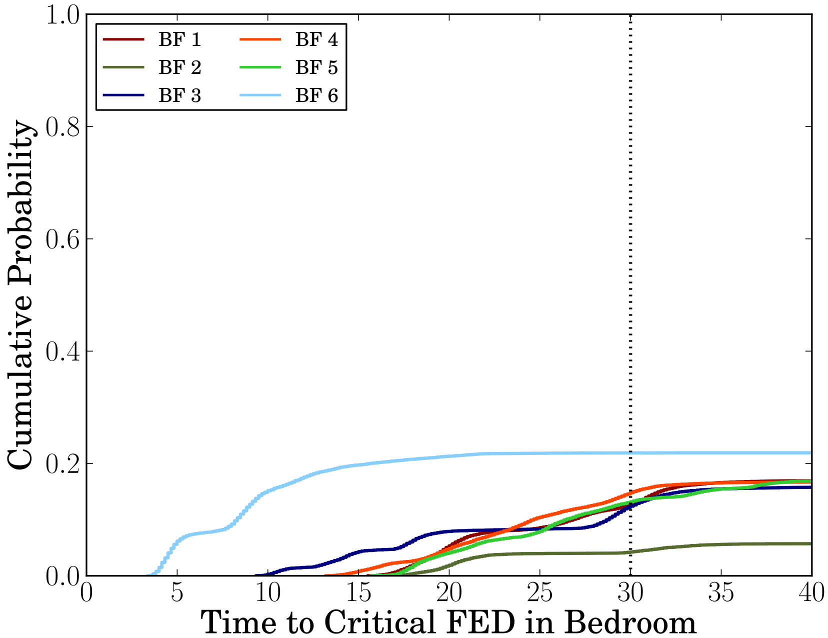

Figure 5.10: Cumulative distribution function for the time at which the bedroom thermal FED exceeds one for all barrier fabrics as predicted using CFAST.

a consequence of the cases in which the chairs with barrier fabric two fail to burn.

As is apparent from Fig. 3.1, the different fabric combinations affect not only the peak HRR, but also the time at which that peak is reached. It is therefore, appropriate to investigate the time at which the critical FED is reached by the various barrier fabrics. A plot of such information is given in Fig. 5.10. Note that for barrier fabric six, thermal hazard in the bedroom becomes a strong possibility at around five minutes. By comparison other barrier fabrics are seen to delay the time to the critical thermal FED until 10 to 20 min after ignition. A particular time may be examined such as 30 min as is represented by the dotted vertical line in Fig. 5.10. At this time, the intermediately performing barrier fabrics are seen to represent a significant advantage over barrier fabric six as the probability of lethal conditions is nearly halved for all cases.

Note that the assumption of the residential layout as shown in Fig. 3.3 might have an influence on the results obtained here. In particular, for scenarios in which the home section of Fig. 3.3 is ventilated to additional rooms, it is likely that the bedroom conditions will not be as severe. Additional rooms were not included in the analysis for the reasons provided in Sec. 3, but future analysis should consider the sensitivity of these results to that assumption.

The conditions in the bedroom have been discussed first since it was observed that flashover is highly unlikely for all of the chair fires. However, for completeness, the temperature and thermal FED in the living room will be described. A plot of the HGL temperature CDF for the living room is provided in Fig. 5.11. Although the chair fires are too small to flashover the compartment for in almost all scenarios, a significant difference in performance is observed. Because chairs with barrier fabric two do not burn in many cases, there is about a 65 % probability that the

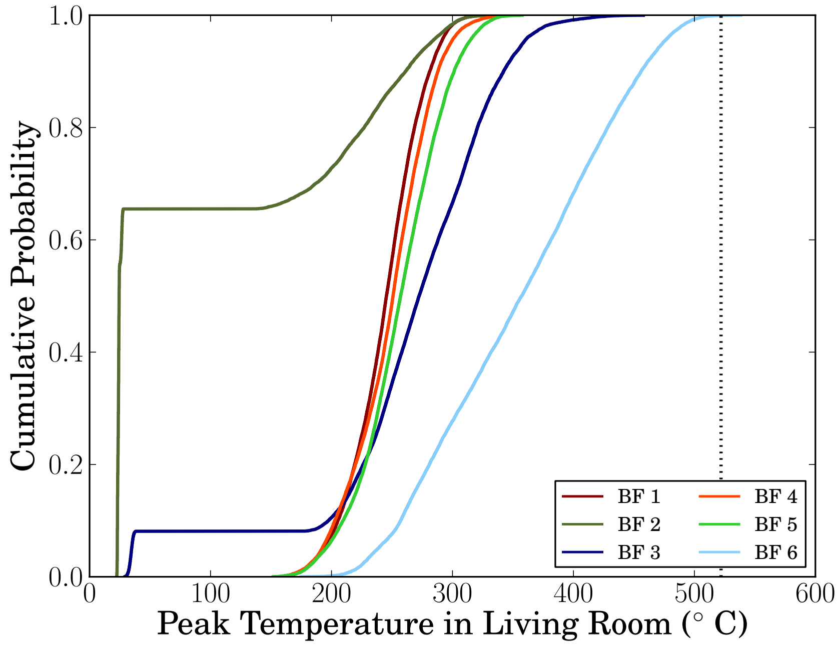

Figure 5.11: Cumulative distribution function for HGL temperature in living room for all barrier fabrics as predicted using CFAST.

room temperature remains ambient for chairs wrapped in barrier fabric two. Furthermore, with the exception of barrier fabrics three and six, there is a greater than 80 % probability that the temperature does not exceed 300 °C in the living room. Such an HGL temperature is certainly hazardous in the living room, but it also corresponds to significantly safer conditions in other parts of the home.

It is helpful to examine the correlations between the various loss metrics. First, focusing on the living room, a scatter plot of living room thermal FED versus living room peak HGL temperature is given in Fig. 5.12. The 120 000 markers in Fig. 5.12 each correspond to a single CFAST simulation. The dotted lines represent critical the values of temperature and FED. Although the living room will not flashover given the chair fires considered, it will almost always be untenable. Only a few cases are thermally tenable because several of the ignited chairs self-extinguish before the polyurethane foam padding becomes involved. Since the thermal FED is largely a function of HGL temperature, there is a clear correlation in the scatter plot.

The correlation between the bedroom FED and the living room HGL temperature is plotted in Fig. 5.14. In this case, as was seen in Fig. 5.9, the majority of scenarios are not lethal for bedroom occupants. It is interesting to note the four distinct groupings of the data in Fig. 5.9. Each of these corresponds to a distinct door opening combination, $\mathscr{D}$. The group of markers with the lowest values of thermal FED corresponds to cases in which there is no ventilation path between the bedroom and the living room—that is, all of the doors to the bedroom are closed. The second lowest group of markers is associated with scenarios in which the hot gases pass down the hallway to bedroom. The third highest group, in which the thermal FED values are close to one, is due to

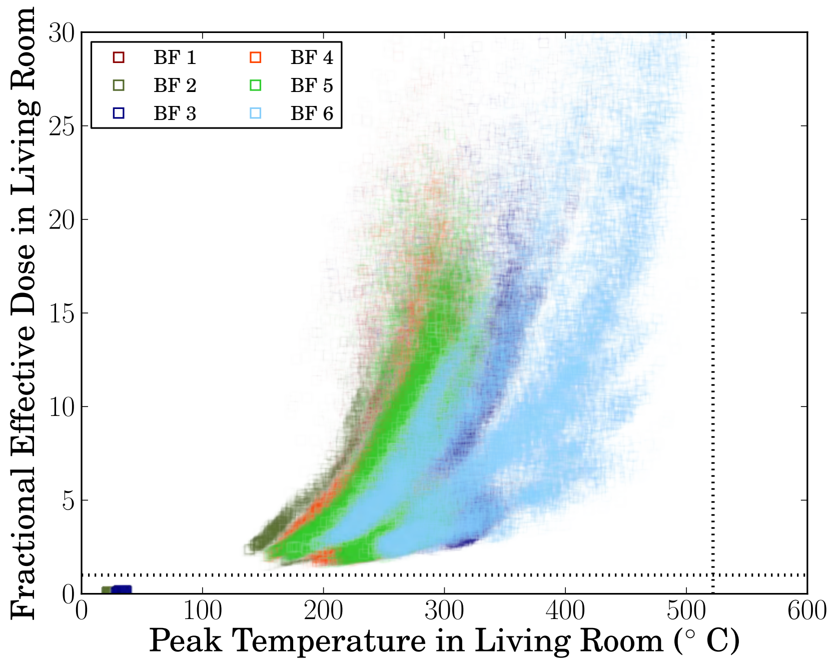

Figure 5.12: Scatter plot of living room fractional effective dose versus living room hot gas layer temperature computed using CFAST with 10 000 samples for each barrier fabric.

the scenarios in which hot gases escape to both the bedroom and the hallway. The final, and most severe, grouping of scenarios corresponds to those cases in which the hot gases move directly and exclusively from the living room to the bedroom.

The data in Fig. 5.9 may be summarized in terms of means and standard deviations. This reduced statistical picture of the data is plotted in Fig. 5.14. The standard deviations are a result of both the uncertainty in the RUF chair fire experiments as well as the uncertainty in the building scenario parameters. It is observed that the average final thermal FED in the bedroom is not much larger for barrier fabric six than it is for barrier fabrics one, three, four, and five. The relatively good performance of barrier fabric two is demonstrated once again.

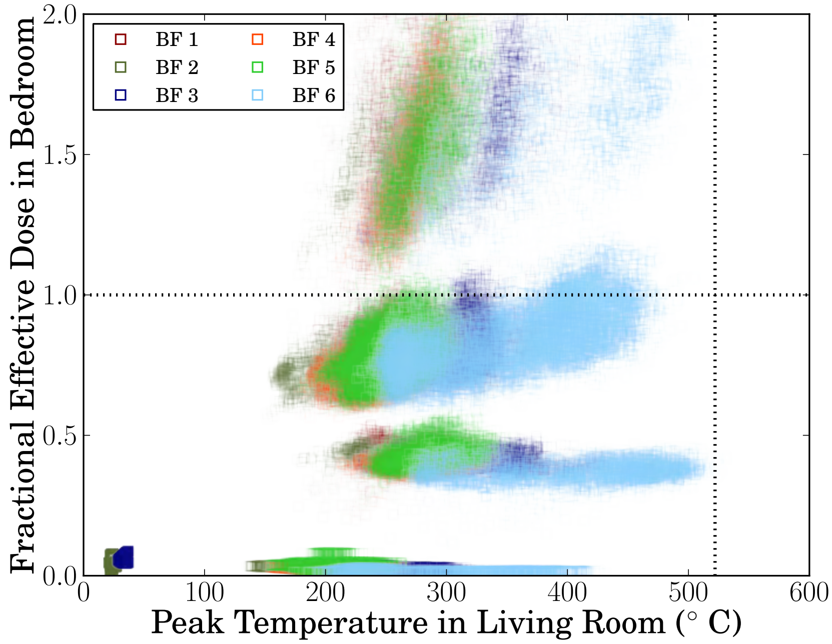

Figure 5.13: Scatter plot of bedroom fractional effective dose versus living room hot gas layer temperature computed using CFAST with 10 000 samples for each barrier fabric.

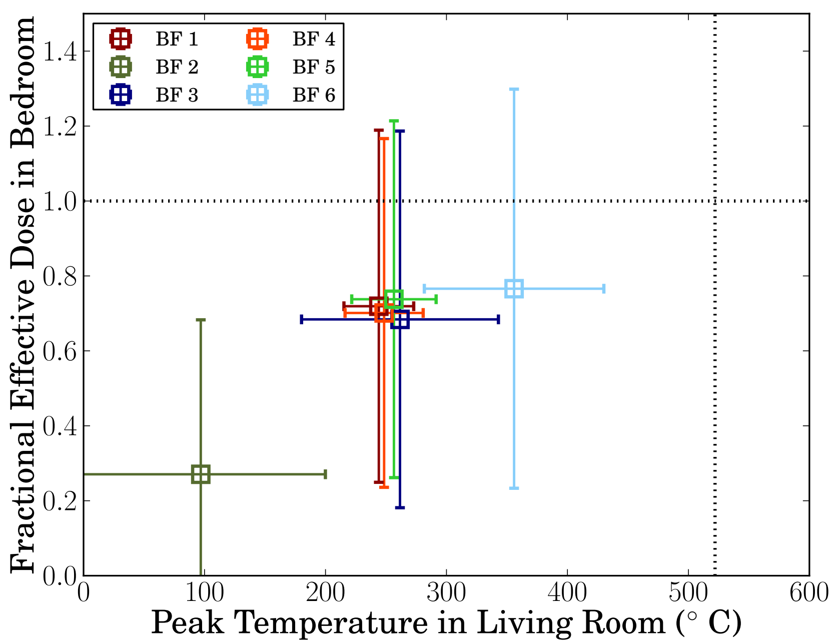

Figure 5.14: Bedroom fractional effective dose versus living room hot gas layer temperature average values computed using CFAST with 10 000 samples for each barrier fabric. The error bars represent one standard deviation.

Section 6

Conclusions

The potential for barrier fabrics to reduce the flammability of residential upholstered furniture (RUF) is being considered by the Consumer Product Safety Commission (CPSC). In order to investigate the effectiveness of barrier fabrics at improving life safety in RUF fires, a probabilistic methodology for estimating fire losses was developed. This methodology is based on Monte Carlo (MC) simulations of fire models. As this report is the first presentation of this methodology, the implementation is still in prototype form. The focus has been on the building statistical data and the theory underlying the approach.

The probabilistic method for estimating fire losses requires a statistical description of the fire scenarios. Such a statistical description was developed from relevant census, code, and survey data. Concurrently, a statistical description of RUF chair fires with different fabric combinations was derived from data provided by the CPSC. The probability distributions describing these scenario parameters may be used to generate an ensemble of residential fire scenarios that is to some degree representative of home fires in the United States.

Two models were used to perform the MC simulations. The first model was the MQH correlation for predicting hot gas layer (HGL) temperature as a function of heat release rate (HRR). The HGL temperature was used as a criterion flashover. While the MQH correlation predicted a significant number of living room flashovers for all fabric combinations and room scenarios in the statistical ensemble sampled, similar calculations using the zone model CFAST indicate that flashover from a single chair is very unlikely for the chairs and floor plan considered. The CFAST model indicates that even though flashover is unlikely in the living room, that lethal conditions may be possible in both the living room and an adjacent bedroom. Lethal conditions were characterized in terms of a thermal fractional effective dose (FED).

A clear distinction between barrier fabrics was observed. Use of the worst barrier fabric resulted in significantly higher temperatures and thermal FEDs in all rooms considered. One of the barrier fabrics consistently performed better than the rest. In many cases this barrier fabric protected the chair from burning, and conditions were safe throughout the structure. The four intermediately performing barrier fabrics provided a significant reduction in HGL temperature in the living room when compared to the worst performing barrier fabric. In terms of the thermal FED, however, the intermediate barriers provided only a marginal improvement over the worst barrier. This is due to the fact that thermal FED is defined as an integrated quantity, and even though the intermediate barriers reduced the peak HRR, they tended to burn for longer periods of time thus steadily increasing the thermal FED. It is unclear if the thermal FED is appropriate for these long time scales.

In any case, the intermediate barriers did tend to delay the time at which a critical thermal FED was reached. In order to quantify the advantage of this delay, it will be necessary to include some analysis of occupant egress in residential scenarios.

The research described in this report has many paths for future development. The MC methodology produces a large amount of data, and it is possible to extract additional useful information from these results. In particular, sensitivity analysis of the uncertain parameters may be easily investigated by producing scatter plots of predicted loss metrics versus the various uncertain parameters. Such plots will allow for identification of those scenario parameters which are most influential on life safety. Those parameters found to be uninfluential do not need to be better characterized or even varied in future simulations. Conversely, those parameters seen to have a significant impact on the loss metrics should be better characterized in terms of their probability distributions. In addition to a deeper analysis of the available data, details should be added to the CFAST model. Specifically, it is important to investigate the hazard consequences of larger RUF fires since those considered in this report did not result in flashover in nearly all of the cases considered. Similarly, the addition of secondary RUF fires into the model will result in more realistic and severe scenarios. It is likely that the consideration of more severe fire scenarios will allow for a more precise differentiation of the fabric combinations under consideration. It was noted that the home model given in Fig. 3.3 might have some limitations due to the lack of fresh air from the rest of the home. The effects of this assumption should be studied by including a door from the hallway to an additional large room to represent the rest of the house or possibly just a door opening to the home exterior. A very practical piece of future work is to use the CFAST model, coupled to a well-chosen set of design fires to identify a critical HRR as was done with the MQH correlation. Future model developments should include the addition of smoke alarms and some consideration of reasonable egress times for building occupants. The limitations of the CFAST model should be explored through the use of more detailed simulations using the Fire Dynamics Simulator (FDS) [33]. The sensitivity of the results to the response of occupants to the HGL height and temperature should be studied. Finally, the methodology could be used to quantify reductions in civilian deaths by focusing on the scenarios in which most fatalities occur according to the fire statistics.

References

[1] M. Ahrens. Home structure fires. Technical Report USS12G, National Fire Protection Association, Quincy, Massachusetts, 2015.

[2] J.R. Hall. Estimating fires when a product is the primary fuel but not the first fuel, with an application to upholstered furniture. *Fire Technology*, 51:381–391, 2015.

[3] R.G. Gann, V. Babrauskas, and R.D. Peacock. Fire conditions for smoke toxicity measurement. *Fire and Materials*, 18:193–199, 1994.

[4] R.W. Bukowski. Evaluation of furniture-fire hazard using a hazard-assessment computer model. *Fire and Materials*, 9(4):159–166, 1985.

[5] R.D. Peacock and R.W. Bukowski. A prototype methodology for fire hazard analysis. *Fire Technology*, 26:15–40, 1990.

[6] F.B. Clarke, R.W. Bukowski, R.W. Steifel, J.R. Hall, and S.A. Steele. The National Fire Risk Assessment Project—Final Report. Technical report, National Fire Protection Research Foundation, Quincy, Massachusetts, 1990.

[7] R.W. Bukowski, F.B. Clarke, J.R. Hall, and R.W. Steifel. The National Fire Risk Assessment Project—Case Study 1: Upholstered Furniture in Residences. Technical report, National Fire Protection Research Foundation, Quincy, Massachusetts, 1990.

[8] V. Babrauskas. Fire hazard and upholstered furniture. In *Third European Conference on Furniture Flammability*, pages 125–133, Brussels, 1992. Interscience Communications Ltd.

[9] R.D. Peacock, P.A. Reneke, R.W. Bukowski, and V. Babrauskas. Defining flashover for fire hazard calculations. *Fire Safety Journal*, 32:331–345, 1999.

[10] P.H. Thomas. Testing products and materials for their contribution to flashover in rooms. *Fire and Materials*, 5(3):103–111, 1981.

[11] B.J. McCaffrey, J.G. Quintiere, and M.F. Harkleroad. Estimating room fire temperatures and the likelihood of flashoverusing fire test data correlations. *Fire Technology*, 17:98–119, 1981.

[12] V. Babruaskas, R.D. Peacock, and P.A. Reneke. Defining flashover for fire hazard calculations: Part ii. *Fire Safety Journal*, 38:613–622, 2003.

[13] T.J. Ohlemiller and R.G. Gann. Estimating reduced fire risk resulting from an improved mattress flammability standard. Technical Note 1446, National Institute of Standards and Technology, Gaithersburg, Maryland, 2002.

[14] R.D. Peacock, J.D. Averill, P.A. Reneke, and W.W. Jones. Characteristics of fire scenarios in which sublethal effects of smoke are important. *Fire Technology*, 40:127–147, 2004.

[15] International Organization for Standardization (ISO). *ISO 13571, Life-threatening components of fire–Guidelines for the estimation of time available for escape using fire data*.

[16] R.R. Upadhyay and O.A. Ezekoye. Treatment of design fire uncertainty using quadrature method of moments. *Fire Safety Journal*, 43:127–139, 2008.

[17] D. Kong, N. Johansson, S. Lu, and S. Lo. A monte carlo analysis of the heat release rate uncertainty on available safe egress time. *Journal of Fire Protection Engineering*, 23:5–29, 2012.

[18] B. Sundström, Research Commission of the European Communities. Directorate-General for Science, Development, Commission of the European Communities, European Commission Measurement, and Testing Programme. *CBUF: Fire Safety of Upholstered Furniture : the Final Report on the CBUF Research Programme*. EUR (Series). European Commission Measurements and Testing, 1995.

[19] V. Babrauskas. Upholstered furniture room fires—measurements, comparison with furniture calorimeter data, and flashover predictions. *Journal of Fire Sciences*, 2:5–19, 1984.

[20] International Code Council, Inc. *International Residential Code*.

[21] K. Ghazi Wakili, E. Hugi, L. Wullschleger, and T. Frank. Gypsum board in fire—modeling and experimental validation. *Journal of Fire Sciences*, 25:267–282, 2007.

[22] U.S. Census Bureau, Suitland, Maryland. *American Housing Survey for the United States: 2013*, 2013.

[23] Paul Emrath. Spaces in new homes. Technical report, National Association of Home Builders (NAHB), 2013.

[24] U.S. Energy Information Administration, Washington, District of Columbia. *Residential Energy Consumption Survey*, 2009.

[25] Eric Jones, Travis Oliphant, Pearu Peterson, et al. SciPy: Open source scientific tools for Python, 2001–. [Online; accessed 2016-03-01].

[26] D.A. Purser. *SFPE Handbook of Fire Protection Engineering*, chapter Assessment of Hazards to Occupants from Smoke, Toxic Gases, and Heat. National Fire Protection Association, Quincy, Massachusetts, 4th edition, 2008.

[27] W.D. Walton and P.H. Thomas. *SFPE Handbook of Fire Protection Engineering*, chapter Estimating Temperatures in Compartment Fires. National Fire Protection Association, Quincy, Massachusetts, 4th edition, 2008.

[28] K. McGrattan, R. Peacock, and K. Overholt. Validation of fire models applied to nuclear power plant safety. *Fire Technology*, 52:5–24, 2016.

[29] F.W. Mowrer and R.B. Williamson. Estimating room temperatures from fires along walls and in corners. *Fire Technology*, 23:133–145, 1987.

[30] R. D. Peacock, K.B. McGrattan, G. P. Forney, and P. A. Reneke. CFAST – Consolidated Model of Fire Growth and Smoke Transport (Version 7) Volume 1: Technical Reference Guide. Technical Note 1889v1, National Institute of Standards and Technology, Gaithersburg, Maryland, 2016.

[31] R. D. Peacock, G. P. Forney, and P. A. Reneke. CFAST – Consolidated Model of Fire Growth and Smoke Transport (Version 7) Volume 3: Verification and Validation Guide. Technical Note 1889v3, National Institute of Standards and Technology, Gaithersburg, Maryland, 2016.

[32] National Fire Protection Association, Quincy, Massachusetts. *NFPA 92, Standard for Smoke Control Systems*, 2012.

[33] K. McGrattan, S. Hostikka, R. McDermott, J. Floyd, C. Weinschenk, and K. Overholt. Fire dynamics simulator, technical reference guide volume 1: Mathematical model. Technical report, NIST, 2015.